ERDC/CHL TR-06-15

Coastal and Hydraulics Laboratory

US Army Corps
of Engineers®
Engineer Research and
Development Center

Half Moon Bay, Grays Harbor, Washington: Movable-Bed Physical Model Study

Steven A. Hughes and Julie Cohen

September 2006

ERDC/CHL TR-06-15
September 2006

Half Moon Bay, Grays Harbor, Washington: Movable-Bed Physical Model Study

Steven A. Hughes and Julie Cohen

Coastal and Hydraulics Laboratory
U.S. Army Engineer Research and Development Center
3909 Halls Ferry Road
Vicksburg, MS 39180-6199

Final report

Prepared for U.S. Army Engineer District, Seattle
P.O. Box 3755, Seattle, WA 98124-3755

Abstract: A 1-to-50 scale physical model of Half Moon Bay, Grays Harbor, WA, was constructed at the U.S. Army Engineer Research and Development Center's Coastal and Hydraulics Laboratory in Vicksburg, MS. The purpose of the physical model was to support studies being conducted by the U.S. Army Engineer District, Seattle. Specifically, the model results will be used to assess the potential long-term response of the Half Moon Bay shoreline to expected storm waves and surge levels, provided the breach fill between South Beach and the bay remains intact. The physical model eroded the June 2003 shoreline until a near equilibrium was achieved in the model with the dune recession line closely matching the existing vegetation line. This result indicated Half Moon Bay is approaching an equilibrium shoreline planform shape as it adjusts from an influx of sediment resulting from the 1993 breach. However, scale effects in the physical model related to sand transport mean that the dune recession reached in the model for a constant water level and wave energy is less than what would occur in Half Moon Bay under the same constant conditions. Therefore, some additional erosion of the dune should be expected in the coming years. The physical model did not include the benefits of placing dredged material in Half Moon Bay. The model demonstrated the gravel/cobble transition material is mobile with substantial erosion and transport of the gravel from the area of original placement toward the eastern portion of the bay.

Contents

Figures and Tables

Figures

Tables

Preface

This technical report describes a movable-bed physical model of Half Moon Bay at Grays Harbor, WA, and results from experiments conducted to examine the response of the existing bay shoreline to storm waves likely to occur at the project site. The study was conducted by the U.S. Army Engineer Research and Development Center (ERDC), Coastal and Hydraulics Laboratory (CHL), Vicksburg, MS, for the U.S. Army Engineer District, Seattle. The purpose of this physical model was to establish a baseline condition that can represent the response of the existing Half Moon Bay shoreline under a specified wave and water level condition, assuming a breach does not occur. Initial funding authority was provided by the Seattle District to CHL on 30 April 2003, and a review draft of this report was submitted to NWS on 31 August 2004. Review comments from the U.S. Army Engineer District, Seattle, Civil/Soils Section were incorporated into the report on 8-28 February 2005, and suggestions from an Independent Technical Review (ITR) panel were incorporated into the report on 1-23 April 2006.

Hiram T. Arden, Navigation Section, Operations Division, was the point of contact for the sponsoring Seattle District, and he provided study oversight and review. Mr. Robert M. Parry, Chief, Navigation Division, Seattle District, provided advice and direction throughout the study.

The physical model study was directed by Dr. Steven A. Hughes, Navigation Division (HN), CHL. Julie A. Cohen, HN-HH, CHL, managed the day-to-day operation of the physical model and assisted in report and figure preparation. Hugh F. Acuff, Jr., HN-HH, provided overall planning and operational guidance throughout the study. The physical model was constructed by craftsmen from the ERDC Department of Public Works (DPW) under the supervision of Charles Brown, construction leadman, and Frank James, construction supervisor. David Daily and Timothy Nisley, Instrumentation Support Division, supported the instrumentation and wave machine requirements. J. Holley Messing, Coastal Engineering Branch Navigation Division, completed word processing and formatting.

This study was conducted during the period May 2003 through August 2004 under the general technical direction of Dr. Nicholas C. Kraus,

Senior Scientists Group, CHL. Administrative supervision was provided by Thomas W. Richardson, Director, CHL; Dr. William D. Martin, Deputy Director, CHL; and Dr. Rose M. Kress, Chief, Navigation Division, CHL. Direct supervision, valuable advice, and insightful review were provided by Dennis G. Markle, former Chief, Harbors, Entrances, and Structures Branch.

Dr. James R. Houston was Director of ERDC, and COL Richard B. Jenkins was Commander and Executive Director.

Unit Conversion Factors

Multiply	By	To Obtain
cubic yards	0.7645549	cubic meters
feet	0.3048	meters
inches	0.0254	meters
miles (U.S. statute)	1,609.347	meters
square miles	2.589998 E+06	square meters
tons (2,000 pounds, mass)	907.1847	kilograms

1 Introduction

Background

The development, operation, and maintenance of navigation channels and facilities at Grays Harbor, WA (Figure 1), have been ongoing since the Rivers and Harbors Act of June 1896 authorized the construction of the south jetty. Initial construction of the north jetty was completed in 1916, and both jetties have required several reconstruction efforts between original construction and present day due to the harsh wave climate on the Washington coast. After rehabilitation of the outer 7,000 ft of the north jetty in 1940, maintenance dredging of the bar and entrance channel was no longer required due to self-scouring induced by the jetty system. Navigation channel maintenance dredging was reinstituted in 1990 with the completion of the Grays Harbor Navigation Improvement Project, and annual dredging of approximately 1.7 million cu yd has been required to maintain the authorized channel dimensions. Erosion on South Beach and on the Half Moon Bay shorelines has prompted disposal of a portion of the dredged material in these areas (Osborne et al. 2003).

In December 1993, persistent shoreline recession near the south jetty culminated in the formation of a breach between the jetty and the adjacent South Beach. In 1994, the U.S. Army Engineer District (USAED), Seattle (hereafter, Seattle District) filled the breach with 600,000 cu yd of sand dredged from the navigation channel as a temporary measure to protect the Grays Harbor Navigation Project and alleviate local concerns. During the seventh winter that the fill was in place (2001-2002), a series of storms damaged the South Beach and modified the Half Moon Bay shoreline, reemphasizing the temporary nature of the breach sand fill.

A comprehensive study (USAED, Seattle 1997) was completed in 1997 to document and evaluate the ongoing erosion problems in the vicinity of the navigation project and to identify the “most appropriate solution for protecting both Federal project features and local improvements.” The study recommended extending the south jetty landward terminus to meet an extension of the Point Chehalis revetment to be built in a southwesterly direction along the Half Moon Bay shore. Placement of dredged sand from channel maintenance within the bay and on the Half Moon Bay shoreline was included in the proposed solution. Extension of the Point Chehalis revetment was completed in 1998, but the proposed jetty extension was

deferred because of slower-than-anticipated erosion of the breach fill and because the City of Westport withdrew its support due to permitting concerns.

A modified plan was formulated for extending the life of the breach fill as a temporary measure until the approved plan for extending the south jetty could be implemented. The plan called for construction of a diffraction mound to reduce diffracted wave heights, placement of gravel/cobble fill extending from the south jetty around a portion of the Half Moon Bay shoreline most susceptible to breaching, and minor repair of the landward end of the south jetty to better withstand undermining by a potential future breach.

In 1999, construction began on a wave diffraction mound on the eastern end of the south jetty as shown in Figure 2. Part of the material for constructing the diffraction mound came from lowering of the landward-most 250 ft of the south jetty from an elevation of +8 ft mean lower low water (mllw) to +2 ft mllw. The placement of approximately 11,600 cu yd of 12-in.-minus rounded cobble and gravel provided only about one-third of a recommended design length for the transition gravel/cobble beach. This reduction in length stemmed from environmental concerns regarding impacts of placing gravel and cobble on a sandy beach.

Concern of a possible breach reoccurrence prompted placement of an additional 16,100 cu yd of gravel/cobble mixture to the Half Moon Bay shoreline in January 2002, extending the shoreline in an easterly direction. Also, 135,000 cu yd of dredged material was rehandled and placed on the breach fill in April 2002. Erosion of both the shoreward and seaward sides of the placed breach fill resulted in overtopping of the breach fill in November 2002. In response to observed erosion, the Seattle District placed an additional 27,000 cu yd of dredged sand in the southwest corner of Half Moon Bay in February 2004 to protect the breach fill. Figure 3 shows a recent (2003) aerial photograph of the Half Moon Bay shoreline.

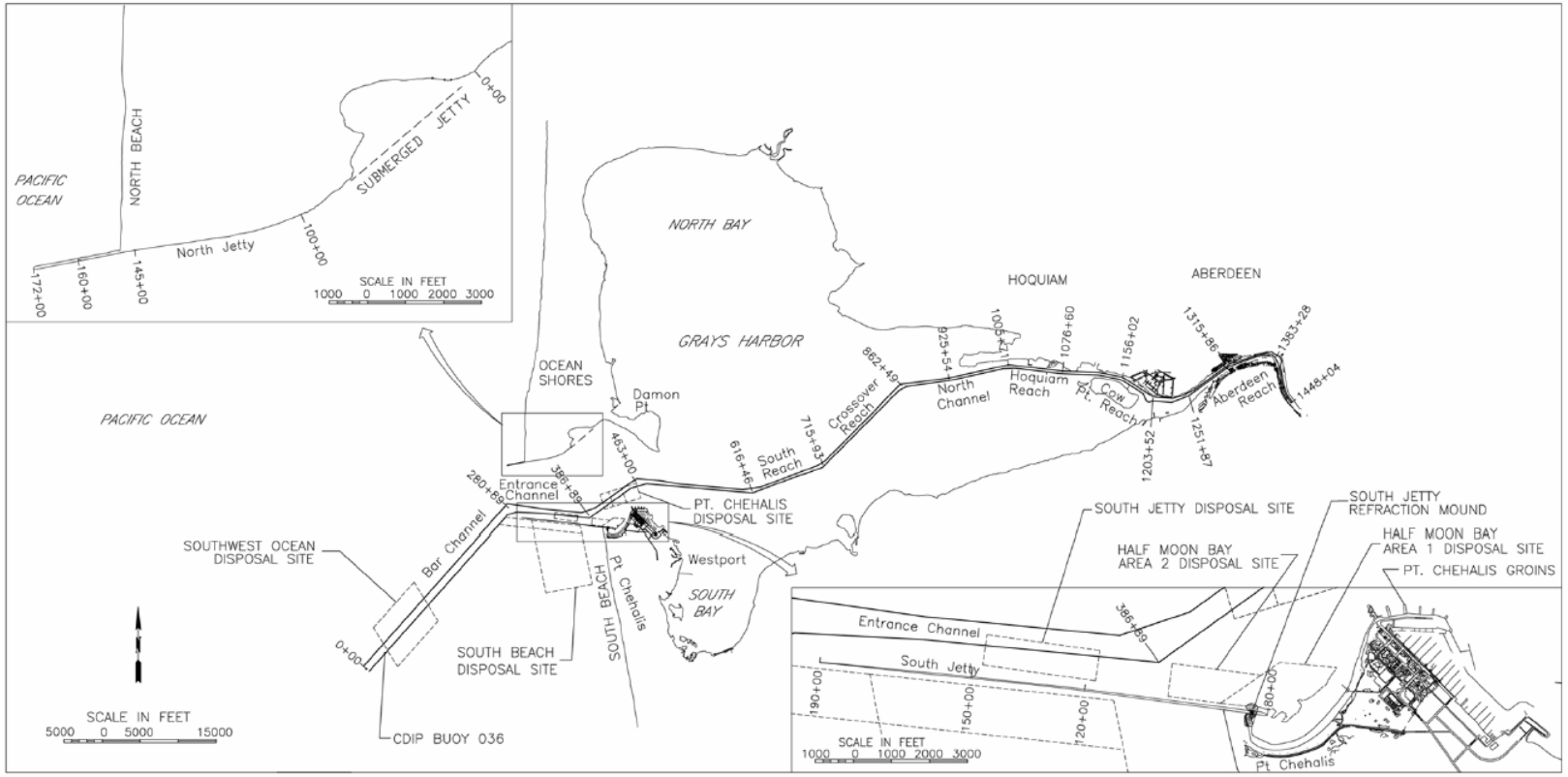

Figure 1. Federal navigation project at Grays Harbor, WA.

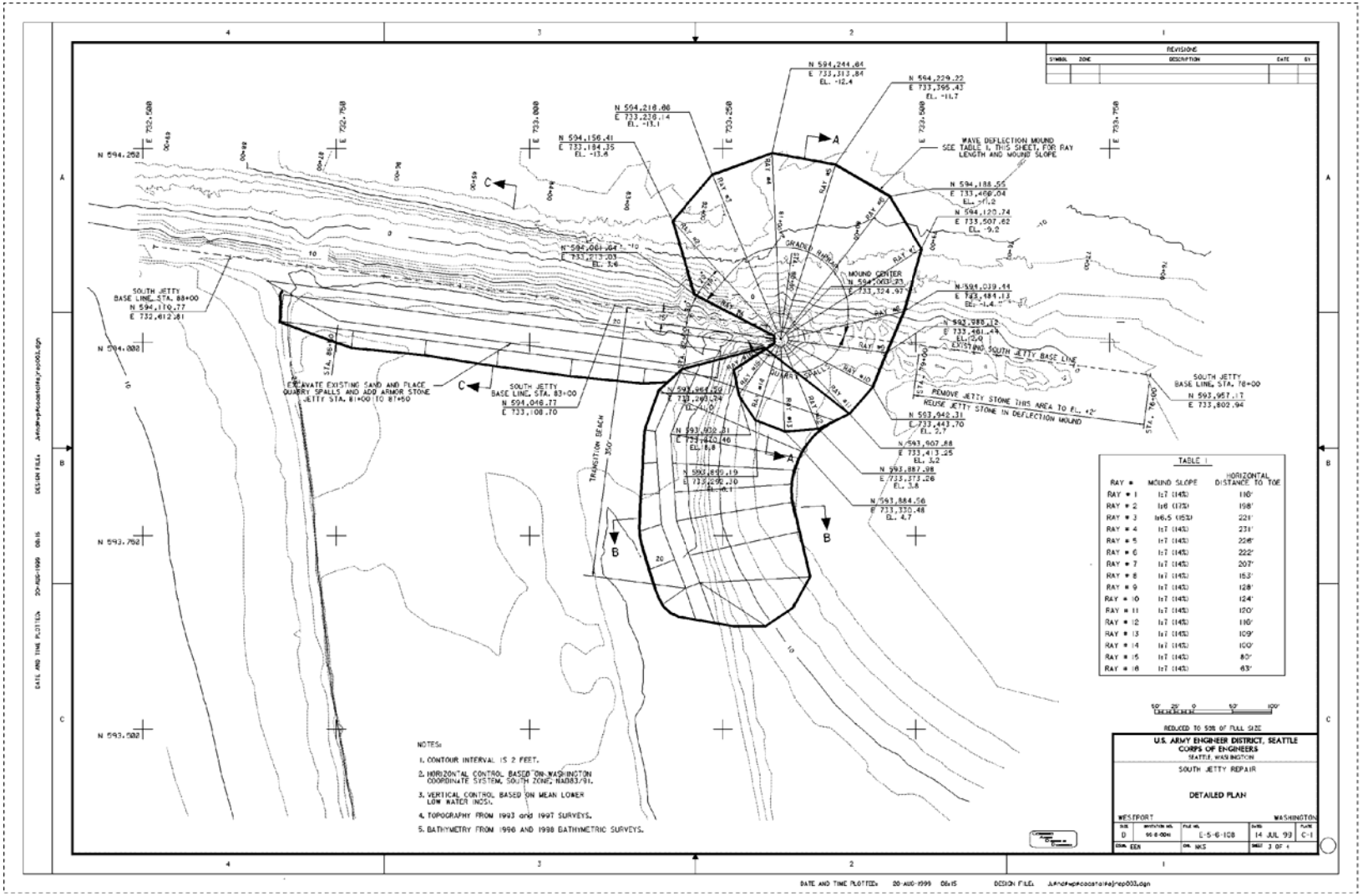

Figure 2. Diffraction mound and initial gravel/cobble beach placement.

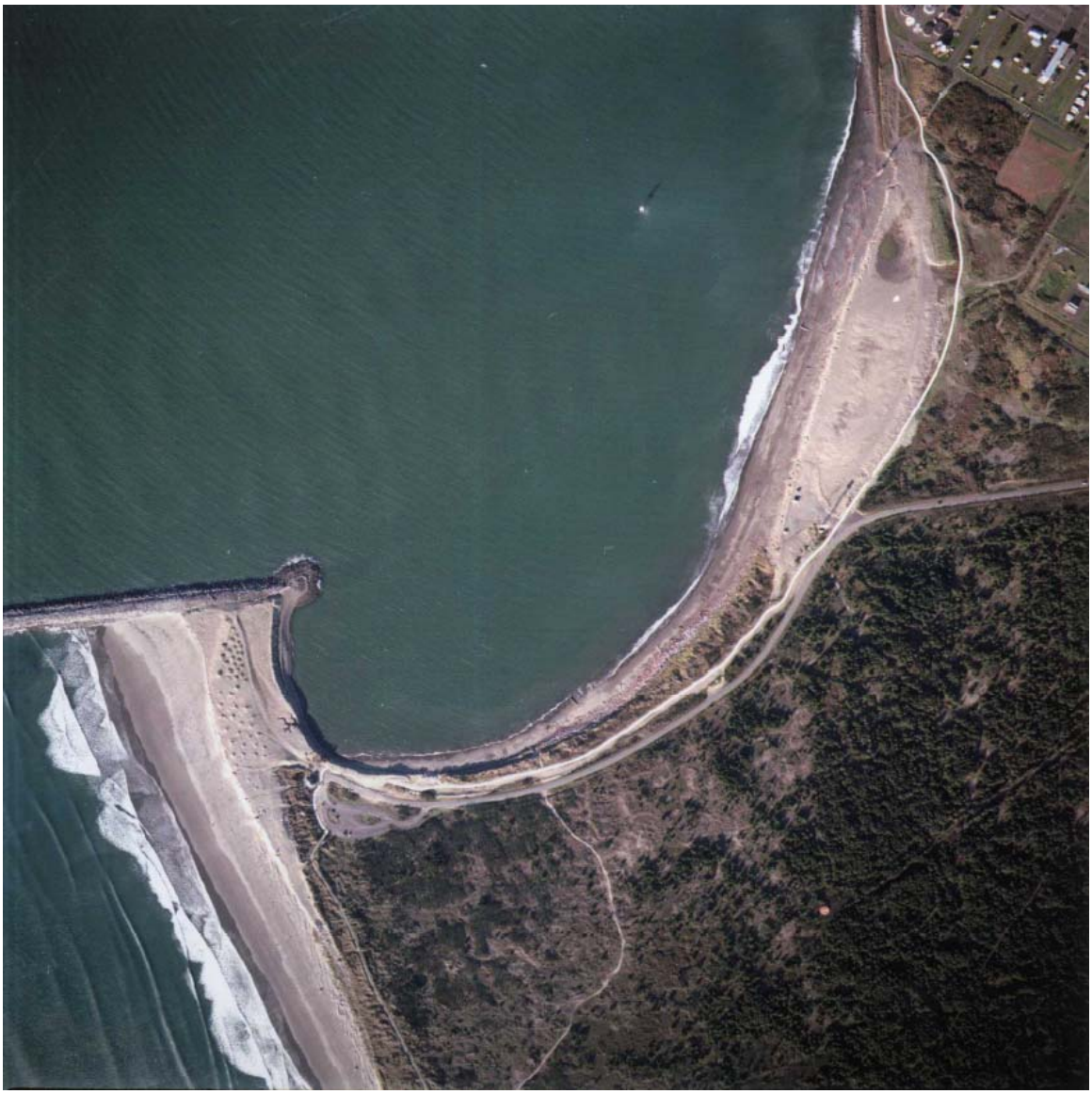

Figure 3. South jetty and shoreline of Half Moon Bay, 31 October 2003.

Grays Harbor Long-Term Management Strategy

The Seattle District initiated the Long-Term Management Strategy (LTMS) in response to persistent loss of sediment from the Grays Harbor project entrance area (including North Beach, South Beach, and Half Moon Bay). It was recognized that recession of South Beach might lead to breaching of the breach fill between the ocean and Half Moon Bay adjacent to the south jetty. The purpose of the LTMS is to assess the threat of breaching at the south jetty, to determine the impact of a breach on the Grays Harbor Navigation Project, and to investigate and recommend the most appropriate strategy for long-term maintenance and protection of the Federal navigation project. The LTMS will document existing condi-

tions, develop and assess engineering alternatives, provide recommendations, and issue a final report. LTMS completion is scheduled for the end of FY06. (Most of the material in this section was summarized from the Seattle District Project Management Plan for the LTMS.)

The initial task of the LTMS is to evaluate the existing condition in the vicinity of the south jetty at Grays Harbor. Specifically, the Seattle District is interested in the time frame for potential breaching of the breach fill between South Beach and Half Moon Bay. Concurrent with the breaching analysis (Wamsley et al. 2005) is documentation of the existing condition in that region of Grays Harbor, and a projection of what the long-term equilibrium planform of Half Moon Bay might be if a breach does not occur and no further remedial action is taken to maintain the present shoreline configuration of Half Moon Bay.

Half Moon Bay Physical Model

A large physical model including the landward terminus of the south jetty at Grays Harbor, the diffraction mound, and all of Half Moon Bay was constructed at the U.S. Army Engineer Research and Development Center (ERDC), Coastal and Hydraulics Laboratory (CHL) in Vicksburg, MS. Funding for model construction and operation was provided to CHL by the Seattle District. The physical model featured fixed-bed bathymetry below the -10-ft mllw contour and a movable-bed above the -10-ft mllw contour. Thus, in the physical model the shoreline and nearshore region of Half Moon Bay were free to respond to wave forcing in a manner similar to what might be expected to occur at Half Moon Bay. The original purpose of the physical model was to support the Seattle District analyses of potential alternatives for stabilizing the Half Moon Bay shoreline. After model construction, the focus was limited by the Seattle District to examining only the response of the existing shoreline to storm conditions.

Physical Model Study Tasks

The movable-bed physical model of Half Moon Bay constructed at CHL was used initially to assist in evaluation of the existing Half Moon Bay shoreline response to storms likely to occur at the project site. The purpose of this study was to establish a baseline condition that can represent the Half Moon Bay shoreline evolution assuming a breach of South Beach does not occur and no further modification of project features are undertaken. This task required that the response of the movable-bed portion of the model be shown to replicate (within the limitations of the physical model-

ing technology) the observed shoreline response that occurred previously. Then, a simulation was performed with the goal of establishing the future quasi-equilibrium shoreline position without further modification. Because of known scaling effects related to sediment transport in small-scale movable-bed models, the equilibrium shoreline established in the physical model will not recede as far as would be expected in the prototype, so it will be necessary to augment the physical model result with an understanding of morphological change based on the concepts of crenulate bay equilibrium.

If the LTMS determines that breaching would cause a threat to the navigation project, the physical model may be used to investigate one or several of the proposed engineering alternatives, as appropriate. In this case, the physical model will allow comparisons of each tested alternative to the baseline condition established previously to gain an understanding of the relative influence of each alternative. This comparison will aid in selection of the most viable alternative that fulfills the LTMS needs when considered along with the economic, environment, and long-term maintenance requirements.

This report focuses on design of the model, model construction, model calibration, and simulation of the "no-project" equilibrium response. If future LTMS action requires additional testing of proposed project modification alternatives, those tests will be documented separately.

Report Organization and Content

The chapters of this report are organized in chronological order from initial design of the model through to interpretation of final results. Chapter 2 overviews the principles of physical modeling, points out the advantages and disadvantages of the technology, and discusses known scale and laboratory effects and how these two effects might influence model results. Chapter 3 covers design of the Half Moon Bay physical model in the context of expected difficulties and limitations of physical facilities available at CHL. Chapter 4 discusses model construction and molding of the movable-bed portion of the physical model. Chapter 5 details the selected key model parameters and operating procedures including instrumentation, measurements, and testing criteria. Chapter 6 presents results from simulations directed at calibrating the movable-bed portion of the model to reproduce known shoreline changes during the 2002-2003 storm season. Results from the existing "no-project" simulation are presented in Chapter 7 along with engineering interpretation of the results in view of the known

difficulties in the modeling technology. Finally, Chapter 8 presents the summary and conclusions from this study.

Units of Measurement

Most dimensional parameters and values cited in this report are given in non-SI units of measurement. Conversion to equivalent SI units can be made using the conversion factors listed on page ix of this report. Parameters related to the hydrodynamic forcing, specifically wave height, storm surge elevation, and water currents, are given in SI units as is customary in the oceanographic literature. Gravel and cobble are given mostly in non-SI units, and sand grain sizes are given in SI units.

Usually, the values of measured model parameters have been scaled to equivalent prototype values so the reader can better understand the model response. However, there are instances where values are reported in model units without specifically stating these are model units. In those cases where prototype or model is not explicitly stated for a parameter, the context will usually reveal whether the value is in model dimensions or equivalent prototype dimensions.

2 Principles of Physical Modeling

This chapter overviews the principles that govern the design and operation of small-scale movable-bed physical models of free-surface flow phenomena. Included is a discussion of the advantages and disadvantages of physical models, along with a description of how the modeling technology can be best applied to Half Moon Bay, Grays Harbor, WA.

Principles of Similitude

The basis of all physical modeling is the idea that the model behaves in a manner similar to the prototype it is intended to emulate. Thus, a properly validated physical model can be used to predict the prototype (real world) under a specified set of conditions. However, there is a possibility that physical model results may not be indicative of prototype behavior due to scale effects or laboratory effects. The role of the physical modeler is to minimize scale effects by understanding and applying proper similitude relationships, and to minimize laboratory effects through careful model operation.

Similarity between the real world (prototype) and a small-scale replica (model) of a coastal project area is achieved when all major factors influencing reactions are in proportion between prototype and model while those factors that are not in proportion throughout the modeled domain are so small as to be insignificant to the process. For coastal short-wave models, three general conditions must be met to achieve model similitude:

a. Geometric similarity exists between two objects or systems if the ratios of all corresponding linear dimensions are equal. This relationship is independent of motion of any kind and involves only similarity in form (Warnock 1950). Geometrically similar models are also known as geometrically undistorted models because the horizontal and vertical length scales are the same. (Departure from geometric similarity is restricted to hydrodynamics of long waves and unidirectional flows.)
b. Kinematic similarity indicates a similarity of motion between particles in model and prototype. Kinematic similarity is achieved when the ratio between the components of all vectorial motions for the prototype and model is the same for all particles at all times (Hudson et al. 1979). In a geometrically similar model, kinematic similarity gives particles paths that are geometrically similar to the prototype.

c. Dynamic similarity between two geometrically and kinematically similar systems requires that the ratios of all vectorial forces in the two systems be the same (Warnock 1950). This means that there must be constant prototype-to-model ratios of all masses and forces acting on the system. The requirement for dynamic similarity arises from Newton's second law that equates the vector sum of the external forces acting on an element to the element's mass reaction to those forces.

Perfect similitude requires that the prototype-to-model ratios of the inertial, gravitational, viscous, surface tension, elastic, and pressure forces be identical. In practice, perfect similitude is impossible at reduced model scale. Fortunately, many coastal problems and flow regimes are adequately modeled by an imperfect similitude where inertia and gravity forces dominate while all other forces are small in comparison.

For convenience, physical modeling similitude requirements are expressed in terms of scale ratios, defined as the ratio of a parameter in the prototype to the value of the same parameter in the model. The scale ratio is represented by the notation:

$$N_X = \frac{X_p}{X_m} = \frac{\text{value of } X \text{ in prototype}}{\text{value of } X \text{ in model}} \tag{1}$$

where N_X is the prototype-to-model scale ratio of the parameter X. For example, the length scale is usually denoted as N_L and the velocity scale is N_V.

Hydraulic similitude

Hydraulic similitude requirements for coastal hydrodynamic short-wave models can be derived (e.g., Hughes 1993) from the continuity and Navier-Stokes equations governing incompressible, free-surface flows. The resulting similitude conditions are listed here. In Equations 2-4 the expressions on the left side give the similitude criteria, which are also given in terms of scale ratios on the right side (Hughes 2003).

1. The model must be geometrically undistorted, i.e., horizontal and vertical length scales are the same.
2. The Froude number, which is the ratio of inertia to gravity forces, must be the same in the model as in the prototype, i.e.,

$$\left(\frac{V}{\sqrt{gL}}\right)_p = \left(\frac{V}{\sqrt{gL}}\right)_m \quad \text{or} \quad \frac{N_V}{\sqrt{N_g N_L}} = 1 \tag{2}$$

3. The Strouhal number, which is the ratio of temporal to convective inertial forces, must be the same in the model as in the prototype, i.e.,

$$\left(\frac{L}{Vt}\right)_p = \left(\frac{L}{Vt}\right)_m \quad \text{or} \quad \frac{N_L}{N_V\, N_t} = 1 \tag{3}$$

4. The Reynolds number, which is the ratio of inertia to viscous forces, must be the same in the model as in the prototype, i.e.,

$$\left(\frac{\rho LV}{\mu}\right)_p = \left(\frac{\rho LV}{\mu}\right)_m \quad \text{or} \quad \frac{N_\rho\, N_L\, N_V}{N_\mu} = 1 \tag{4}$$

where

V = characteristic velocity
G = gravitational acceleration
L = characteristic length
t = time
ρ = fluid density

and the subscripts p and m represent prototype and model, respectively.

The geometric similarity criterion (condition 1) coupled with the Froude Criterion (condition 2) assure that all terms in the governing flow equations are in similitude with the exception of the viscous terms. Froude similarity includes the turbulent Reynolds shear stress terms; thus, macro features of turbulent dissipative processes are also in similitude.

Viscous effects can only be modeled if the Reynolds Criterion (condition 3) is met along with the Froude criterion in a geometrically similar model. In general this is practical only at prototype scale (full-size scale). Consequently, coastal short-wave models can be either nondissipative where viscous and capillary effects are negligible, such as waves prior to breaking; or the model can have highly turbulent flow dissipation over a relatively short distance, such as during wave breaking on a structure or a beach (Le Méhauté 1976). In reality, there will always be a small amount of wave

attenuation due to viscous frictional losses and surface tension effects, but these scale effects can be minimized to the point of insignificance.

The hydrodynamic time scale for Froude-scaled hydrodynamic models is obtained by solving Equation 2 for N_V and substituting into Equation 3 to give:

$$N_t = \sqrt{\frac{N_L}{N_g}} \tag{5}$$

Because the gravitational force will be the same in the model as in the prototype, the ratio N_g will be unity, and it is usually not included in the scaling criteria. Other scale ratios derived from Froude and Reynolds scaling are given in most similitude texts (e.g., Hughes 1993).

Sediment transport similitude

Noncohesive sediment (sand) in the nearshore marine environment will remain stationary so long as the wave- and current-induced bottom shear stresses are less than the critical shear stress needed to mobilize the sand grains. Once the critical shear stress for a particular sand size and sand density is exceeded, incipient motion of sediment begins. In some cases the fluid flow shear stresses are low, and the sand moves primarily as bed load. In other situations, the flow conditions might be energetic with high bottom shear stresses and significant turbulence causing the sand grains to be mobilized upward into the water column where they are transported as suspended load. As might be expected, both types of sediment transport occur in most coastal regions. Where waves and currents are energetic, such as during a storm, suspended load transport is likely to be more dominant than bed-load transport. Conversely, in sheltered areas, the suspended grains will settle out of the water column, and any continued sediment transport will be dominated by bed load.

The requirements for similitude of movable-bed physical models are reasonably well understood, but more often than not completely fulfilling these similitude requirements in a small-scale model is difficult to achieve. A totally correct movable-bed model would be able to maintain similitude of both bed load and suspended load, as well as being able to scale the incipient motion of the sediment particles. Unfortunately, there will probably never be a completely correct sediment transport physical model at any scale smaller than prototype. Thus, it should come as no surprise

that “movable-bed scale model investigations of coastal erosion and sediment transport are probably the most difficult hydraulic models to conduct” (Hudson et al. 1979).

Similitude of sand transport by bed load

Kamphuis (1975) summarized the requirements for scaling bed load movable-bed physical models, and he listed four different model classifications based on which of the five necessary criteria were met by the model. The “Best Model” met three of the five criteria (similitude of grain-size, grain density, and densimetric Froude number). The key scaling requirement for the Best Model is that the model sand have the same density as the prototype sand, and the sand grain size scales according to the model length scale, i.e.,

$$N_d = \frac{d_p}{d_m} = N_L \tag{6}$$

where d_p and d_m are the prototype and model sand grain sizes, respectively. There remains a scale effect related to nonsimilitude of Reynolds number, but this is not a severe restriction because it only influences viscous effects related to sediment transport, and these occur only during low flow velocities or during flow reversal in the model. For the most part, the sediment will be transported in a fully-developed turbulent boundary layer which will be correctly reproduced in a Froude-scaled model. Hughes (1993) also noted that sediment fall speed is not in similitude in the Best Model unless both the model and prototype grain sizes fall in the range 0.13 mm < d < 1.0 mm. If this criterion is not met, then sand grains thrown into suspension in the model will take relatively longer to fall to the bottom than in the prototype. Thus, the model sand grains may be transported farther by suspension than they should.

Two of the bed-load modeling criteria listed by Kamphuis (1975) involved using model lightweight model sediments to simulate the motion of sand in the prototype. These models were referred to as the “Lightweight Model” and the “Densimetric Froude Model.” These approaches have proven successful for specific situation, but they are not practical for the movable-bed model of Half Moon Bay because of the large quantity of material needed. Thus, these two similitude models will not be discussed further.

Whereas the Best Model is preferred, it is not often obtained due to the requirement of scaling the sediment the same as the model length scale. For most situations this would result in model sediment sizes that fall into the range of cohesive sediment, and this introduces a new set of forces not present in the prototype noncohesive sediment. Consequently, the only viable alternative is to use a model sand that has the same density as the prototype but still has a grain-size large enough to remain in the noncohesive sand range (grain-size larger than about 0.1 mm). This results in what Kamphuis called the "Sand Model," and it is the most common of movable-bed models.

The major Sand Model scale effects arise from the fact that the model sand grains are relatively larger than the prototype grains. In a Sand Model, sediment incipient motion is slower to occur (requires relatively higher flow velocity); sediment transport quantities may not be correct, particularly at lower flow velocities; and sediment will stop moving in the model before it should. Despite these shortcomings, the Sand Model will indicate regions of erosion and deposition, and it will demonstrate the relative influence of modifications made to the physical setting. Movable-bed model results can be used in a quantitative sense provided the model has first been calibrated by reproducing successfully erosion and deposition patterns observed in the prototype being modeled.

Similitude of sand transport by suspension

Suspension-dominated transport is quite different from bed-load transport, and not surprisingly, movable-bed modeling of suspended sediment transport requires consideration of different physical parameters of the process. Inevitably, this leads to scaling criteria for suspended load that are different from bed-load transport criteria, which means in the model one of the transport modes (depending on which one is not properly scaled) will have a scale effect associated with it.

Hughes (1993) reviewed various proposed sets of similitude relationships for movable-bed modeling of suspension-dominated regimes, and he promoted the scaling criteria originally proposed by Dalrymple and Thompson (1976) that is based on assuring similarity of the sediment grain "fall speed parameter." The two criteria of the "Fall Speed" model are that the hydrodynamics are scaled according to the geometrically undistorted Froude similitude relationship, and that the model have the same sediment fall speed parameter as the prototype.

Dean (1973) introduced the dimensionless fall speed parameter as:

$$P_{\omega} = \frac{H}{\omega T} \tag{7}$$

where H is the wave height, T is the wave period, and ω is the sediment fall speed. Equating the fall speed parameter in the prototype to the fall speed parameter in the model, i.e.,

$$\frac{H_p}{\omega_p T_p} = \frac{H_m}{\omega_m T_m} \tag{8}$$

and rearranging into prototype-to-model ratios of each variable yields:

$$\frac{H_p}{H_m} = \frac{T_p}{T_m}\frac{\omega_p}{\omega_m} \text{ or in terms of scale-ratio notation } N_H = N_T N_{\omega} \tag{9}$$

Recognizing the N_H is the same as the length scale N_L, and substituting the Froude time scale from Equation 5 gives the necessary scale ratio for sediment fall speed, i.e.,

$$N_{\omega} = \sqrt{N_g N_L} \tag{10}$$

Fulfilling the scaling requirement given by Equation 10 has been shown to give good model reproduction of sediment transport processes driven by turbulent and energetic wave conditions such as experienced in the surf zone during storms (Hughes and Fowler 1990). Thus, it is most appropriate for modeling beach erosion by storm waves or scour by turbulent wave action. The fall speed scaling relationship allows the model sand grain-size to be larger than the size dictated by the Best Model criteria for bed-load transport. Therefore, the surf zone portions of the movable-bed model are expected to provide reasonable response, but those portions of the model where conditions are less energetic and sediment transport is primarily by bed load will not exhibit the correct erosion and deposition quantities. Nevertheless, the general patterns of erosion and deposition should resemble those of the prototype even though the quantities are suspect. The model could in the future be used to compare project engineering alternatives to assess relative performance of each alternative. The same limitations as previously described would apply in the comparisons. In other words, absolute erosion and deposition quantities would not be cor-

rect, but the relative effectiveness of the compared alternatives would be qualitatively correct.

Similitude of gravel and cobble transport

A portion of the shoreline in Half Moon Bay extending from the diffraction mound was protected by a placed layer composed of gravel and cobble material. This layer extends generally from between the elevations +4 ft to +25 ft mllw. The gravel/cobble protection ranges in size between 2 in. to 12 in. in diameter. Sediment in this size range moves as bed load in all but the most extreme wave or flow conditions. Therefore, the same similitude requirements given by the Best Model for bed-load sediment transport apply for gravel and cobble transport. The model material representing the gravel and cobble should have the same density, and the prototype grain-size distribution should be scaled according to the sediment diameter scale given in Equation 6. Reproducing the grain-size distribution instead of just the mean gravel/cobble diameter becomes more important as the size range of the prototype material increases.

Physical Model Advantages

Small-scale physical models are essentially analog computers of all the physical processes being simulated with the model. Nonlinearities and complex physical interactions between fluid and solid boundaries are faithfully reproduced without compromise provided the model has been scaled correctly and laboratory effects are controlled. For this reason, small-scale physical models offers an opportunity to examine those processes that are beyond theoretical understanding or are too complicated to represent adequately with simplified analytical or numerical modeling tools. The following is a list of advantages associated with physical models (Hughes 1993).

a. Physical models incorporate and integrate the fully nonlinear governing equations of the modeled process without simplifying assumptions.
b. Complex boundaries and bathymetry can be included without difficulty.
c. The small size of the model permits easy data collection.
d. Model forcing conditions can be easily simulated and controlled.
e. Similitude requirements for many problems are well understood and easily implemented.
f. Visual feedback from a physical model often reveals aspects of the physical process that had not been considered previously. Observations also help us to understand the differences that arise from changing the forcing conditions, and they often stimulate new ideas or alternative solutions.

g. Engineering solutions can be optimized in a physical model to achieve project functionality at minimum expense.
h. Often physical models are a cost-effective option relative to alternate study methods.

The benefits arising from physical model studies depend largely on the careful operation of the model coupled with a full understanding of the potential problems and shortcomings that may exist because of scale or laboratory effects.

Physical Model Disadvantages

The major disadvantages associated with small-scale physical models relate to either scale effects or laboratory effects.

Physical model scale effects

Scale effects in coastal hydrodynamic models result primarily from the Froude scaling assumption that gravity is the dominant physical force balancing the inertial forces. The other physical forces of viscosity, elasticity, and surface tension are incorrectly scaled with the belief that these forces contribute little to the physical processes. Scale effects in physical models are analogous to decreased accuracy that occurs in numerical models when complex physical processes are represented by simplified mathematical formulations (Kamphuis 1991).

In movable-bed models the primary scale effect occurs because most often it is not possible to scale the model sediment size according to the model length scale. Other scale effects might occur for flow through rubble-mound structures, or some aspects of water percolation at the shoreface. Sand ripples that form in movable-bed models are not in similitude, and they represent a full-scale phenomenon.

Physical Model Laboratory Effects

Laboratory effects in coastal physical models are primarily related to the following:

a. Physical constraints on flow in the model are caused by the need of representing a portion of the prototype in a finite amount of space. Model boundaries may exist where there is no boundary in the prototype. Waves reflect off model boundaries and introduce reflected wave trains back into

the simulated wave field. This problem is partially solved using energy dissipating beaches composed of gentle slopes and rubberized horsehair mats that can minimize reflection to less than 5 percent.

b. Mechanical means of wave and current generation may introduce unintentional nonlinear effects. The most common example is incorrect reproduction of bound long waves that sometimes cause problems for harbor basins. The model engineer must attempt to make the mechanical waves resemble reasonably well the waves observed in nature.

c. Prototype forcing conditions are simplified and only a subset of all possible conditions can be selected for testing. A common laboratory effect in wave basins is when long-crested unidirectional waves are generated to approximate directional waves that occur in nature. This compromise is not considered serious if the testing covers multiple approach angles, but the engineer must assess the approximation to determine whether it is reasonable. Another example is simulating a storm using a constant water level as opposed to a time-varying surge hydrograph.

Laboratory effects in physical models are analogous to problems in numerical models caused by numerical approximation to the equations, roundoff and truncation errors, and computer speed, memory, and availability (Kamphuis 1991).

Other Physical Model Disadvantages

Cost of physical model construction and operation is an important factor to consider. Construction costs increases directly with the model area, so the reduction in potential scale effects that arises from larger models will come at higher costs. Operation of a physical model requires skilled engineers and technicians, and significant time and effort is spent minimizing laboratory effects and assuring quality measurements. Also, time scales in physical models are determined by the similitude relationships so some time-dependent simulations make take a long time to complete (when compared to numerical modeling).

Even though data acquisition in a physical model is much easier than field data collection, there are inherent limitations. The number of measurement locations in the model is limited by available instrumentation and data channels. Therefore, careful consideration must be given about what to measure and where to place the instruments.

Physical Model Appropriateness

In many cases a coastal problem can be examined by several different methods including numerical models, physical models, analytical techniques, statistical analyses, and desktop studies. Selecting which techniques are most suited to a particular problem requires the following: (a) knowledge of the primary forcing and responses that shape the coastal processes in the problem area, and (b) an understanding of how well the forcing and response are replicated by the alternative technologies. Often multiple technologies are employed with each providing part of the answer.

Physical models are appropriate where the hydrodynamic physical processes are complex (wave nonlinearities, wave/current interactions, complex bathymetry, numerous boundaries), and where the response to the hydrodynamics is not well understood or quantified. In addition, the similitude relationships for the dominant processes must be known, and the potential scale and laboratory effects are thought to be surmountable.

Beach and nearshore erosion qualifies as a complicated response to the hydrodynamic forcing, but whether or not a physical model can successfully replicate the response will depend on compensating for the sediment scale effect and forcing the model with correct hydrodynamics. More confidence is given to movable-bed models that have been calibrated. Model calibration involves reproducing in the model a known beach or nearshore evolution observed in the past. Sometimes it is necessary to manipulate the forcing to overcome the sediment scaling effect. Once model calibration has been achieved, project response to future modifications or to changes in the forcing can be predicted with more confidence. Prediction of absolute changes at a project site requires a good calibration.

There may be situations where data are not available for calibrating a movable-bed model; and even if data are available, sediment scale effects may render the calibration unsuccessful. In these cases, the movable-bed physical model is less useful for prediction of absolute changes in the prototype, but the model is still appropriate and useful for examining relative changes resulting from different project alternatives. The main caveat is that the model is known to be eroding and depositing sediment in the proper locations, even though the quantities are not quite correct because the relatively larger sand grains in the model stop moving before they would in the prototype. For example, comparisons can be made between project engineering alternatives to see which alternative does a better job

of shore protection, or quelling downdrift beach erosion, or preventing channel shoaling. Absolute quantities are not obtained, but effective engineering solutions can be identified and optimized in an uncalibrated movable-bed physical model.

3 Physical Model Design

This chapter describes the design of the Half Moon Bay physical model. Included is a discussion of the dominant physical processes governing shoreline evolution in Half Moon Bay, the rationale for scale selection, and a summary of potential scale effects and how they might influence model results.

Dominant Physical Processes in Half Moon Bay

Field observations and site measurements in Half Moon Bay indicate that waves are the primary forcing for moving sediment on the beach and in the nearshore zone. Large storm waves, usually concurrent with elevated water levels, propagate up the wide gap between the two parallel rubble-mound jetties and diffract into Half Moon Bay as they pass the eastern end of the south jetty. Diffraction of the waves into the sheltered region south of the diffraction mound helps to reduce wave energy by spreading energy along the wave crest. But during severe storms there is still an abundance of energy in the waves as they break against the shoreline. Diffraction is a leading wave transformation causing alongshore variation in breaking wave height and the resulting planform configuration of the bay.

Recession of the shoreline during storms is caused by the violent and turbulent flows in the breaking waves suspending sand into the water column where it is then moved to a different location by the water current. Away from the wave breaking process there is less flow turbulence to suspend the sand grains, and relatively more of the sand transport is by bed load. Gravel- and cobble-sized material on the beach at Half Moon Bay is also moved by the energetic wave action, but because of the increased size, it can be assumed that most gravel/cobble transport occurs as bed load. Even if large stones are thrown into suspension, they quickly settle on the bed before moving far.

The theory of crenulate-shaped bays (Silvester 1991) postulates that planform shape equilibrium occurs when the diffracted wave front breaks normal to the shoreline at all locations, and there is no alongshore current generated. However, crenulate-shaped bays will retain their planform shape provided there is no gradient in alongshore sediment transport. This does not mean that sediment transport has ceased; it means that the gradient of alongshore sediment transport is not sufficient to change the gen-

eral shoreline planform shape. Distribution of sand on shore-normal profiles seaward of the shoreline will vary with wave conditions and water level. More severe storm conditions could cause the shoreline to recede while still retaining the approximate crenulate-bay planform shape.

Previous studies indicated that wave orbital motion and ebb-tidal current are responsible for removing sediment from the seaward portion of Half Moon Bay, but tidal current does not appear to contribute to the nearshore current that moves the sand within the bay, whether by suspension or bed load. Measurements and numerical model simulations (Osborne et al. 2003) have indicated tidal current, while strong farther out in the Grays Harbor entrance channel, is relatively weak throughout the tidal cycle in Half Moon Bay. Sediment losses from Half Moon Bay generally seem to occur as wave-induced current moves sand along the shoreline and in the nearshore toward Point Chehalis. Once the sediment reaches Point Chehalis, the tidal current begin to dominate the sediment transport process. Wind-generated current may influence physical processes within Half Moon Bay, particularly during severe storms with strong onshore winds. However, quantifying wind-driven current is difficult, so there is no good estimate of what this current might be and how it might influence the Half Moon Bay evolution.

In summary, the main physical processes that need to be recreated in the movable-bed physical model are the following:

a. Elevated water levels.
b. Storm waves.
c. Wave diffraction, refraction, and shoaling processes.
d. Wave-generated current.
e. Sand transport by suspension.
f. Sand transport by bed load.
g. Gravel transport by bed load.

Absent from the physical model are tidal current (thought to be small), wind-driven current (unknown influence), and other physical processes that may have some minor sway on the shoreline equilibrium, but are thought to be orders of magnitude less influential than these dominant processes.

Model Scale Selection

Selecting physical model scale ratios requires consideration and assessment of multiple requirements and limitations. The model must include as much of the project site area as needed to simulate the physical forcing, but this area is constrained by the size of the available space in the model facility. Those physical processes identified as being the dominant forcing in the project area must be scaled according to established similitude criteria at a scale as large as can be accommodated in the model facility in order to minimize potential scale effects. Existing wavemakers must be able to reproduce the maximum waves to be used in testing at the selected scale. If the wavemaker is insufficient in this regard, either new equipment must be sought, or the model scale must be reduced to meet the requirement. Known scale effects, laboratory effects, and other limitations must be assessed to determine possible impacts on model results. The following sections detail the scale section processes for the Half Moon Bay physical model.

Model purpose

The physical model was constructed to support the LTMS of the Seattle District. The primary purpose of the physical model originally was to evaluate engineering alternatives that might be considered as long-term solutions to prevent breaching of the breach fill separating South Beach from Half Moon Bay, and to investigate modifications that would alleviate long-term shoreline erosion in Half Moon Bay. Model design needed to support a wide variety of possible engineering alternatives including such possibilities as beach nourishment, gravel protection, rubble-mound structures, and dredged sand placement in the nearshore. The first aspect of model design was to consider how much of the region adjacent to Half Moon Bay needed to be included in the model in order to simulate the wave forcing and also cover the range of potential alternatives.

Modeled region

Once the determination was made that tidal current does not contribute substantially to shoreline evolution in Half Moon Bay, the necessary area to be modeled consisted only of the bay itself, and enough of the adjacent Grays Harbor entrance channel to simulate incoming storm waves from the appropriate approach angles. The red box shown in Figure 4 outlines the approximate region of Grays Harbor that needed to be reproduced by

the physical model. This area measures about 7,000 × 7,000 ft, or about 1.3 miles square.

Figure 4. Region of Grays Harbor entrance modeled in physical model.

The largest shelter space at CHL that was available during the time of this study measured about 150 × 140 ft. Therefore, the length scale giving the largest model that could accommodate the selected region shown in Figure 4 was:

$$N_L = \frac{L_p}{L_m} = \frac{7{,}000\ \text{ft}}{150\ \text{ft}} = 46.7 \tag{11}$$

From experience it was known that model construction would intrude slightly into the modeled area, so the length scale was increased (model size decreased) to $N_L = 50$. Also, this scale ratio makes it easier to perform mental scale conversions with less chance of error. The next step was to determine the corresponding similitude criteria for waves and sediment transport and to evaluate the capability of available wavemakers to assure the desired conditions can be generated in the physical model.

Hydrodynamic similitude criteria

Small-scale model simulation of all free-surface flow phenomena, such as waves, must adhere to the Froude scaling, which means simply that the model must be geometrically undistorted (horizontal and vertical length scales are the same), and the model velocity scale and time scale must con-

form to the scaling relationships given by Equations 2 and 5, respectively. For a model length scale of N_L = 50, the required velocity scale is given by:

$$N_V = \sqrt{N_g N_L} = \sqrt{(1)(50)} = 7.1 \tag{12}$$

and the hydrodynamic time scale (wave period scale) becomes

$$N_T = \sqrt{\frac{N_L}{N_g}} = \sqrt{\frac{(50)}{(1)}} = 7.1 \tag{13}$$

where the gravitational scale ratio, N_g is unity.

Wave generation capability

Estimates of key testing parameters were identified from wave height and water level measurements at Grays Harbor and from information provided by the Seattle District. These parameters are shown in Table 1 with the model equivalents determined using the length scale ratio of N_L = 50. Maximum water level (storm surge), wave height, and wave period were scaled from prototype values to give corresponding model values. The total water depth was a limitation of the model facility, so that value was scaled up to prototype to assure it would be sufficient. Finally, the depth at the wavemaker is the total water depth subtracted from the elevation of the maximum water level.

Table 1. Prototype and model parameter values.

Parameter	Prototype Value	Model Value
Maximum water level	+4 m (+13 ft) mllw	+8 cm (+3.2 in.) mllw
Depth at wavemaker	-15.2 m (-50 ft) mllw	-31 cm (-1.0 ft) mllw
Total water depth	19.2 m (63 ft)	38 cm (1.26 ft)
Maximum wave height	6 m (19.7 ft)	12 cm (4.7 in.)
Maximum wave period	16 sec	2.26 sec

An existing plunger-type wavemaker with total length of 80 ft was able to generate regular waves in the maximum water depth that met the maximum wave conditions. This wavemaker has a prismatic-shaped wave board that generates waves with an up-and-down vertical motion. The wave board can produce regular or irregular waves. Because of the irregular nature of random seas, irregular waves more closely replicate nature and are preferred in the physical model. However, it requires more capa-

bility to generate irregular significant wave heights (H_{mo}) than it does to generate regular waves of the same height.

Experience with the available wavemaker indicated that it probably could not produce the specified maximum wave height condition using irregular waves. However, the prototype value came from measurements in deeper water, and wave transformation studies had shown that irregular wave heights within the modeled region closer to Half Moon Bay are substantially less. For this reduced value of maximum wave height, engineers felt the target wave condition could be achieved. Therefore, the wavemaker was considered adequate and appropriate for generating waves at the chosen length scale.

Sand transport similitude criteria

The similitude requirement for bedload-dominated sediment transport is that the model sediment grain size must be reduced from prototype according to the model length scale as expressed by Equation 6. Thus, the model grain-size requirement would be:

$$d_m = \frac{d_p}{N_L} = \frac{(0.5\ \text{mm})}{(50)} = 0.01\ \text{mm} \tag{14}$$

The derived size for model sediment is well into the range of cohesive sediment, and thus it cannot be considered viable for modeling sediment to simulate bed-load transport of noncohesive sand. The smallest grain size in quartz sand that is readily available in large quantities is d_m = 0.125 mm. The only alternatives were: (a) to increase the model scale to satisfy the bed-load transport criterion using the smallest noncohesive grain size available, or (b) to keep the model scale as it was, and accept the sediment scale effect. Using the 0.125-mm sand in the model would require a model length scale of (0.5 mm)/(0.125 mm) = 4. A 1:4 model of Half Moon Bay is neither practical nor economically feasible. Therefore, the physical model is constrained to using model sand with d_m = 0.125 mm, and model results must be evaluated with the knowledge of the bed-load transport scale effect.

The similitude requirement for sediment transport in suspension is given by Equation 10. The criterion states that the prototype-to-model ratio of sediment fall speed must be the same as the model velocity scale as determined by the Froude criterion. Estimation of sediment particle fall speed

is not precise, and several methods are commonly used. For this model study the method given by Hallemeier (1981) was used to estimate the sand fall speeds for the prototype and model grain sizes. Fall speed is a function of both water temperature and density. For the prototype, salt water at 10°C was assumed, giving an estimated fall speed of ω_p = 5.9 cm/sec. For the model, the fresh water temperature was assumed to be 20°C, yielding a fall speed ω_m = 1.4 cm/sec. The resulting prototype-to-model ratio of sediment fall speed was:

$$N_\omega = \frac{(5.9\ \text{cm/s})}{(1.4\ \text{cm/s})} = 4.2 \tag{15}$$

which is smaller than the required fall speed ratio N_ω = 7.1. This means there will be also a scale effect associated with regions of the model where suspended load transport is thought to be dominant. However, this scaling effect is not too severe, as discussed in the following paragraphs, particularly in view of variations in fall speed estimates that arise using the available method.

Gravel/cobble transport similitude criterion

The mixture of gravel and cobble placed as protection on the Half Moon Bay shoreline just landward of South Beach ranges in size from about 2 in. up to 12 in. (50 mm to 300 mm). Figure 5 shows a section of the gravel transition in June 2003.

Because the gravel material moves primarily as bed load, the gravel and cobble size distribution should be scaled the same as the model length scale N_L. This requirement gave the following sizes for the lower and upper ends of the grain-size distribution in the model.

$$d_m(\text{low}) = \frac{d_p(\text{low})}{N_L} = \frac{(50\ \text{mm})}{(50)} = 1\ \text{mm} \tag{16}$$

$$d_m(\text{high}) = \frac{d_p(\text{high})}{N_L} = \frac{(300\ \text{mm})}{(50)} = 6\ \text{mm} \tag{17}$$

Field sampling of the gravel/cobble material on the Half Moon Bay beach provided a grain-size distribution that was scaled to model size as shown in Figure 6 by the black dashed line. The prototype distribution was well

simulated by a mixture of three different sediment sizes in the model as shown by the solid red line in Figure 6.

Figure 5. View of transition gravel protection from diffraction mound.

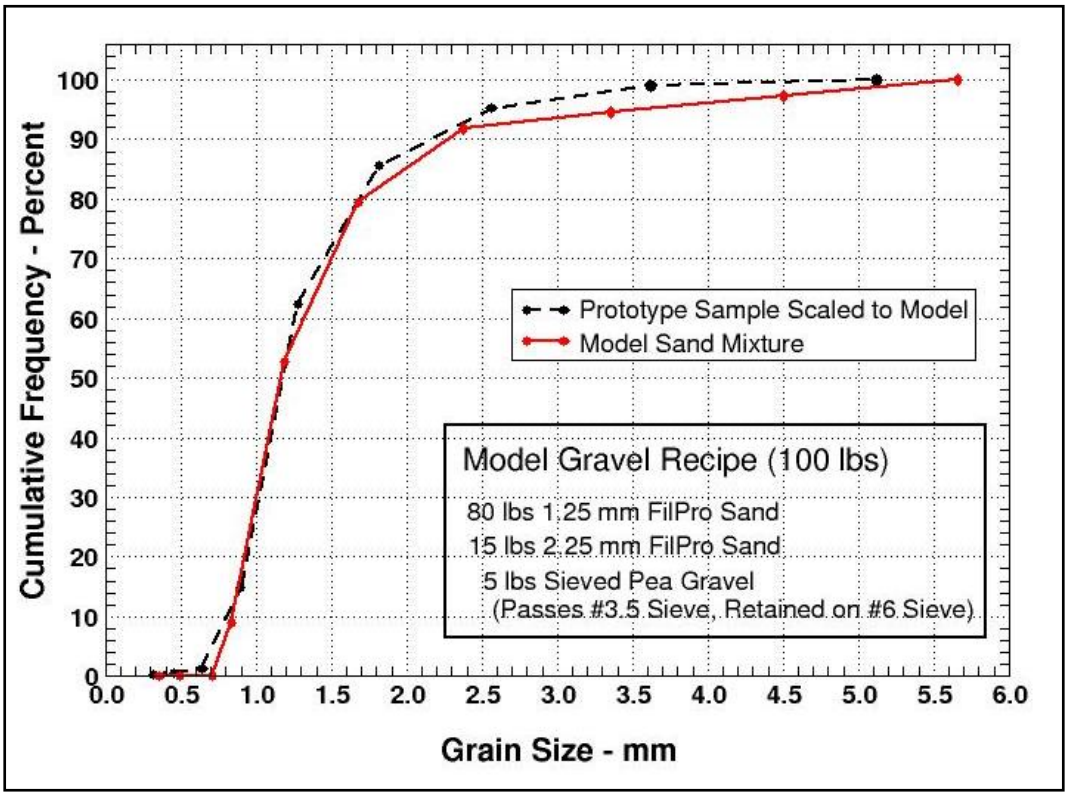

Figure 6. Scaling of prototype gravel/cobble distribution in physical model.

Table 2 summarizes the prototype and model parameters related to the movable-bed portion of the physical model.

Table 2. Prototype and model sand, gravel, and cobble parameters.

Parameter	Prototype Value	Model Value
Beach sand	0.50 mm	0.125 mm
Sand fall speed	5.9 cm/sec	1.4 cm/sec
Gravel – smallest size	50 mm	1 mm
Median gravel/cobble size	70 mm	1.4 mm
Cobble – largest size	300 mm	6 mm

Summary of model scaling

The important model scale ratios (value in the prototype divided by the equivalent value in the model) are listed in Table 3. The fundamental scaling parameter is the length scale, N_L = 50, which can be interpreted as 1 ft in the model equals 50 ft in the real world. Two columns are shown in the table for scale ratio. The Target Scale Ratio is the scale ratio dictated by the similitude criteria. The Actual Scale Ratio is the scale ratio implemented in the physical model. As seen in the table, the sand size scale and the sediment fall speed scale do not meet the strict similitude criteria. However, this does not necessarily render the physical model invalid. It does mean that scale effects must be evaluated and model results must be explained in terms of the scaling shortcomings.

Table 3. Model scale ratios and prototype equivalence.

Scale	Target Scale Ratio	Actual Scale Ratio	Model Equivalence
Length scale	N_X = 50	N_X = 50	1 ft = 50 ft
Time scale	N_T = 7.1	N_T = 7.1	1 s = 7.1 sec
Velocity scale	N_V = 7.1	N_V = 7.1	1 ft/s = 7.1 ft/sec
Sand size scale	N_d = 50	**N_d = 4**	0.125 mm = 0.5 mm
Gravel size scale	N_G = 50	N_G = 50	1 mm = 50 mm
Sand fall speed scale	N_ω = 7.1	**N_ω = 4.2**	1 cm/s = 4.2 cm/sec

Physical Model Layout

The layout of the modeled region of Half Moon Bay in the selected model shelter is shown in Figure 7 oriented with north to the top of the figure. The model basin measured 150 ft in the east-west direction and 140 ft in the north-south direction. The landward portion of the south jetty is seen

on the lower left portion of Figure 7 with Half Moon Bay taking up the lower right side. Approximately 3,050 ft of the south jetty and 300 ft of the south jetty remnant structure were reproduced in the model. The wave machine was located to the left side in the figure, and it could be positioned at different angles to simulate waves propagating into Grays Harbor.

All bathymetry lower than -10 ft mllw (mean lower low water) was reproduced in the model with a fixed bed constructed of concrete. Detailed digital bathymetric data collected by the Seattle District in 2003 were scaled to model dimensions using a prototype-to-model length scale of N_L = 50 and molded in the model from the -10 ft mllw depth seaward to a depth of -40 ft mllw. Seaward of the -40 ft contour the bed was molded at a 1:10 (vertical-to-horizontal) slope to the basin floor located at -50 ft mllw. (Note that elevations are given in prototype dimensions.) The location of the transition between the -40 ft and -50 ft contours can be seen in Figure 7. The remainder of the basin floor to the north and west of the transition was flat.

The shoreline and dune region extending from -10 ft to +25 ft (+30 ft in places) mllw was reproduced using a fine, noncohesive quartz sand having median grain-size diameter d_m = 0.125 mm. This portion of the model (movable-bed) responded to waves acting at elevated water levels. The extent of the model sand portion is shown by the “J-shaped” outline in the southeast corner of the layout of Figure 7. The movable-bed was sculpted based on 10 profiles lines measured in Half Moon Bay in June 2002. The profile lines are shown in Figure 8, and they were fairly evenly spaced along the bay shoreline. Templates were constructed for each profile line, and between adjacent profiles an additional template was cut based on interpolation between profiles. Figure 9 illustrates a typical profile cross section of the movable-bed bathymetry. Approximately 45 tons of sand were used in the Half Moon Bay model, and a mixture of sand and two sizes of gravel was used to represent the gravel beach transition, extending from the diffraction mound to just past Profile Line 3 (Figure 8).

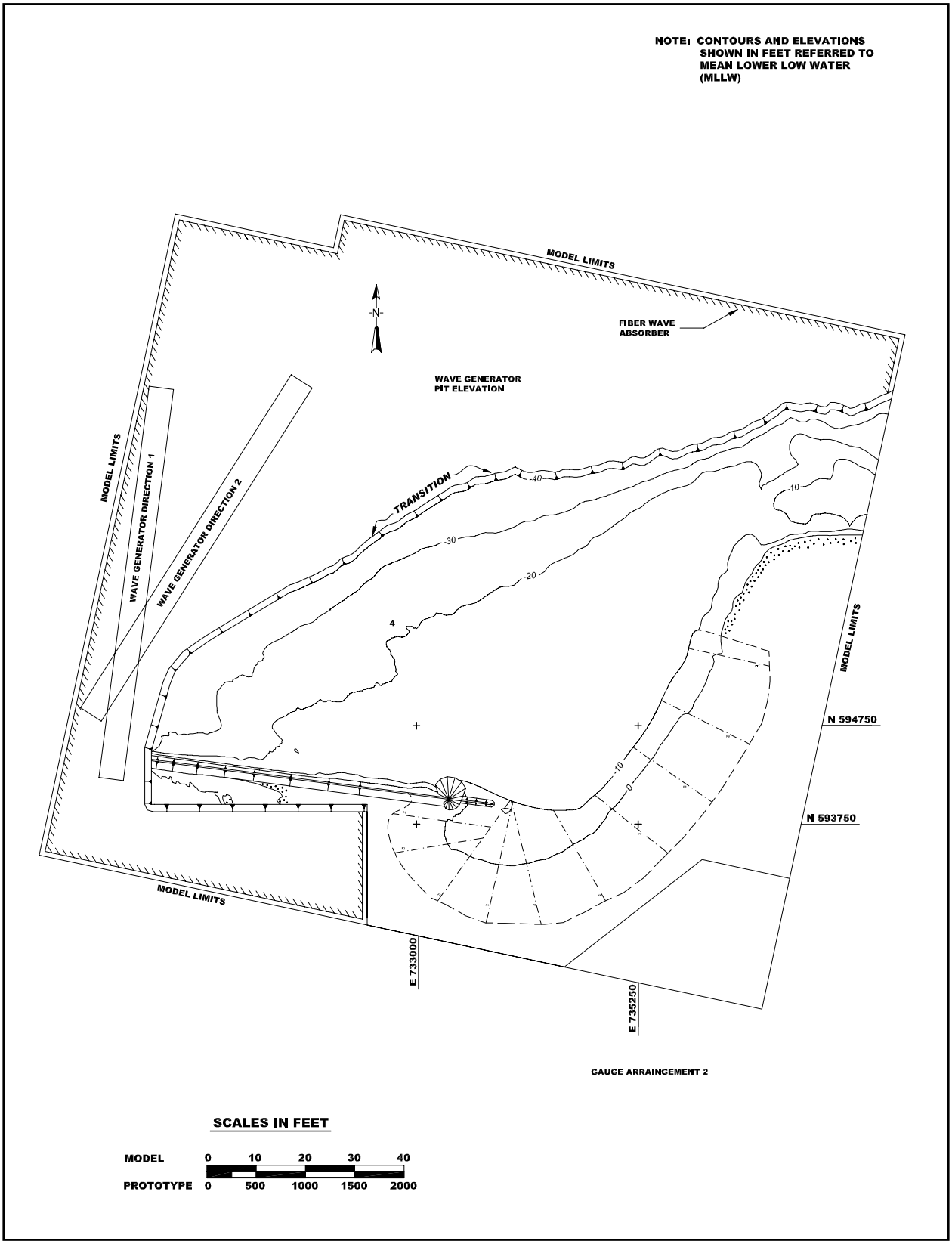

Figure 7. Basin layout for Half Moon Bay physical model.

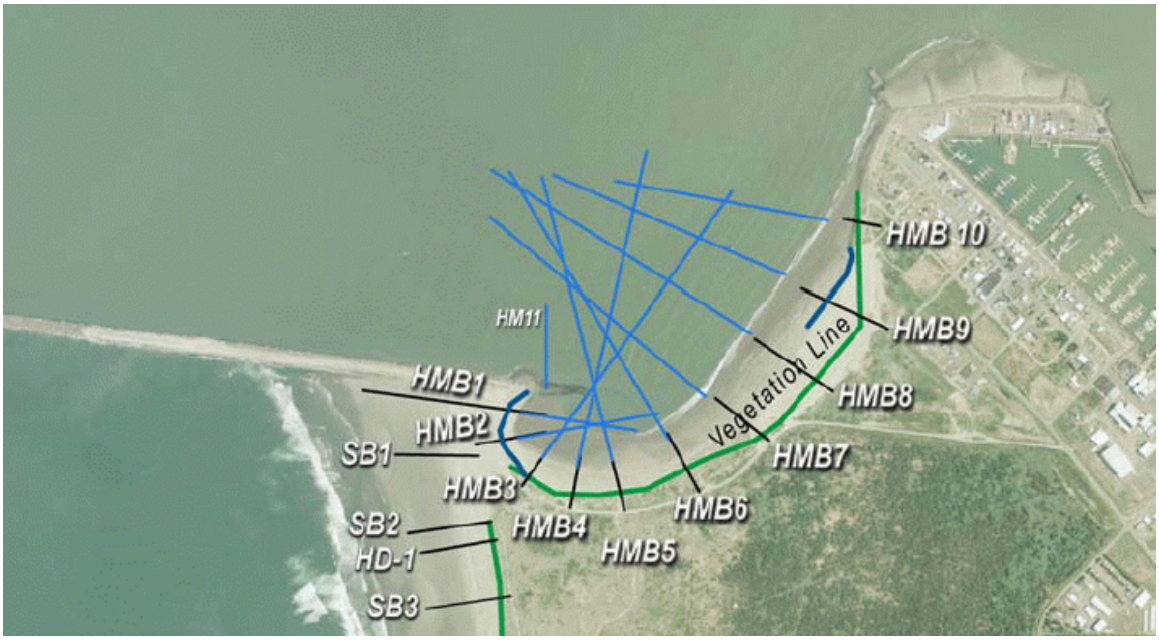

Figure 8. Location of profile lines used for beach and nearshore surveys at Half Moon Bay.

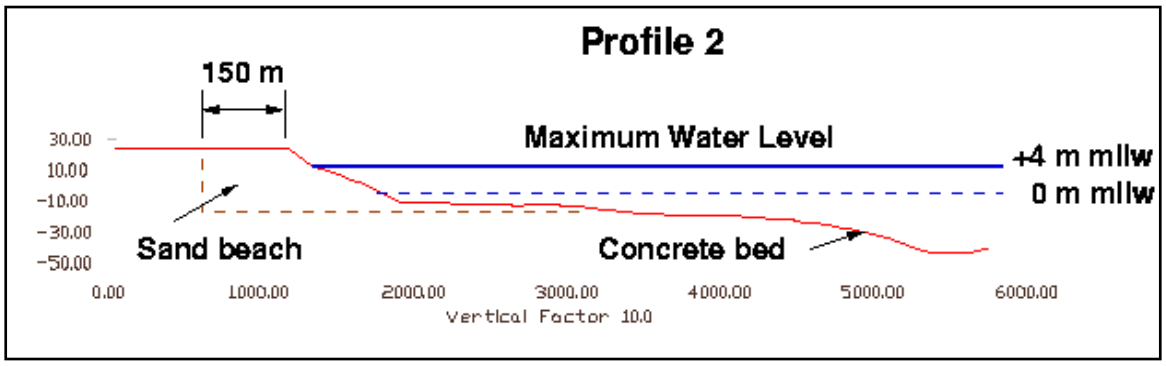

Figure 9. Typical model cross section showing movable-bed portion above –10 ft mllw (axis units are prototype feet).

Potential Scale and Laboratory Effects

Scale effects and laboratory effects were summarized in general terms in Chapter 2, and briefly mentioned in the previous sections discussing similitude criteria. An assessment of how these scale and laboratory effects might influence results obtained from the Half Moon Bay physical model is given in the following paragraphs.

Scale effects in Half Moon Bay physical model

At the selected model length scale, hydrodynamics are in similitude so there is no appreciable scale effect related to the hydrodynamics. All wave-related phenomena such as wave shoaling, diffraction, reflection, and wave breaking will be in similitude with the prototype. Wave-induced current

will be correct, and all nonlinear aspects of the wave motion also will be correct. There may be a slight scale effect related to wave runup on the beach because water will not percolate through the smaller grain sizes of the model as easily as in the prototype. Thus, the model wave runup could be slightly greater. However, the relatively larger bottom friction in the model will help to offset any increase in runup. Flow over and through the diffraction mound will be in similitude because the rubble-mound is large enough to preclude any scale effects related to laminar flow conditions within the stone matrix.

The physical model was conducted using fresh water to simulate the salt water environment at Grays Harbor. This is a practical compromise to avoid corrosion of laboratory facilities and delicate instrumentation. The slight difference in water density between model and prototype has virtually no impact on hydrodynamics as proven by many studies over the past 50 years (Hughes 1993).

Gravel transport in the physical model will be in similitude because the gravel/cobble grain-size distribution was scaled according to the model length scale. Gravel erosion, deposition, and transported quantities should be indicative of prototype behavior under the same forcing conditions.

There is a scale effect associated with sand transport in the physical model. For bed-load sediment transport, the model sand is relatively larger than it should be. Consequently, beach erosion and deposition that occurs in the model under bed-load conditions is not expected to be quantitatively correct. Model erosion and shoreline recession will be less than would occur in the prototype under similar wave conditions, and sand being transported by bed load will stop moving at relatively higher current velocity than in the prototype. Therefore, the location of deposition areas between prototype and model may not correspond exactly.

A somewhat less severe scale effect is likely to occur for sediment moved in suspension. Although the sediment fall speed scale ratio is not what it should be, it is not too far from being correct, particularly given the variation in estimates of fall speed given by different authors. Model sand thrown into suspension will settle back to the bed slightly faster than in the prototype. This could result in a bit less erosion by turbulent wave breaking than would occur in the prototype.

It is difficult to gauge the extent of difference between model and prototype due to the scale effects related to sediment transport, but the calibration phase of the study provided some indication of what to expect. Qualitatively the physical model generally eroded where erosion would occur in the prototype and deposited sand in the same general area where deposition would occur in nature. The main difference was model erosion was less than what occurs in the prototype under the same hydrodynamic forcing.

Because of the known scaling effects, adjustments to the model hydrodynamic parameters may be needed to achieve a calibration of the model. Applying the same adjustments in subsequent tests of different model configurations allows quantitative estimates to be made of erosion. Even if model calibration is less than fully successful, the physical model can provide valuable information about the relative effectiveness of one engineering alternative compared to other alternatives (or the do-nothing alternative).

Laboratory effects in Half Moon Bay physical model

The key laboratory effects in the Half Moon Bay physical model were related either to wave generation, water level, or model boundaries. Waves were generated by a plunger-type wave maker that reproduced long-crested, irregular waves scaled to match wave spectra typical of storms in the northwest or long-crested regular waves with wave height and period similar to the typical storms. Wave approach direction was fixed by the orientation of the wavemaker within the basin. The use of long-crested waves to represent multidirectional wave conditions in the prototype was a reasonable compromise, especially at Grays Harbor where incident storm waves are channeled by the parallel jetty system. The jetties also restrict the approach direction of the more severe storm waves to a narrow window that could be replicated in the model. To assure the long-crestedness of the wave was not affecting wave transformation, measurements were collected in the model and compared to field measurements gathered in and around Half Moon Bay.

Irregular wave trains are more realistic, but morphological changes in the movable-bed portion of the model take more time with irregular waves because not all the waves are large enough to move sediment. However, this variation in wave heights results in smoother shoreline and nearshore bathymetry. Conversely, shoreline evolution under regular waves occurs more rapidly because each incoming wave has sufficient energy to move

sediment. The regularity of the forcing also creates pronounced features in the bathymetry such as exaggerated bar/trough systems and alongshore morphological variations that probably would not occur in nature. A viable compromise was to alternate bursts of regular and irregular wave trains. The regular waves did much of the erosion work and the irregular waves helped smooth the bathymetry.

Water level is recognized as the greatest contribution to beach recession during storms. Over the course of a storm, the normal tide fluctuation is superimposed on the storm surge. The greatest erosion happens when the peak surge level coincides with the high tide level. Water level in the Half Moon Bay model was kept static at the level corresponding to maximum water level. This assured that maximum erosion occurred in the physical model associated with that water level, and it alleviated some of the scale effects related to sediment transport. In nature, storms end, water level returns to normal, and coastal processes continue (usually at a slower pace). Sediment that was eroded from the dune area and deposited on the beachface during the storm might be further reworked and moved offshore as the surge level decreases. These additional processes were not simulated in the physical model with a static water level. Consequently, it should be expected that post-storm profiles measured in the prototype will be different than those obtained in the model because additional processes have helped shape the prototype beach profiles. The main objective of the modeling was to reproduce shoreline and dune recession in the model similar to that observed in the prototype.

Model boundaries are responsible for two laboratory effects: unwanted reflections and unwanted current patterns. Reflections from vertical walls in the basin were kept to a minimum by placement of rubberized “horsehair” mats that are effective in absorbing wave energy. Wave guides (vertical walls) were used at the north end of the wavemaker to prevent immediate diffraction of waves toward the north (Figure 7). Diffraction would reduce wave height along the crest, and this gradient could induce unwanted current. During the calibration phase of testing it was observed that alongshore current in the vicinity of Point Chehalis was too strong. This current was believed to be caused by wave diffraction after the waves passed the end of the wave guide. This problem was alleviated by placement of a groin constructed of horsehair bales extending seaward from Point Chehalis toward the end of the wavemaker at approximately the same location of the first groin at Point Chehalis.

4 Physical Model Construction

Construction costs are a large part of a physical model study. Before committing to a physical model, there should be reasonable expectation that the benefits to be derived are greater than the cost of constructing and operating the model. The Half Moon Bay physical model was originally designed and built with the goal of evaluating engineering alternatives for long-term stabilization of the bay. After model construction, the study scope was changed by the Seattle District, and model testing was limited to simulation of the existing shoreline configuration. Determination of whether or not to proceed with testing of alternatives will depend on the findings of the LTMS.

Once the region to be modeled was scaled to fit within the available space, plan view drawings were prepared (Figure 7), and correspondence between prototype and model coordinate systems was established. Construction then proceeded on the fixed-bed portion of the model.

Fixed-Bed Bathymetry

The procedure for constructing fixed-bed models is to begin with a flat, horizontal floor, place compacted sand on the floor up to about 2 in. from the required elevation, then fill in the remaining elevation with mortar that sets into a hard surface. The construction technique is guided by templates that are spaced throughout the model at approximately 4-ft spacing.

Prototype bathymetry for the fixed-bed portion of the model between elevations -10 ft and -40 ft mllw was scaled to model dimensions and contoured on a plan view drawing in AutoCAD software. Template lines were selected based on the contours. When possible, the template lines were kept parallel and evenly spaced; but in some locations variation was needed to assure accurate molding of the bathymetry. Experience by the model designer helped establish a useful set of templates. The software produced profiles for each template along with the information necessary to position the template spatially in the model. Full-sized drawings of the templates were produced, and the model shop at ERDC cut the templates out of medium gauge sheet metal.

Fixed-bed bathymetry construction started in the deeper portion of the model near the wave machine location and proceeded toward the eastern

shore of Half Moon Bay. Each template was positioned, and the elevation was adjusted to close tolerance. After several templates had been placed, the space between adjacent templates was filled with construction-grade sand that was then wetted and compacted. Finally, ready-mixed concrete mortar was placed, and the surface was floated to a smooth finish level with the top of the templates. It was also necessary to hand-finish the bathymetry to capture local variations between templates that had been noted on the drawings. The construction technique is illustrated by the photographs in Figures 10-14.

Figure 10 shows the start of model construction with the concrete placed between the first three templates. The sloping section is the transition between the -40 ft contour and the basin floor at -50 ft mllw. The templates for the south jetty are shown on the right side of the photograph. Holes in the jetty templates assure jetty permeability.

Figures 11 and 12 show sand placement between model templates. In both photographs the sand had not yet been compacted and graded to final elevation before placing concrete. In Figure 12 the tops of the templates are at the same elevation representing -10 ft mllw in the prototype. This served as the base for the movable-bed portion that was placed as an overlay.

Figure 13 shows the model builders finishing the concrete for the region of Half Moon Bay closest to South Beach. The vertical section was the model baseline that was set back from the present shoreline about 500 ft all around the bay. The entire flat area shown in Figure 13 was later filled in with sand and molded to the correct shape.

Figure 14 shows the nearly completed fixed-bed portion of the model from a viewpoint seaward of South Beach looking east. South Beach was not reproduced in the physical model.

Figure 10. View from wavemaker location looking landward up navigation channel.

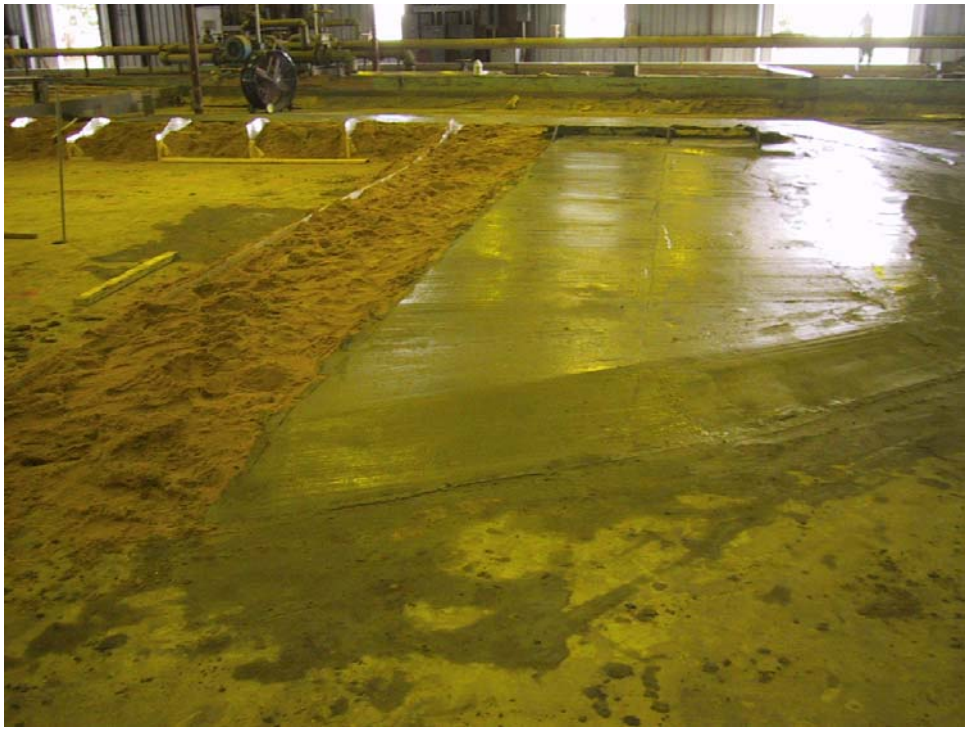

Figure 11. View from navigation channel looking south toward south jetty.

Figure 12. View from Half Moon Bay looking west toward South Beach.

Figure 13. Finishing fixed-bed portion in westward region of Half Moon Bay.

Figure 14. Half Moon Bay looking eastward from South Beach.

Movable-Bed Bathymetry

After completion of the fixed-bed portion of the model, the concrete was painted, and a black contour line was added at the -10-ft mllw elevation denoting the demarcation between fixed-bed and movable-bed regions of the model. Landward of the demarcation line, the bathymetry was molded in fine sand having a median diameter of 0.125 mm. Approximately 45 tons of model sand was ordered and placed in the Half Moon Bay model. This small-diameter, finely sorted sand was purchased from U.S. Silica Company, and it arrived in 100-lb bags. This F95 grade sand is typically used in sandblasting, but experience has shown it is an excellent sand for movable-bed models.

Figure 15 shows initial sand placement in the physical model in the region of the diffraction mound. The black line indicates the transition between fixed-bed and movable-bed. The baseline is shown as the transition between sand and concrete at the highest elevation of the dune. The setback to the baseline is more than adequate to cover any erosion that might occur. The diffraction mound has been constructed atop the sand. In the Figure 15 photograph, the jetty remnant eastward of the diffraction mound had not yet been constructed. Figures 16 and 17 are additional photographs of the initial sand placement.

Figure 15. Construction of diffraction mound at eastward end of south jetty.

Figure 16. Initial sand placement shown looking eastward from South Beach dune.

Figure 17. Initial sand placement looking northeast toward Point Chehalis.

The initial placement resulted in most of the required sand volume being placed in approximately the correct position. The next step was to flood the model and run some waves to compact the model sand and wash out the silt. After that, the final movable-bed bathymetry was molded using reverse templates suspended on horizontal beams. As discussed earlier, these templates were based on 10 profile lines surveyed in June 2002 approximately evenly spaced along the Half Moon Bay shoreline. Templates used between the profile lines were based on a hand-adjusted interpolation between measured profile lines.

Figure 18 illustrates the movable-bed molding processes. On the particular profile shown here, the initial sand placement was not sufficient to bring the profile to the required grade, so additional sand was brought in and placed on the profile. The newly added sand was wetted and compacted to the proper grade. In Figure 18, ripples are observed that were created by waves that compacted the initial placement.

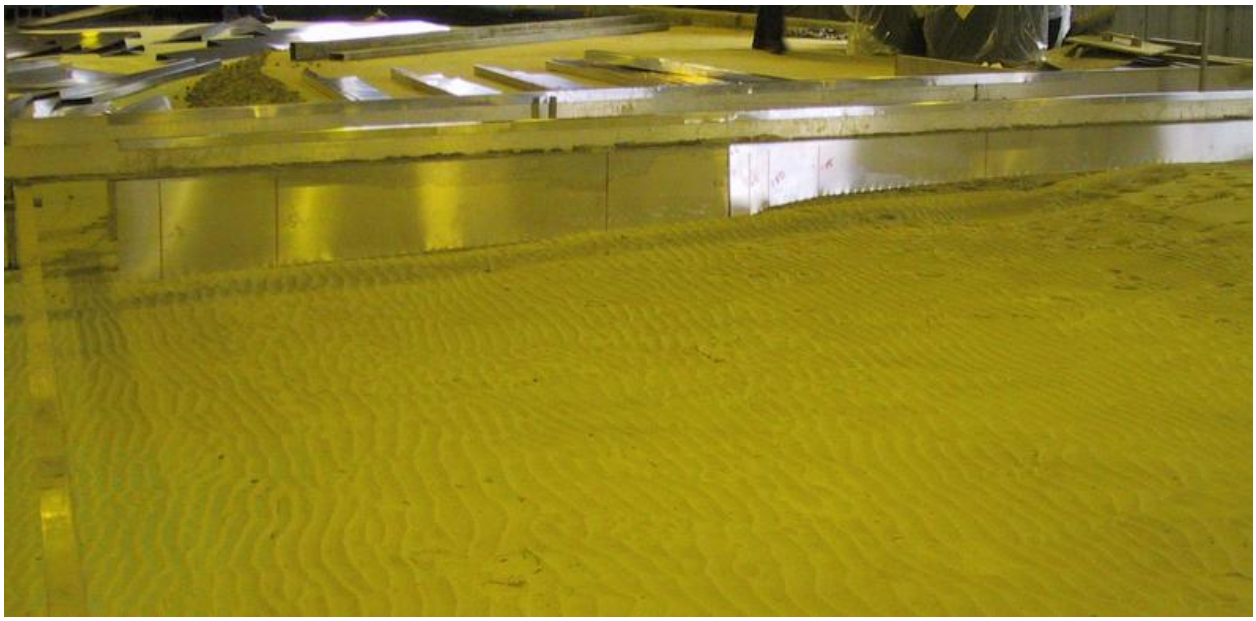

Figure 18. Suspended template for movable-bed grading near Point Chehalis.

Figures 19, 20, and 21 further illustrate the movable-bed molding processes. Between adjacent templates, straightedges are used to bring the bed to approximate elevation. Then the model craftsmen complete the section using hand trowels to mold and compact the sand in place. This was a labor-intensive procedure, taking approximately a week to remold the movable-bed after each experiment. During experiments, waves and wave-induced current transported sand to different locations in the model basin. Transported sand had to be moved back manually during remolding at the end of the experiment. No sand was lost to the system, so it was not necessary to add additional sand while remolding.

Figure 19. Molding Half Moon Bay movable bed.

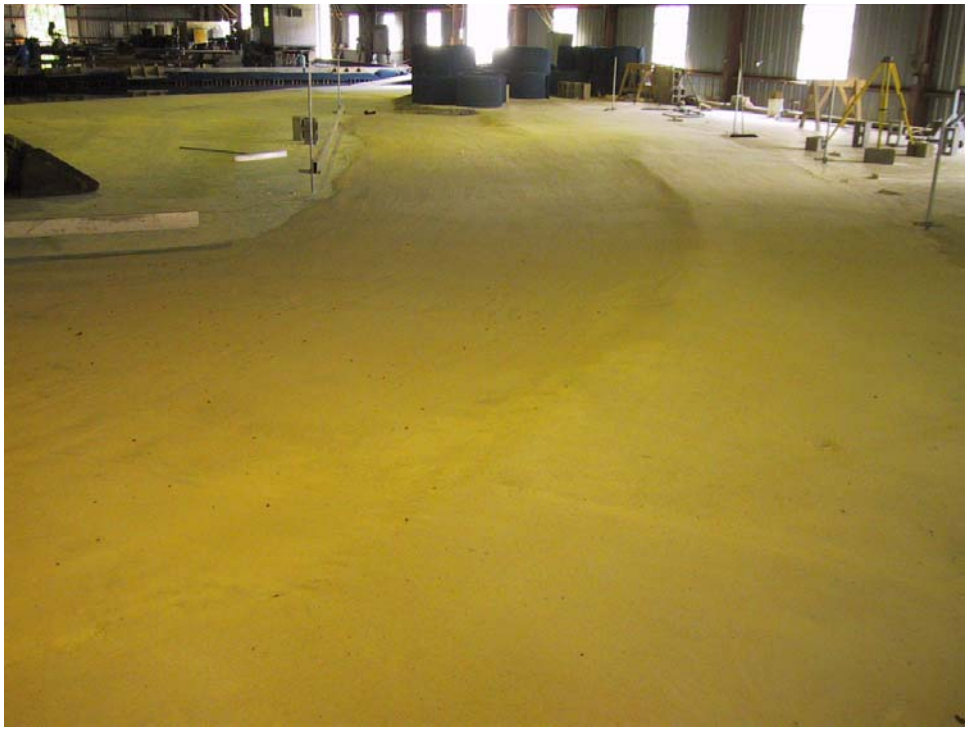

Figure 20. Completed portion of movable bed looking northeast toward Point Chehalis.

Figure 21. Molded beach looking westward toward south jetty.

Gravel Transition

Final distribution of the gravel over the profiles from mean high water (mhw) to the dune crest in the transition area in Half Moon Bay was not well known, so several assumptions were necessary. From the time of initial gravel placement until profiles were acquired, the gravel beach had been subjected to storms that reworked the material from its original dumped placement. Total placement volume was known, as well as the profile shape from the 2002 survey and the approximate alongshore extent of the placement.

In the Half Moon Bay model, the scaled total quantity of gravel/cobble material was evenly distributed over the alongshore extent of the gravel transition area. The gravel was molded into the shape of the measured profiles, and it extended from the +4- to the +25-ft mllw elevations. The thickness of gravel over the sand bed was assumed to be uniform over the entire profile. Although a uniform distribution is likely not fully representative of the prototype, lack of field data necessitated this assumption. Most of the gravel transition nearest the diffraction mound appears to be relatively stable according to field profiles. However, the gravel transition has experienced considerable movement in the vicinity of profile line P3.

Figures 22 and 23 show the gravel transition region in the physical model immediately after model remolding. Note the jetty remnant extending from the diffraction mound in Figure 23. After completion of the movable-bed portion, profiles in the model were recorded on the same 10 profile line positions as in the prototype.

Figure 22. Placed gravel transition looking southeast from south jetty.

Figure 23. Gravel transition seen from navigation channel.

5 Physical Model Parameters and Operating Procedures

The physical model is similar to an analog computer by responding to wave forcing with a reaction governed by physical forces. This chapter overviews the wave conditions selected for driving the physical model, describes the instrumentation used to record model response, and discusses the procedures followed when operating the physical model. Model results can be negatively influenced if proper operating procedures are not followed.

Model Wave Conditions

Field measurements of wave conditions in Half Moon Bay were obtained during the period 9 December 2003 to 10 January 2004 at the four locations shown in Figure 24. During this period the zeroth-moment wave height at the Coastal Data Information Program (CDIP) 3601 offshore buoy reached a maximum of H_{mo} = 7.2 m with a corresponding peak period of T_p = 14 sec. The mean direction for the offshore maximum wave condition was west-southwest.

Figure 25 shows a plot of the time series of H_{mo} from the four inshore locations and the CDIP buoy. Inshore Gauge 1 (-20-ft mllw contour) and Gauge 2 (-10 ft mllw) near Point Chehalis saw the largest wave heights with the maximum measured H_{mo} just over 3 m. At Gauge 3 (-5 ft mllw) there was some reduction in wave height that can be attributed to diffraction into Half Moon Bay, but the greatest reduction was seen at Gauge 4 (-5 ft mllw) where much lower wave heights were recorded. Gauge 4 was located in the protected lee of the diffraction mound and submerged jetty remnant.

Wave roses for wave height and direction measurements at each gauge location are shown in Figure 26. The roses indicate a progressive reduction in H_{mo} between field Gauges 2, 3, and 4, and they show increasingly narrow directional spread as waves propagate from offshore to the nearshore region of Half Moon Bay. Wave direction at Gauge 4 is mostly to the south, parallel to the breach-fill shoreline, indicating the waves have diffracted nearly 90 deg from the wave incident wave direction.

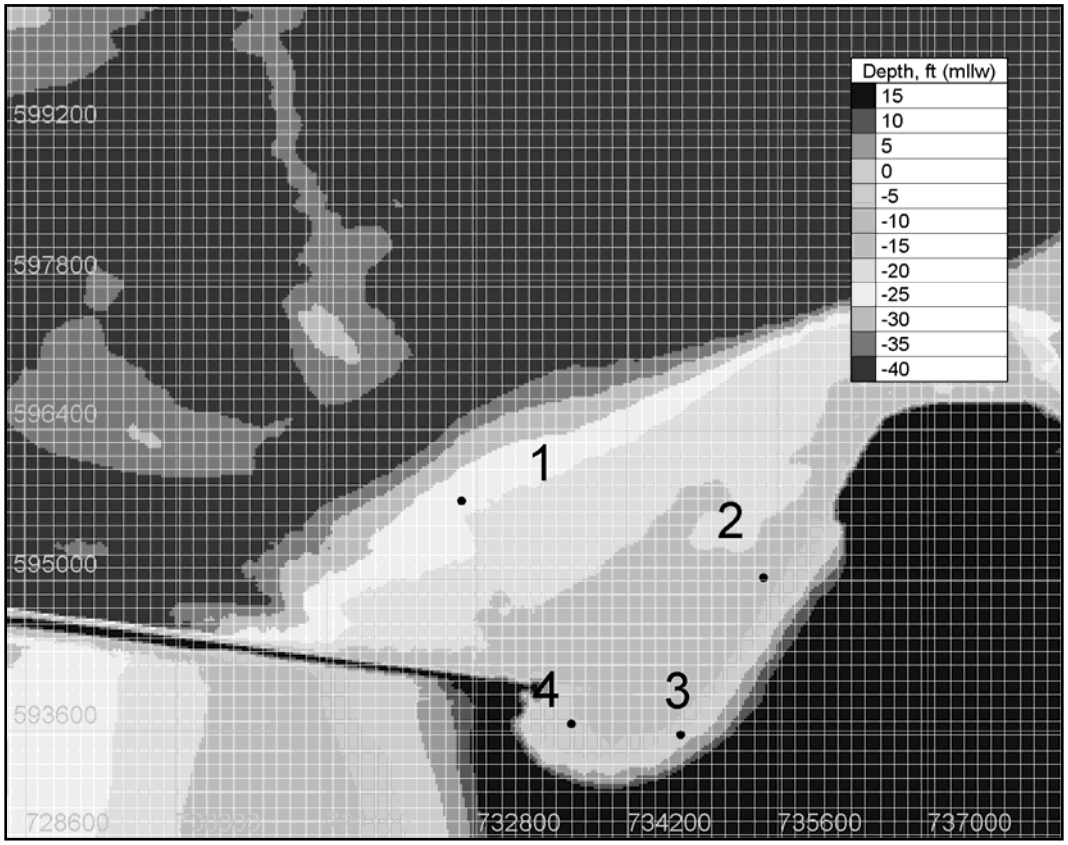

Figure 24. Field wave gauge locations in Half Moon Bay.

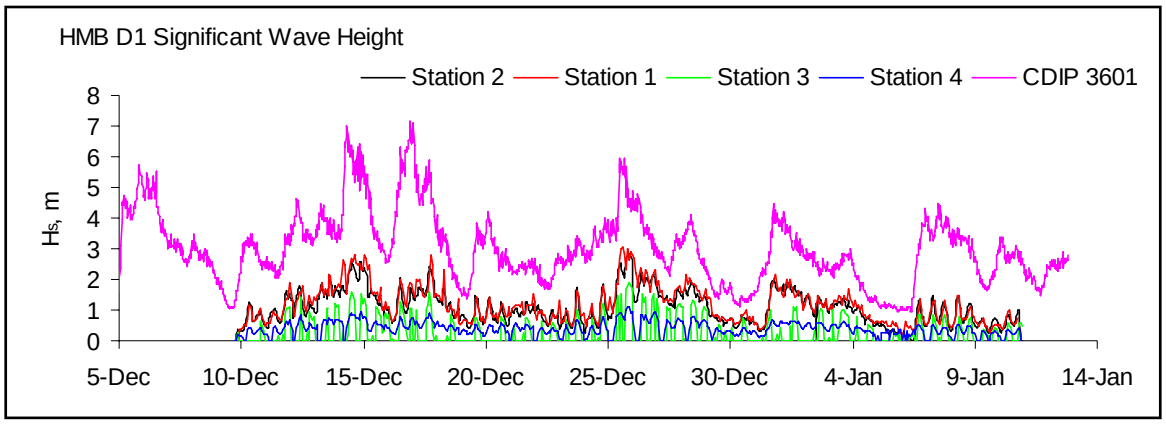

Figure 25. Time series of H_{mo} for offshore and Half Moon Bay gauges.

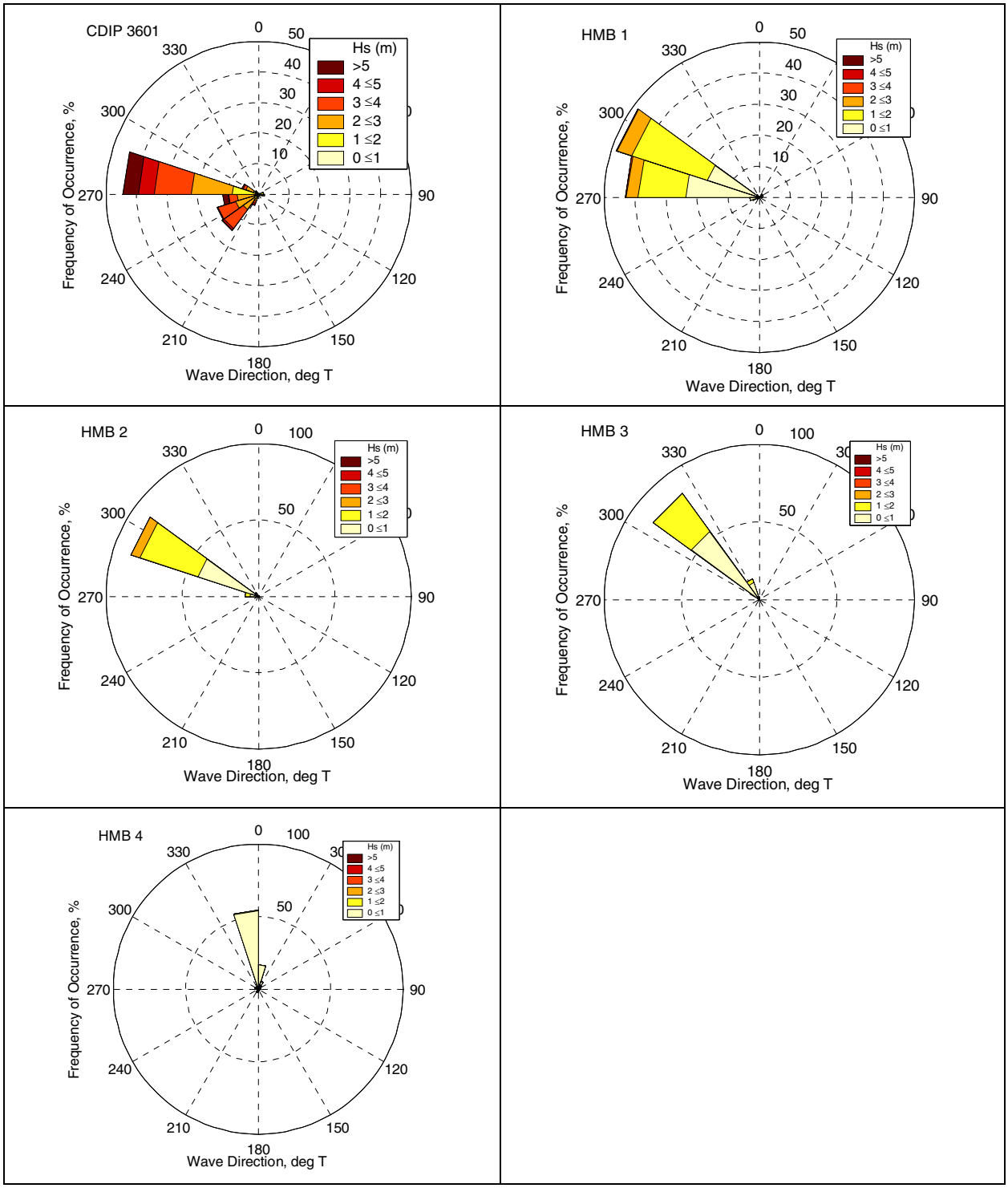

Figure 26. Wave roses for wave height and direction measured at CDIP and inshore wave gauges.

The field wave measurements served as the basis for design wave conditions in the Half Moon Bay physical model. Waves in the model were generated with a computer-controlled, vertical displacement plunger-type wave machine shown in Figure 27. This wavemaker could produce long-

crested, regular and irregular waves, but it could not generate wave spectra with directional spreading. However, the wave approach angle to Half Moon Bay is limited by the dual jetties at Grays Harbor, so waves reaching the study area cannot have much directional variability. It was concluded that representation of directional wave trains in nature by long-crested waves propagating in a single direction in the model was a reasonable compromise.

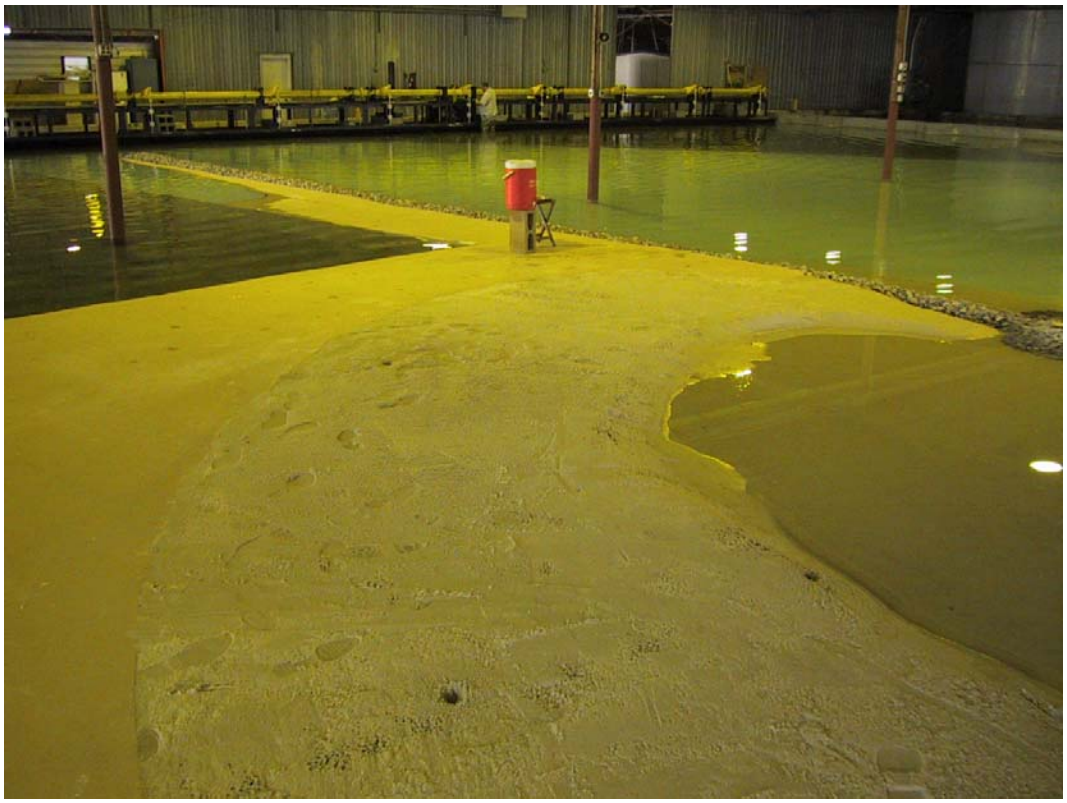

Figure 27. Plunger-type wave machine used in Half Moon Bay physical model.

Spectral representations of wave conditions characteristic of those measured at field wave Gauge 1 were scaled to model size spectra. A computer program created a time-series of sea surface elevations that matched the spectral description. There is no practical relationship for converting from sea surface elevation time series to equivalent wave board stroke time series for plunging-type wavemakers. Therefore, it was necessary to calibrate the wave machine following a standard procedure used at CHL. Based on past experience with this wave machine, an approximate stroke time series was generated to command the wave machine. This signal was run in the basin at the design water level, and measurements were made at a number of wave gauges. These measurements were analyzed, and a gain factor was calculated that would uniformly increase or decrease the wave

board stroke signal to match the target spectrum. Then the test was repeated with the new board signal. Once the measured spectra matched the target spectra, the command signals were saved for future use.

For model testing, waves can be either irregular or regular wave. Irregular waves are preferred because they are more realistic. Movable-beds in physical model respond more smoothly to irregular waves, and the morphologic features better resemble those of nature. The consistency of regular waves causes movable-beds to have more rhythmic features such as exaggerated bar-trough systems. Also, change occurs more rapidly under regular waves because all waves have sediment moving capacity, whereas with irregular waves, only some of the waves can move sediment.

Model Instrumentation

Waves

Waves were measured throughout the Half Moon Bay model using capacitance-type wave gauges mounted on tripods at fixed locations. The capacitance gauges measure the vertical variation of the water surface as the waves move past the gauge position. As mentioned, waves were run in bursts ranging between 10 and 30 min. Wave data were not collected for every wave run; but when data were collected, the sampling rate of 20 Hz, and the duration of the wave record spanned the entire wave run.

All wave gauges were mounted on remotely-controlled stepping motors that permit the gauges to be raised and lowered precise vertical distances for calibration. Wave gauges were calibrated daily with the water at test level and motionless. The gauges were first raised 10 equal increments, then lowered 20 equal increments, and finally raised 10 equal increments to bring the gauges back to their original vertical positions. Data collected at each stopping point were analyzed to establish the relationship (usually linear) between water elevation at the gauge and frequency output by the gauge. Provided all gauges exhibited the expected calibration, the calibration relationship was saved in a file for later application to the measured raw wave data.

Standard analysis of the recorded wave gauge signal included time series analysis for representative statistics such as significant wave height ($H_{1/3}$) and mean wave period (T_m), and the wave height distribution. Frequency-domain analysis decomposed the measured irregular wave time series under the assumption that the measurement can be represented by the

summation of many sine waves of differing amplitudes and periods. The main result from frequency-domain analysis was a wave energy spectrum indicating the distribution of wave energy over the range of wave frequencies (inverse period). The square root of the area under the spectrum times four is known as the "zeroth-moment wave height, or H_{mo}. This parameter is often called significant wave height because for narrow-banded spectra in deep water, H_{mo} is approximately equal to $H_{1/3}$. The other key parameter taken from frequency-domain analysis is the wave period associated with the spectral peak, T_p. Figure 28 illustrates a typical output plot from the Generalized Experiment Control and Data Acquisition Package (GEDAP™) analysis package. Shown in the figure are the plotted time series in model-scale engineering units, analyzed wave spectrum, and both frequency- and time-domain representative parameters in model units.

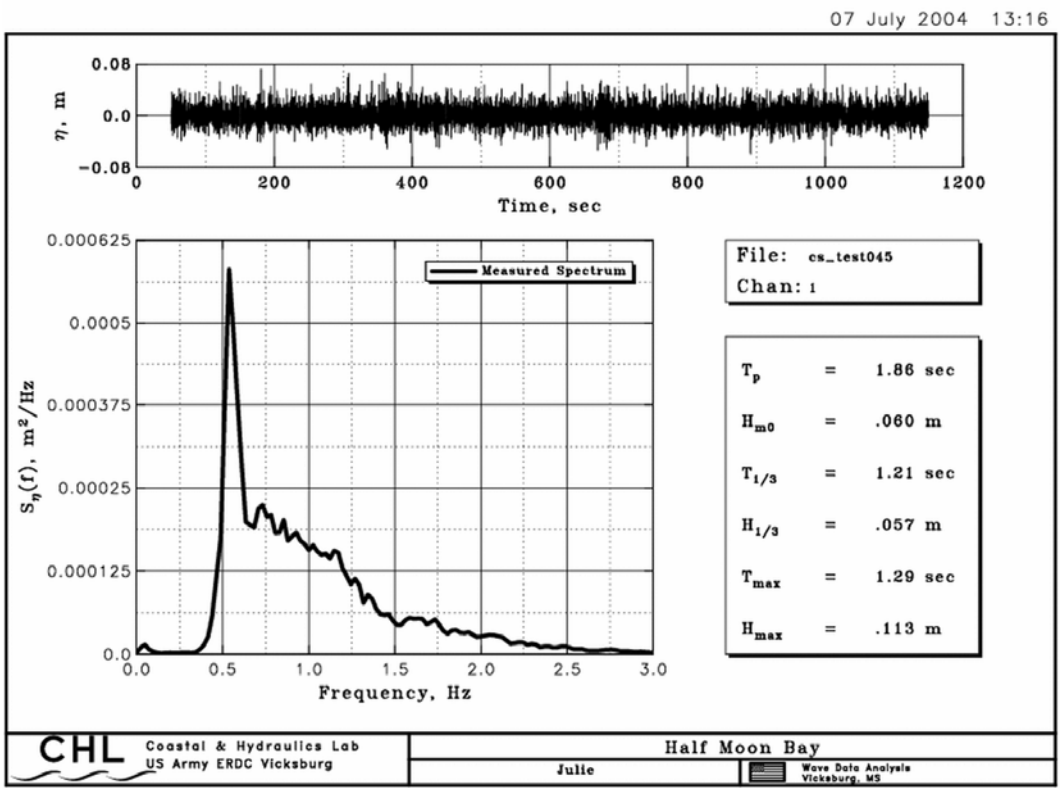

Figure 28. Wave analysis output from model wave measurements.

Wave measurements were acquired at a minimum of nine locations throughout the Half Moon Bay physical model. Six locations (Gauges 4-9) were placed in the Half Moon Bay nearshore region or out in the Grays Harbor entrance channel on the molded bathymetry as shown in Figure 29. Four of these gauges correspond to the field wave gauges shown in Figure 25. Table 4 gives the correspondence between the field and model

gauge numbers. Three gauges were positioned on a line parallel to the wave machine a distance of 12 ft from the face of the wave generator. These gauges were used to evaluate the generated waves before they underwent wave transformation in the model. For the second calibration test, an additional four wave gauges were placed in the nearshore zone for a total of 13 wave gauges.

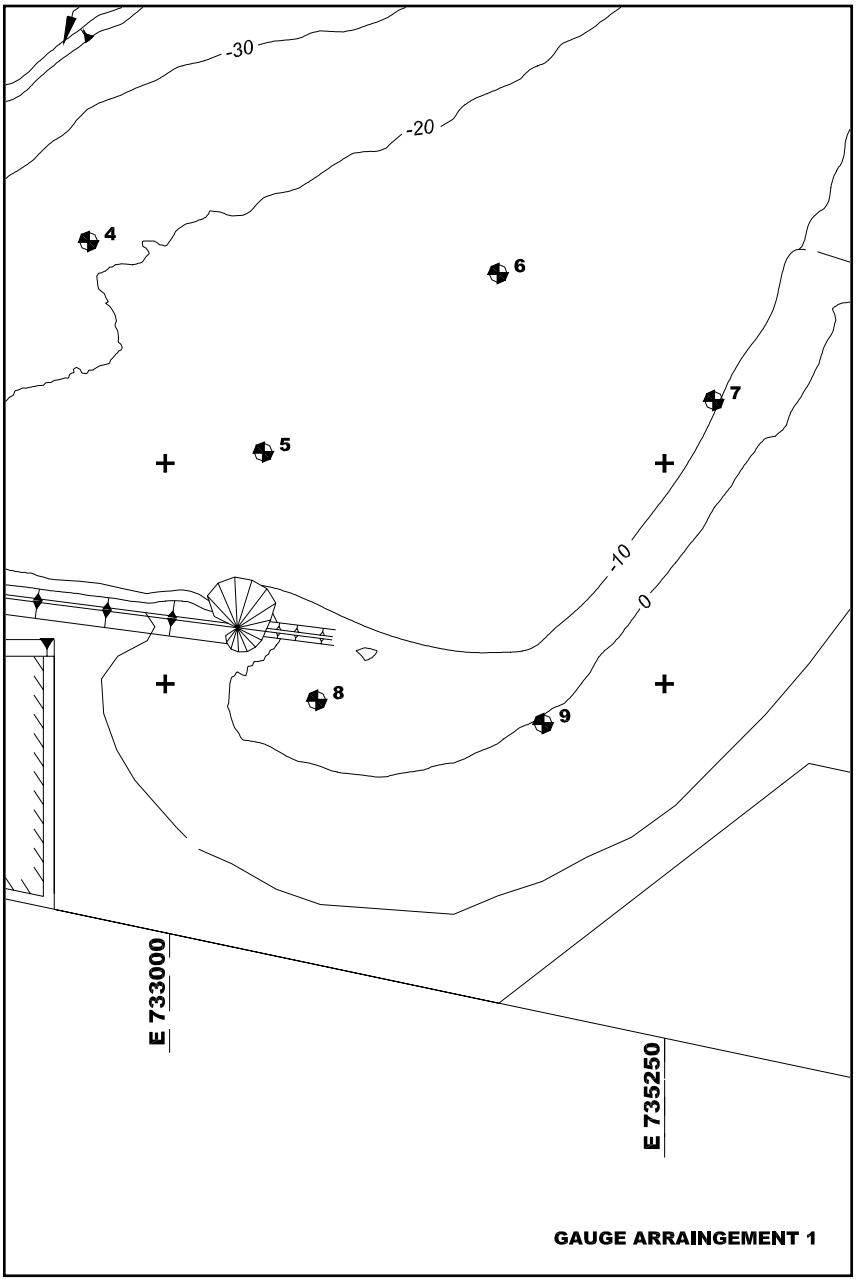

Figure 29. Wave gauge locations in Half Moon Bay physical model.

Table 4. Correspondence between field and model wave gauges.

Field Gauge Number	Model Gauge Number
1	4
2	7
3	9
4	8

Current

The current in Half Moon Bay is generated primarily by waves. The tidal current, although strong out in the main entrance channel, appear to be relatively weak within the bay (Osborne et al. 2003). During all but extreme conditions, most of Half Moon Bay has reached a planform conforming to the crenulate-bay theory (Silvester 1991). The exception is the region nearest the diffraction mound that has been protected by placement of the gravel/cobble material. Wave-driven current in the bay moves along the shoreline toward Point Chehalis. Because of the bay's near-equilibrium bay planform, the longshore current is not as large as on the open coast.

At the beginning of testing, dye was injected at various points in the physical model to indicate the general current patterns under storm wave action. The dye revealed a slow moving current at most locations with the exception of the region just offshore closer to Point Chehalis. Here, the water had a stronger velocity directed to the north past Point Chehalis. It was later determined that this longshore velocity was a laboratory effect caused by wave diffraction in the model, and it was corrected (Chapter 6).

After correction of the laboratory effect causing an unrealistic longshore current near Pt. Chehalis, it was judged that the model correctly simulated the wave processes of refraction by bottom bathymetry and diffraction around the south jetty terminus; and consequently, the corresponding wave-induced current would also be correctly simulated. In general, the current was not measured routinely in the physical model during calibration tests and testing of the existing condition. For those occasions when the dye injection indicated unusual model current response, a Nixon Streamflo micro-impeller current meter was used. This instrument measures current with a five-bladed fan that spins as flow moves past the blades. A counter logs the number of impeller revolutions as a function of time, and outputs the average over a user-selected time interval to a remote display. The counter frequency is converted to engineering units of

flow speed by a calibration curve provided by the manufacturer. The Nixon Streamflo meter measures flow only in the direction aligned with the impeller, and it cannot distinguish flow direction. For this reason, the instrument is not suited for measuring wave orbital velocities, but it is appropriate for measuring the mean longshore current produced by wave action. The impellor probe was supported on a stand with the impellor positioned about at middepth.

Movable-bed profiles

Shoreline response in Half Moon Bay resulting from the combination of wave condition and water level was the primary output of the movable-bed physical model. Profiles extending from the dune seaward to depth elevations between -6 to -10 ft mllw were measured using the custom-built bed profiler shown in Figure 30. The profiler is a thin aluminum rod (with a wheel on one end) connected to a rotating support mechanism that is mounted on a 5-m-long horizontal support beam. A hand crank at one end moves the profiler rod horizontally, and as the rod moves, it rolls along the bed undulations. As the profile rod is traversed, the instrument continuously samples two potentimeters. One potentimeter gives horizontal position along the rail, and the second measures the angle of the profiling rod relative to horizontal. These two measurements, coupled with knowledge of the support beam location in the horizontal and vertical planes, are sufficient to resolve the *x*, *y*, and *z* values for each sampled point acquired over the profile.

A wheel on the lower end of the profiler rod allows the profiler to move along the movable bed and capture the undulations without altering the profile along the track. A counterweight serves to adjust the weight of the wheel on the bed. The main advantage of this profiler system is the capability to measure both the subaqueous and subaerial portions of the profile with or without draining the basin. Automatic recording of data makes profile measuring quick and easy. The profiler beam is supported on each end by a vertically-adjustable base. The beam had a slight sag over its span, so it was necessary to add a midspan support as shown in Figure 30.

Figure 30. Movable-bed profiler moving over beach near diffraction mound.

Profiles were surveyed along transects corresponding to profile lines P1 to P10 in the prototype (see Figure 8). For each profile, the profiler beam had to be lifted into position aligned along the profile line, and the elevation of both ends and the middle was adjusted to the horizontal datum. Even though the profiler is capable of operating with the water level up, it was easier to drain the basin down to the -10-ft mllw contour before commencing measurements for the following two reasons: (a) During model testing, the nearshore wave gauges and associated cabling made it difficult to move the profiler between profile lines, and (b) the sand bed in the flooded model could not support the weight of a technician without significant deformation. The surveyed profiles were converted to units of prototype-scale feet and referenced to the Washington State Planes coordinate system for comparison with profiles measured at Half Moon Bay. Because of the time necessary to drain the basin and measure the profiles, a set of profiles was typically collected only at the beginning and end of each major model test or after significant changes in hydrodynamic forcing.

Shoreline and beach scarp positions

During experiments, daily interim monitoring of the dune scarp location and the still-water level (+12 ft) shoreline gave an indication of amount of erosion or shoreline change that occurred during that day's runtime. Measurements were made using a standard tape measure and recording the distance between the scarp or shoreline and the baseline represented

by the edge of the concrete where the sand dune ended. Shoreline and scarp data were acquired at profile lines P1 through P10, and at several intermediate locations between the standard profile lines. Horizontal measurements were converted to units of prototype feet and referenced to the Washington State Planes coordinate system before entering into the Regional Morphology and Analysis Package (RMAP) software (Batten and Kraus 2004) for comparison with shoreline and scarp observations acquired at Half Moon Bay.

Model Operation

Generally, the following standard procedures were followed during the conduct of a test in the Half Moon Bay physical model.

a. The movable-bed sand was regraded to the June 2002 configuration using templates supported on horizontal beams (see Chapter 4). Model gravel/cobble material that had been moved during the previous experiment was scraped up and removed. The final task in remolding the sand bed was rebuilding the gravel/cobble transition, and checking the elevations of the diffraction mound and jetty remnant.
b. Once the initial condition was established, profiles were surveyed on profile lines P1 through P10, and the distance of the sand dune crest back to the concrete base line was verified and recorded. After surveying, the nearshore wave gauges were moved back into position.
c. The model was flooded up to the elevation for the test, and an automatic system was started that monitored the water level, adding water when needed. Water slowly leaked out of the basin overnight, so each morning during multi-day tests it was necessary to add water to return the water level to the correct elevation. Throughout the day manual checks of water level were also performed.
d. Most mornings before commencing runs for the day, the wave gauges were calibrated while the water elevation was motionless. Typically, the calibration procedure took 30 min. On rare occasions a gauge would fail calibration and have to be fixed or replaced.
e. Waves were run in bursts according to the sequencing schedules described in Chapters 6 and 7. Between bursts, 10 to 15 min were allowed for the basin to settle before initiating another wave sequence. Allowing for calibration and settling time between runs, it was possible to obtain between 4.5 to 5.5 hr of waves run in the model during an 8-hr working day.
f. During multi-day experiments, the dune scarp and shoreline (relative to storm water level) were recorded at the end of the workday. Wave data were not recorded for every run, but when data were collected, analyses

were usually performed that same day. Same-day analysis assured the correct waves were being generated, and it links the raw data with the appropriate calibration files.

g. Photographs and video documentation were acquired as necessary to document erosion progression in the model. Dye was injected to observe the current patterns and confirm the current was responding as expected.

h. Profiles were surveyed on lines P1 through P10 at the end of the test to document the total change in shoreline position and cross-shore configuration that had occurred during the experiment.

Test Termination Criterion

The wave conditions run in the Half Moon Bay physical model were nearly constant, and they were run at a static water level representing the +12-ft mllw storm surge elevation. Eventually, this relatively static hydrodynamic condition forced the movable-bed portion of Half Moon Bay into a state near equilibrium for that constant water level and wave height. This was a state where sand was still being moved around in the model, but no further recession of the shoreline or dune was occurring for the specified wave and water level.

The main criterion for estimating whether or not a near equilibrium had been established during an experiment was monitoring the dune scarp and shoreline position. Once these measurements cease changing over more than two or three measurement cycles, then it was reasonable to assume that little additional erosion would occur unless the water level or wave condition changed.

6 Calibration for Shoreline Recession

Calibration of the Half Moon Bay movable-bed physical model for shoreline recession was a necessary precursor for evaluating physical model shoreline change caused by storm waves and high-water level elevations. At the selected model length scale, hydrodynamics were in similitude, and the gravel material was scaled correctly to simulate bed-load movement. However, the sand portion of the beach was not correctly scaled for bed-load transport because the sand in the model was relatively larger than it should be (Chapter 2). Consequently, beach erosion that occurred in the model was expected to be less than would occur in the prototype under similar wave conditions.

Calibration Strategy

Under the constraint of the known sediment transport scale effect, the aim was to demonstrate model calibration by reproducing shoreline recession that occurred in the prototype. This was a difficult task because the prototype erosion represented the culmination of several months of different storms at different water levels with longer time periods of lesser waves at lower water levels between storms. The resulting beach profiles recorded after the end of the storm season are the integration of this entire storm sequence. Included in the sequence were those times when sediment eroded from the dunes was reworked to positions lower on the profile by calmer wave conditions at normal water levels, thus down-cutting the profiles in the vicinity of the shoreface. Reproducing the same time-varying sequence of waves and water levels in the physical model was not possible primarily because of the time required to simulate such a sequence in the physical model.

The necessary compromise was to attempt model calibration for shoreline recession by simulating storm wave conditions at the maximum water level until near equilibrium in the model. Comparison of the resulting model shoreline recession, dune erosion, and profile change with prototype equivalents indicated whether this compromise was satisfactory. The tacit assumption was that the prototype recession does not represent an equilibrium condition because the storms ended before the bay shoreline had time to adjust to a new equilibrium. Running the model to a near-equilibrium condition was judged to offset partially the sediment scaling effect. Another way to achieve shoreline recession correspondence

between model and prototype would be to increase the model hydrodynamic parameters to induce greater erosion, and thus compensate for the sediment scaling effect. This approach was not followed because increasing the storm surge level would cause extensive overtopping at Point Chehalis and the adjacent beach, and little benefit could be achieved with increasing wave height because the waves break before diffracting into Half Moon Bay.

The best possible outcome of the calibration testing would be good replication of both the shoreline recession and profile development. Such a good comparison would validate the compromises previously described, and the model could be expected to simulate properly the absolute effects of engineering changes to the bay under similar hydrodynamic conditions. The more likely outcome would be shoreline recession at the right locations, but not as much recession as observed in the prototype. Similarly, profiles would show correct erosional trends, but erosion magnitude would not be as much as the prototype, and the profiles would not be down-cut by wave action at lower water levels. Even with this more probable outcome, the model can still serve to examine the relative changes brought about by engineering modifications to the bay, but absolute shoreline recession magnitudes would be somewhat in doubt with the prototype expected to have more recession than indicated by the model.

In summary, the calibration testing procedures were necessary for several reasons.

a. Calibration testing aided the model engineers understand how the model reacted to the hydrodynamic forcing.
b. The severity of sediment scaling effects was assessed.
c. The calibration experiments identified laboratory effects that needed to be corrected.
d. The engineers gained much insight on how model results should be interpreted in terms of probable prototype response to similar forcing conditions.

Historic Erosion Event Selected for Calibration

The event selected for calibration of the Half Moon Bay movable-bed physical model was actually the cumulative erosion resulting for a collection of storms that occurred between June 2002 and March 2003. During this time period, significant erosion was observed in the vicinity of profiles

P3 and P4 shown in Figure 8. Figures 31, 32, and 33 compare beach and dune profiles bracketing the selected time frame.

Figure 31 shows no erosion for profiles P1 and P2 that are nearest to the diffraction mound and well protected from relatively small waves diffracted around the south jetty terminus. Note the additional dune elevation resulting from placement of 135,000 cu yd on the breach fill separating South Beach from Half Moon Bay in April 2002. Profile P3 exhibited significant erosion during the time span. This transect may have been located just beyond the gravel/cobble protection which was terminated short of design length by funding constraints. Observed erosion at profiles P3 and P4 may indicate an effect related to the western terminus of the transition gravel. Under the assumption that the reach of shore protected by the gravel/cobble is not in equilibrium, the unprotected shore immediately downdrift of the gravel termination point would be expected to see increased erosion and greater recession. This study did not investigate whether or not the gravel-protected shore is at equilibrium. Such a determination should be based on field observation over an extended time period. Recession of the dune on profile P3 was approximately 75 ft between June 2002 and March 2003.

Shoreline recession of similar magnitude as profile P3 was observed on profile P4 as shown in Figure 32. The main difference between profiles P3 and P4 is that the dune crest position appears to have remained stationary at its historical position on profile P4. Only minor erosion was seen on the upper portions of profiles P5 and P6, with as much as 100 ft of recession seen around the 0-ft mllw contour.

Figure 33 indicates the profiles nearer to Point Chehalis experienced virtually no recession during the storm season even though this portion of Half Moon Bay receives more energetic wave conditions than the shore farther to the west. The decrease in crest elevation for profile P8 was probably caused by mechanical removal of material placed on the breach fill in April 2002. Adjacent profiles did not show this elevation decrease.

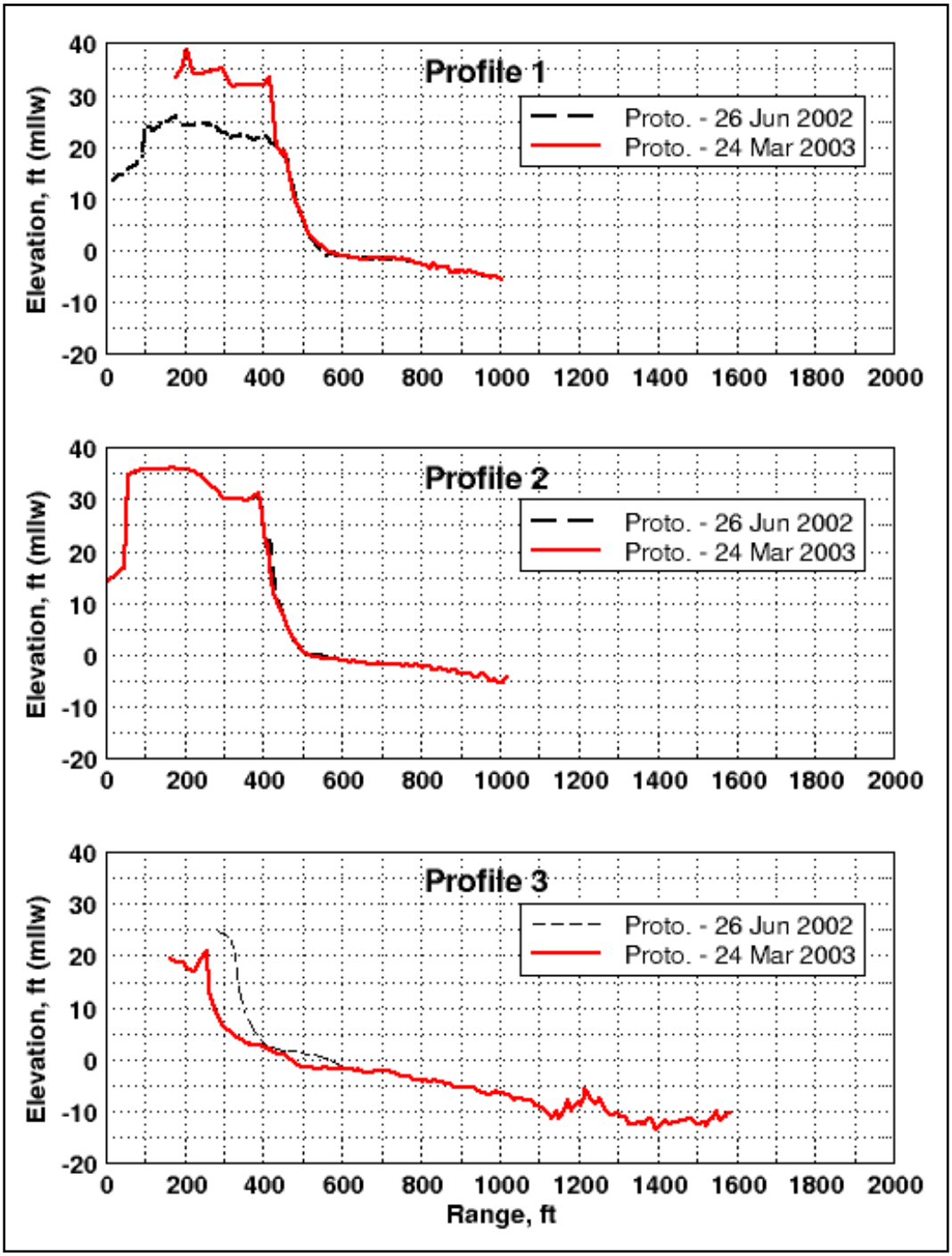

Figure 31. Prototype profile change between June 2002 and March 2003, profiles P1-P3 (vertical scale is exaggerated relative to horizontal scale).

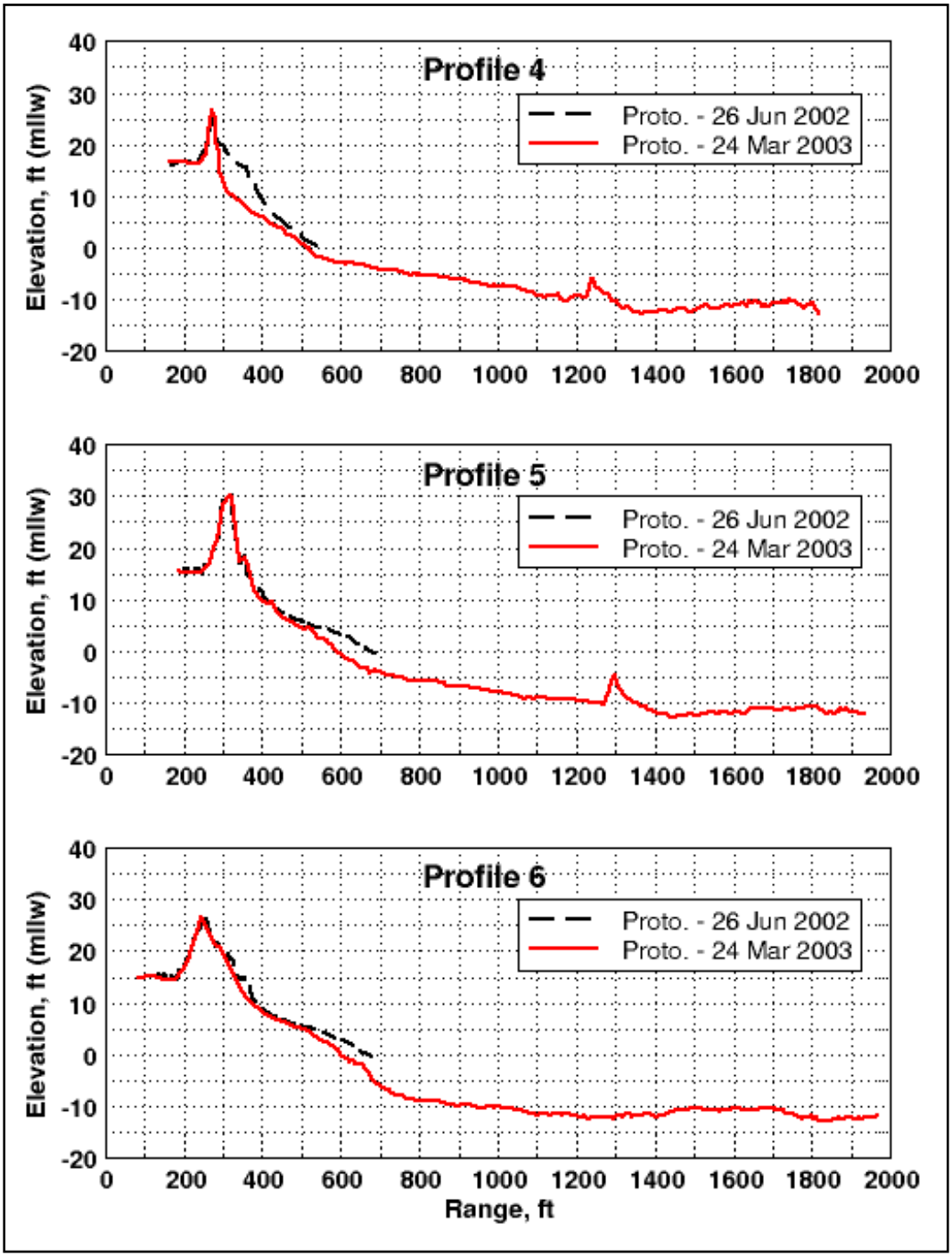

Figure 32. Prototype profile change between June 2002 and March 2003, profiles P4-P6 (vertical scale is exaggerated relative to horizontal scale).

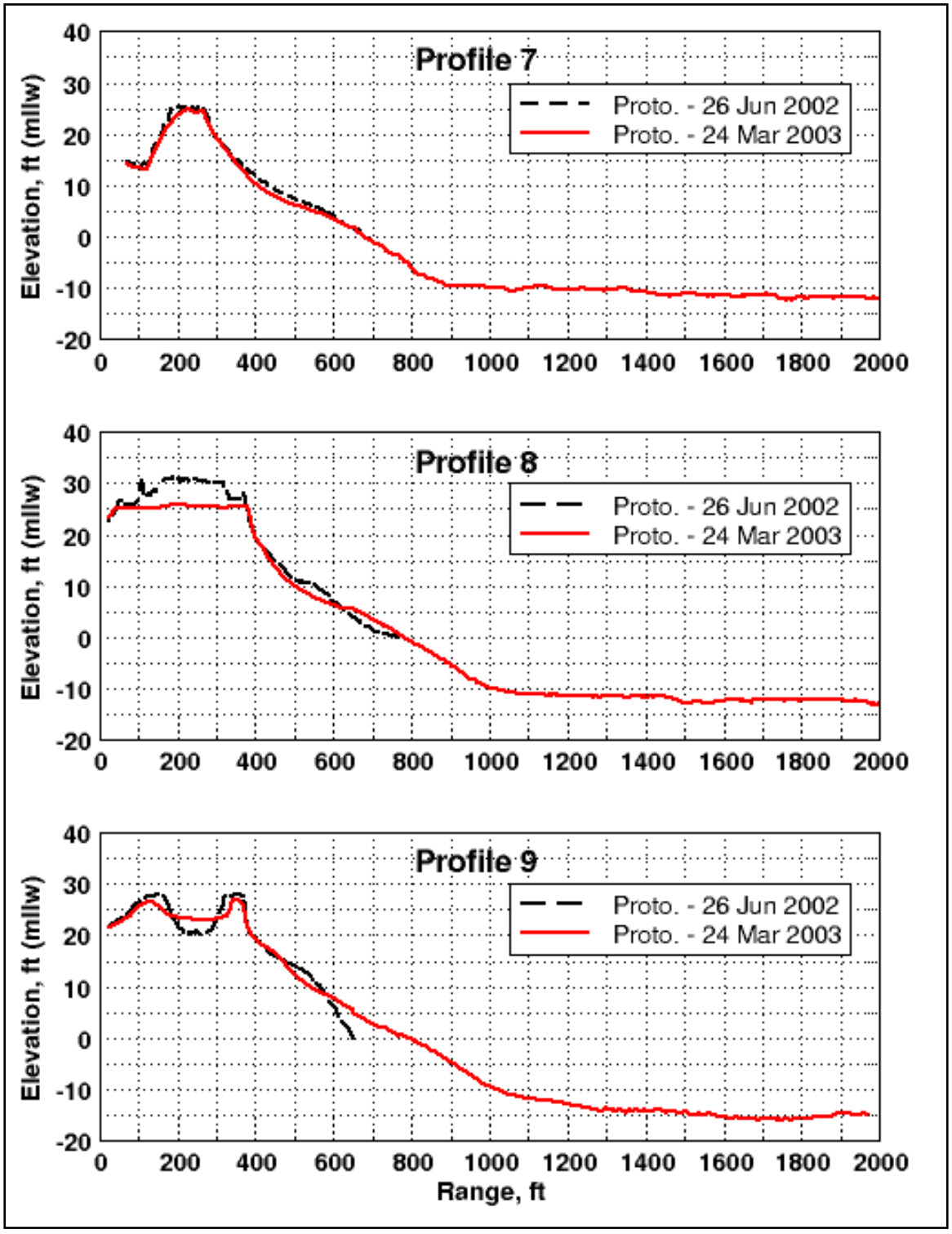

Figure 33. Prototype profile change between June 2002 and March 2003, profiles P7-P9 (vertical scale is exaggerated relative to horizontal scale).

First Movable-Bed Model Calibration Experiment

Because this large physical model is complex, calibration was expected to be an iterative process among the many variables and possible configurations. Past experience with movable-bed model calibration suggested the first attempt to calibrate the Half Moon Bay movable-bed model would not be completely successful. However, valuable knowledge was gained on how the model responded to wave forcing, where erosion and deposition occurred, and how laboratory and scale effects influenced the results.

The plunger-type wave machine for the first calibration experiment was oriented perpendicular to the south jetty so the long-crested waves generated by the machine propagated straight up the Grays Harbor entrance from an angle of approximately 277 deg. This approach angle characterized the predominant wave direction for the CDIP offshore buoy, but not necessarily the direction from the nearshore field wave Gauge 1 (see Figure 26). Testing began on 1 April 2004, with irregular waves represented by a TMA spectral shape and scaled to model size according to Froude scaling as described in Chapter 3. The prototype-scale target spectrum had a significant wave height of H_{mo} = 6 m with a peak spectral wave period of T_p = 16 sec. However, this condition was measured in deeper water, and wave transformation effectively reduced the significant wave height to around H_{mo} = 3 m by the time the waves reached the -20-ft mllw contour (see wave Gauge 4 in Figure 29). The wave machine was unable to generate the 6-m significant wave height, but it could generate irregular waves of height larger than those recorded at the -20-ft contour gauge. The larger waves in the wave train would break while still in the main entrance channel before even reaching a line perpendicular with the diffraction mound. Wave breaking also occurred as waves were diffracted and traveled over the submerged jetty remnant. Guide vanes were placed perpendicular to the wave machine on the north side and extended about 45 ft into the model area. These guide vanes reduced diffraction of the waves into the region of the basin to the north, and thus countered the laboratory effect due to the finite length of the wave machine.

The largest waves reaching the shoreline were along the reach extending from Point Chehalis around to about profile line P8 (Figure 8). In this region, wave heights are not reduced much by wave diffraction. The smallest waves occurred along the sheltered shoreline in the lee of the diffraction mound because the waves had undergone an almost 90-deg change of direction due to diffraction, a significant reduction in wave height, and often wave breaking across the jetty remnant.

This same irregular wave time series realization was run repeatedly in bursts of 20 min followed by about a 10- or 15-min settling time. During the first day, waves were run for a total of 150 min. The shoreline did not experience any significant recession during this first day of testing.

On the morning of 2 April 2004, a new irregular wave signal was generated that was more narrow-banded ($\gamma = 10$) with the expectation that this spectrum would contain more of the higher waves, and thus increase the slight erosional trends observed in the model. This new signal was run for a total of 180 min over the course of the day. Erosion was observed in the vicinity of profile P3, but not to the extent needed for calibration. It was concluded that sediment scaling effects were hindering the erosion, so it might be necessary to increase the wave energy by generating regular waves. With irregular waves only a few waves move the wave machine to its maximum stroke, but with regular waves maximum stroke can be used for every wave. Consequently, there is appreciably more energy in the regular wave train.

The regular wave train had a scaled wave period representing a prototype period of T = 16 sec, and a wave height of nearly H = 5 m. The regular waves were run continuously, and almost immediately an increase in movable-bed erosion was noted. Perhaps the most significant change was erosion of the profiles closest to Point Chehalis. In this region, a bar-trough was formed by the regular waves, and a significant amount of sediment was removed. This trend was counter to the results shown on the prototype profile measurements. In the vicinity of profiles P3 and P4, the rate of erosion increased, but the ultimate magnitude appeared that it would reach only about half of what was needed for calibration. Profile lines were measured on 19 April 2004. Measured dune recession at profile P3 was equivalent to only 23 ft in the prototype. This recession was well short of the 75-ft dune recession seen at Half Moon Bay.

Another unrealistic aspect of running strictly regular waves was the formation of protruding features in the Half Moon Bay planform. Apparently, the regularity of the waves and the along-crest height variation during diffraction created zones of decreased sediment mobility that resulted in buildup of salients along the shoreline. These features are contrary to the relatively smooth shape of the actual Half Moon Bay shoreline, and the salients were not formed when using irregular waves.

The large distance between the jetties permits a somewhat limited wave-angle window for waves approaching Half Moon Bay, and field observations indicated a 25-deg clockwise rotation of the wave generator would be a reasonable change in wave direction. The model was drained, and the wave machine was reoriented so it would produce long-crested waves coming at an angle of 295 deg rather than the original 277 deg. The new wave angle represented the mid-angle of the most energetic direction band measured at the field wave Gauge 1 as shown in Figure 26. This orientation was a more realistic representation of the field data, and the change of approach angle would increase the wave energy reaching the western portion of Half Moon Bay, and perhaps alleviate somewhat the excessive erosion observed closer to Point Chehalis. Testing resumed with irregular and regular waves at the end of April 2004.

In addition to changing the incident wave approach angle, the peak period was reduced from 16 to 13 sec for both regular and irregular waves. It was noticed that the shorter period waves were more effective in eroding the beach. The longer waves had a bit more wave runup, but the shorter waves seemed to bring the wave energy farther inshore before breaking.

Wave conditions were run for an additional 22 hr in the physical model. Significant erosion occurred at profile P3, and some erosion occurred at profile P4. When the testing reached the point that the rate of erosion around profile P3 had become small, it was decided to terminate the first calibration test and survey profiles. Profile lines were surveyed on 15 May 2004. Figure 34 shows the erosional development at profile P3. The final horizontal dune recession was about 65 ft with more than half of the recession occurring after the wave machine approach angle was changed. The model dune recession was comparable to that measured at Half Moon Bay between June 2002 and March 2003. Figure 35 shows the study area near the completion of the 22-hr test.

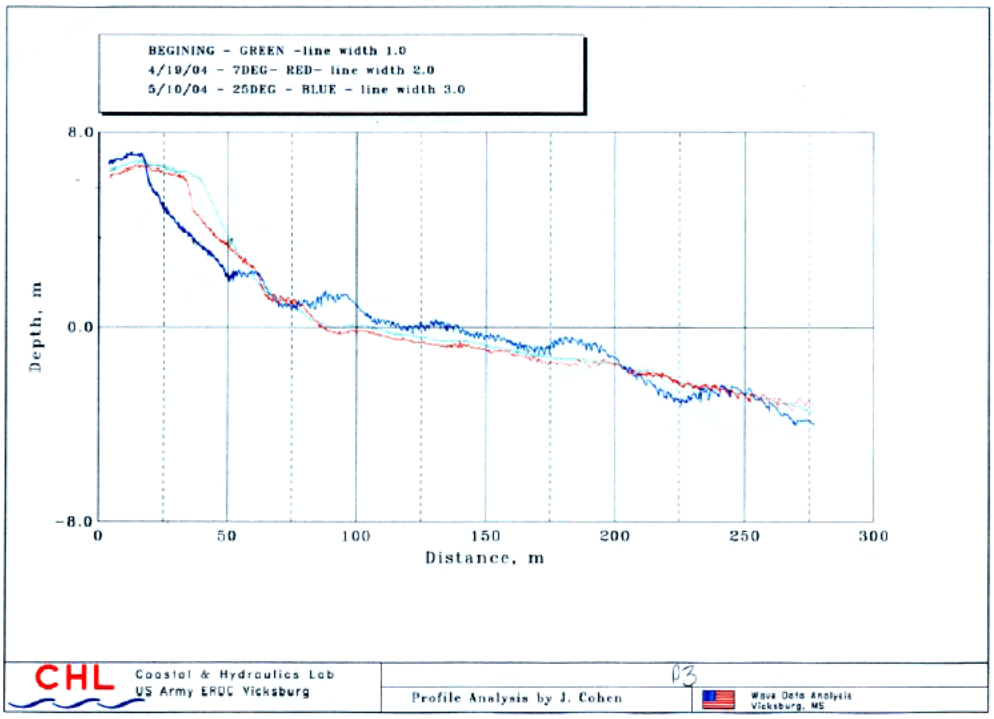

Figure 34. Erosion on profile P3 during first calibration experiment.

Figure 35. Overhead view of model near end of first calibration experiment.

Second Movable-Bed Model Calibration Experiment

In the time leading up to the start of the second calibration experiment, available water level records from Westport were analyzed for expected frequency of occurrence of extreme high tides. This analysis suggested the model be operated at the +11.0 - 12.0-ft mllw water level. The +12.0-ft mllw water level was adopted for the second calibration test.

After 1 week of remolding the movable-bed to the June 2002 bathymetry, reinstallation of the gravel/cobble transition, and surveying of initial profiles, the physical model was once again ready for testing. One of the lessons learned from the first calibration experiment was that the larger waves approaching from the 295 deg were effective in eroding the beach in the region of profiles P3 and P4; however, farther east along the shoreline there was a small buildup of shoreline position because sand moving out of the eroding area was not being distributed farther along the shore. It was discovered that altering the more energetic regular wave condition (H = 6 m and T = 13 sec) with a milder regular wave condition (H = 3 m and T = 12 sec) promoted better distribution of the sand within Half Moon Bay through improved longshore transport.

Different wave sequences were tested to find the best combination for beach/dune erosion. The 6-m, 13-sec regular wave was used to establish the overall magnitude of dune recession, and the 3-m, 12-sec regular wave established the longshore sediment transport pattern from the south jetty towards Point Chehalis. Table 5 shows the two sequences tested in the physical model.

Of the two tested options, Sequence No. 2 gave improved performance in producing recession along the shoreline and moving the eroded sand and gravel in the alongshore direction. It also was noted that the smaller regular wave condition caused less basin oscillation, so it could be run for 60 min without creating an adverse basin oscillation.

Table 5. Regular wave sequences tested during second calibration.

Wave Parameters (Prototype Scale)	Minutes Duration (Model Scale)
Sequence No. 1 (120-min run time)	
H = 6 m, *T* = 13 sec	30
Basin settling	15
H = 6 m, *T* = 13 sec	30
Basin settling	15
H = 3 m, *T* = 12 sec	60
Basin settling	10
Sequence No. 2 (90-min run time)	
H = 6 m, *T* = 13 sec	30
Basin settling	15
H = 3 m, *T* = 12 sec	60
Basin settling	10

After 5 days testing (24.5-hr total run time) dune recession at profile P3 was equivalent to 31 ft in the prototype. It appeared that more of the 6-m, 13-sec regular wave condition was needed to promote erosion of the dune. From that point on, the run plan was modified to include the 120-min Sequence No. 1 after every six of the 90-min sequences. Testing was terminated on 14 June 2004, after a total of 34.5 hr of wave action.

Figure 36 shows the western end of Half Moon Bay in the physical model at the end of testing. Note how the gravel/cobble transition has been eroded and transported eastward. Figure 37 is a close-up view of the dune recession.

The overhead view (Figure 38) shows how the gravel moved eastward along the shoreline. Figure 39 illustrates the similarity between the prototype and model beaches and dune scarps.

Figure 36. Erosion at western end of Half Moon Bay physical model (second calibration experiment).

Figure 37. Dune scarp and gravel/cobble removal between profiles P2 and P3 (second calibration experiment).

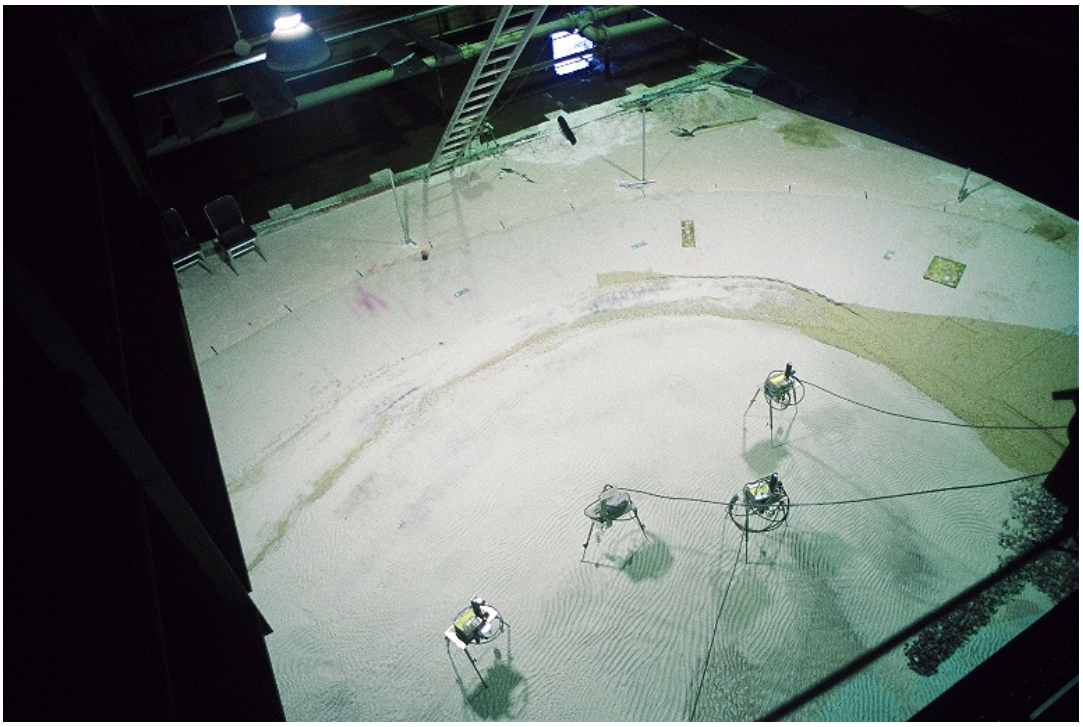

Figure 38. Overhead view of physical model after second calibration experiment.

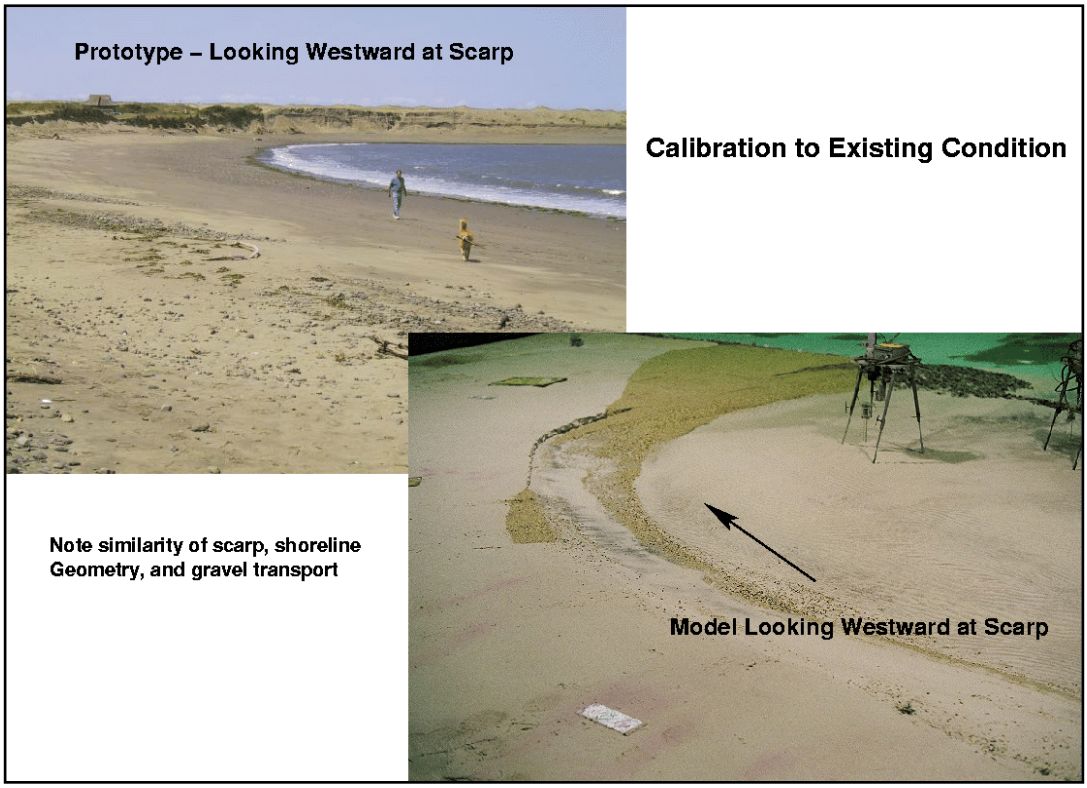

Figure 39. Similarities between prototype and model beach and dune scarp (second calibration experiment).

Final dune recession at profile P3 in the model was the equivalent of 60 ft in the prototype. This is less than the target recession of 75 ft; but given the known sediment scaling effect, this was considered to be a reasonable result for similarity of dune recession. The markers (plus signs) in Figure 40 show the final dune recession positions for positions located between profiles P1 to P5 in the physical model compared to the prototype 2003 shoreline recession shown by the solid line labeled "Shore 2003." (The seaward solid line is the 2002 shoreline, defined as the intersection of the beach with normal high tide level.) Beach scarp erosion in the region between profiles P1 and P4 shows reasonable correspondence to observed erosion that occurred at Half Moon Bay between June 2002 and March 2003.

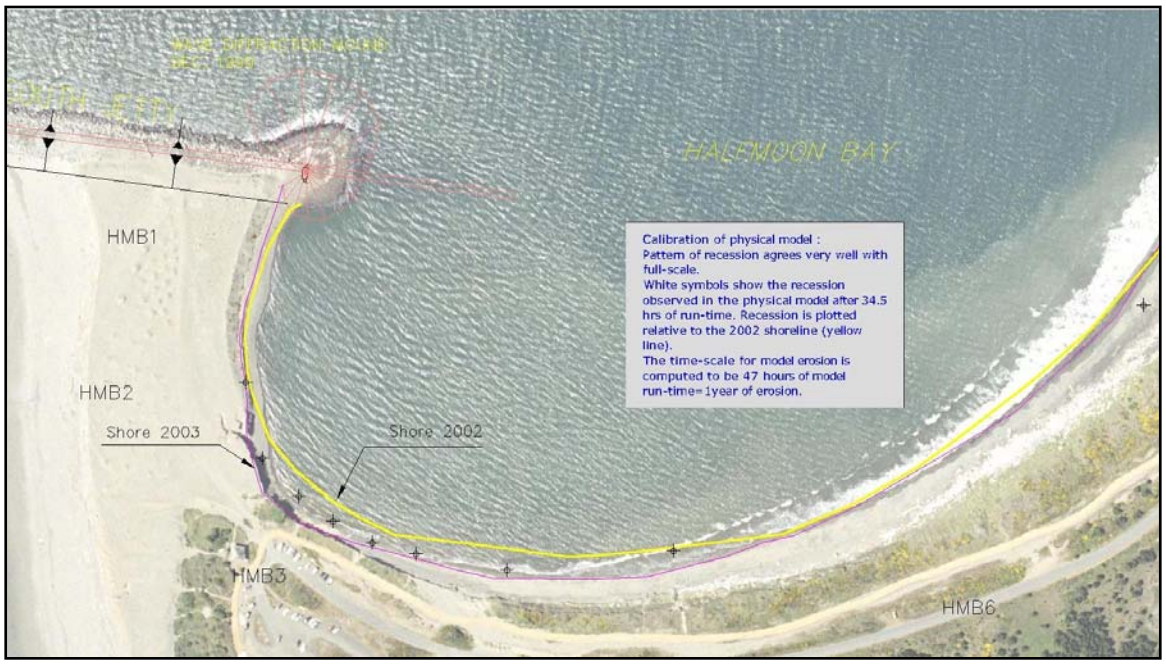

Figure 40. Shoreline recession in physical model compared to 2003 shoreline (photograph date 16 June 2003).

Profiles P1 through P9 were surveyed in the physical model at the end of the second calibration experiment, scaled up to prototype units, and plotted along with the prototype profiles from June 2002 and March 2003. Comparisons for profiles P1-P3, profiles P4-P6, and profiles P7-P9 are given in Figures 41, 42, and 43, respectively.

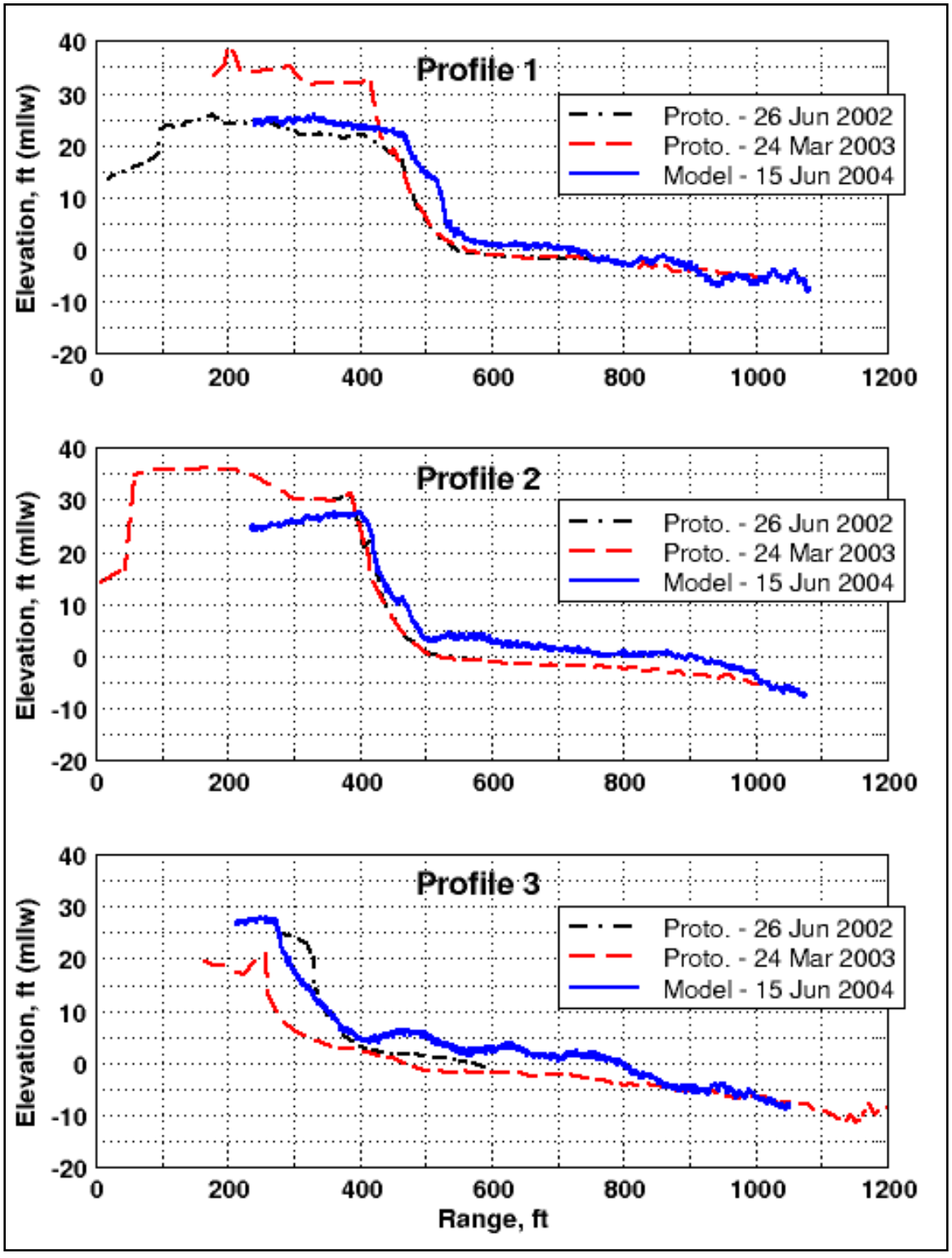

Figure 41. Prototype to model comparison – Profiles P1, P2, and P3 (vertical scale is exaggerated relative to horizontal scale).

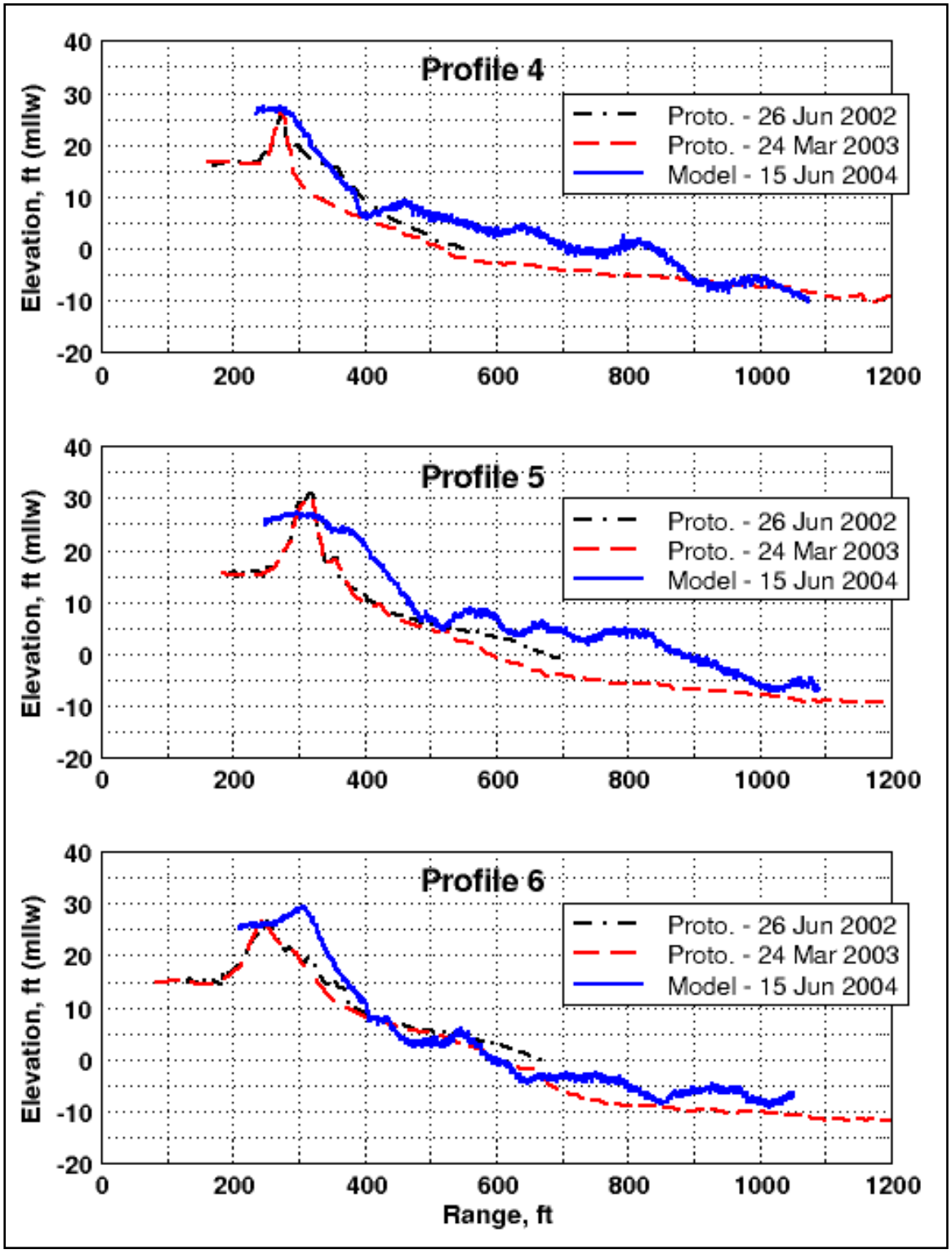

Figure 42. Prototype to model comparison – Profiles P4, P5, and P6 (vertical scale is exaggerated relative to horizontal scale).

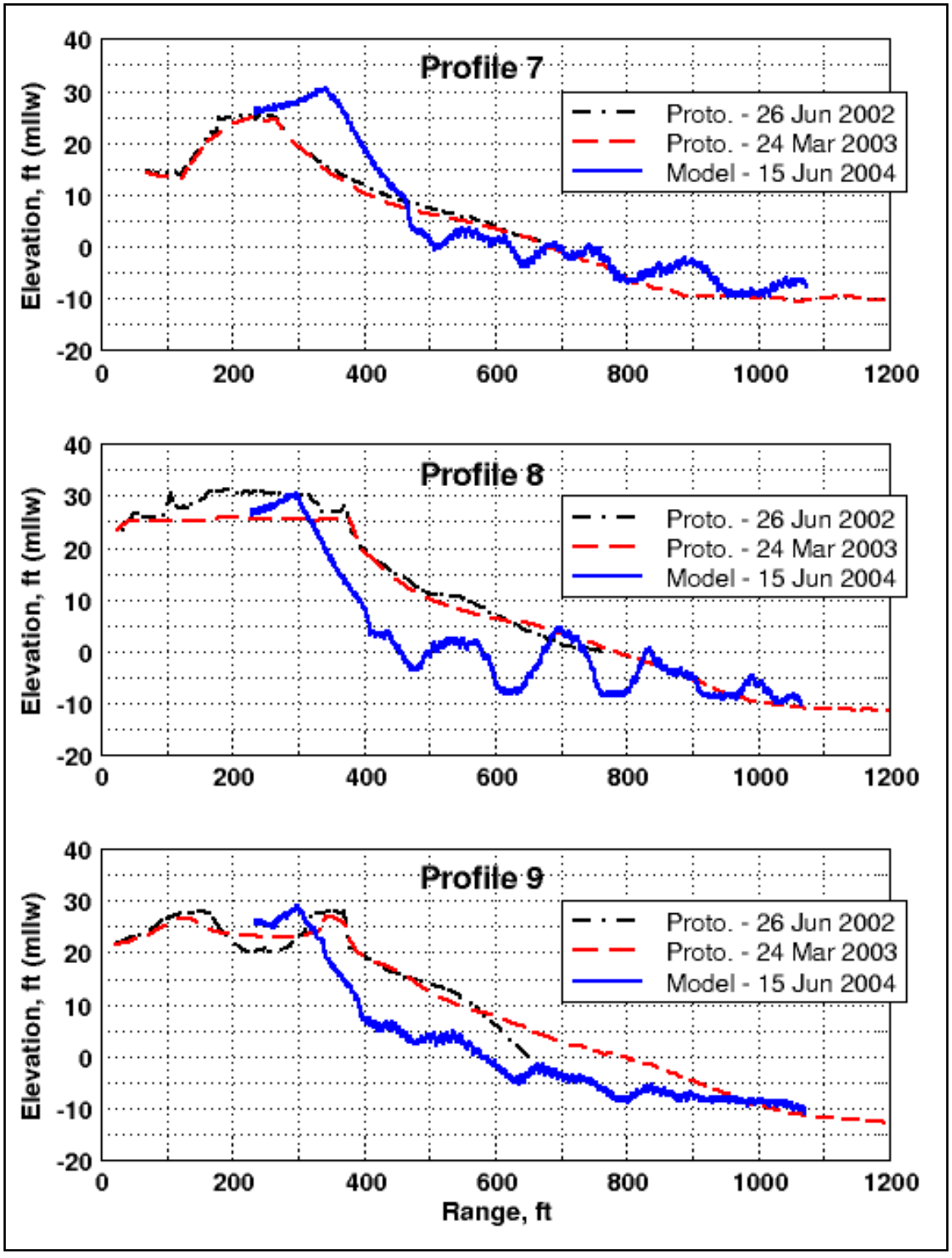

Figure 43. Prototype to model comparison – Profiles P7, P8, and P9 (vertical scale is exaggerated relative to horizontal scale).

In the western end of Half Moon Bay, the profiles exhibited erosion where expected. Profile P1 is protected by the gravel/cobble fill placement, and little erosion occurred on this profile. However, the upper plot of Figure 41 indicates accretion in the model that is incorrect, and this was most likely due to an error in locating the model profile in Washington State Plane coordinates. Profile P2 shows no recession, but there was some sand accretion between +5 ft and -5 ft mllw.

Dune recession at profile P3 was about 15 ft short of the target recession, considered a reasonable result, but the profile comparison indicates that there was insufficient erosion of the beach face between elevations +15 ft down to +5 ft mllw. It was hypothesized that the lack of sufficient profile erosion at profile P3 might be caused by conducting the simulation at a constant storm water elevation. In the prototype, the beach profiles would continue to be cut downward as the storm ended and the water level fell to normal levels. As the water level fell, sediment would be moved farther seaward. In fact, the lowering of the beachface portion of the profile in the prototype may have occurred over a fairly long time. Because of time constraints, variable water level was not simulated in the physical model, so the hypothesis remains unproven.

Profile P4 experienced considerable variability over the course of the experiment as salients built up during the more energetic waves and were subsequently removed during milder wave sequences. The upper plot of Figure 42 indicates some dune recession, but not as much beach erosion as observed in the prototype. Sand eroded from other parts of the model was deposited on profile P4 between +10 ft and -5 ft mllw. A constant storm surge water level, and the fact that bedload transport is deposited sooner in the model than it should, probably contributed to the profile P4 differences.

The prototype comparisons between June 2002 and March 2003 showed little difference for profiles P5 through P9. Because these profiles are more exposed to both storm waves and everyday normal wave action, there is a possibility that severe erosion may have occurred during storms in that time period, but recovery of the profiles took place before profiles were surveyed, thus masking the storm impact. In the physical model profiles P5, P6, and P7 showed accretion of the dune and upper beach, whereas profiles P8 and P9 showed greater erosion than expected. This was an unexpected result that appears to be tied to regular waves approaching

from a nearly shore-normal direction, and an unrealistically strong longshore current moving toward Point Chehalis.

The regularity of the waves incident to the beach in the eastern end of Half Moon Bay formed a pronounced bar-trough system, indicating turbulent water motion with suspended sediment transport being a significant portion of the overall sediment transport. Sand thrown into suspension was more easily transported by the abnormally strong alongshore current. A large quantity of sand from the reach between profiles P6 and P9 was swept past Point Chehalis and deposited farther north in a portion of the basin where wave action was not correctly simulated. The longshore current is analyzed in the following section.

In summary, the second calibration experiment was not fully successful because the model did not adequately reproduce the same profile development as observed in the prototype at Half Moon Bay. In the western end of the bay, the profile recession was similar to that observed in the prototype, but the profiles did not cut down vertically far enough. It was hypothesized the excess vertical elevation of the profiles stemmed from running the model only at the higher water level. In nature, the wave action with falling water level would move sediment on the beach face to a lower location on the profile, and this process would have continued for several months. Time constraints in the physical model did not permit longer simulations. However, dune recession in the western end of the bay did reasonably approximate the field observations, and this recession indicated that the wave test sequences were a reasonable simplification of the actual history of waves that caused the erosion during the period June 2002 to March 2003.

In the eastern portion of Half Moon Bay, some profiles exhibited too much accretion above +10 ft mllw, and excessive erosion of the profiles closest to Point Chehalis. This nonsimilarity was thought to be caused by excessive longshore current magnitudes. Tests conducted after the calibration revealed this current was a laboratory effect that could be corrected for subsequent testing.

Model Longshore Current in Eastern Half Moon Bay

During the latter stages of the second calibration experiment, engineers became aware of excessive erosion of profiles closest to Point Chehalis (see Figure 43). The discrepancy between model and prototype erosion was thought to be caused by the strong alongshore current moving sand north-

ward past Point Chehalis and out of the testing area. Dye placed in the nearshore region confirmed the strong current velocities.

After conclusion of the second calibration test, both regular wave conditions used in the calibration (see Table 5) were run in the basin, and shore-parallel current measurements were made in the model at the locations of model wave Gauges 6 (offshore) and 7 (nearshore) as detailed in Figure 29. The current was measured with a Nixon micro-impeller meter that averaged velocities over 10-sec model time (71-sec prototype scale). Because only one current meter was available, the test had to be run twice to obtain measurements at both the nearshore and offshore locations.

Figure 44 plots the shore-parallel current magnitude at both locations for the more energetic H = 6-m, T = 13-sec regular wave condition. Current magnitude and time have been scaled to equivalent prototype values. Initially, the current was stronger at the onshore gauge location; but after about one-third of the run, the current had become stabilized at a magnitude of about 0.9 m/sec (prototype) at both locations. This magnitude was about twice as large as field measurements acquired at the location of the nearshore gauge position. Measurements obtained in the model for the less energetic H = 3-m, T = 13-sec regular wave condition revealed no significant longshore current, thus indicating that wave height played a key role in current generation.

It was concluded the model current was a scale effect caused by a wave height differential along the wave crests. Wave diffraction at the northern end of the wave generator (farthest away from Half Moon Bay) was minimized by the vertical wave guide placed perpendicular to the wave crests. However, at the terminus of the wave guide, the waves then started to diffract into the quiescent region of the basin, setting up an along-crest height differential. This height differential created a longshore current flowing northward parallel to the wave crests. Because this same physical mechanism does not exist in the prototype, the current observed in the laboratory is a laboratory effect that needed to be corrected or minimized. The laboratory effect first manifested itself at the onshore location where the along-crest height variation was maximum. Over time, momentum transfer between the nearshore and offshore positions equalized the current, so the magnitude was similar at both locations.

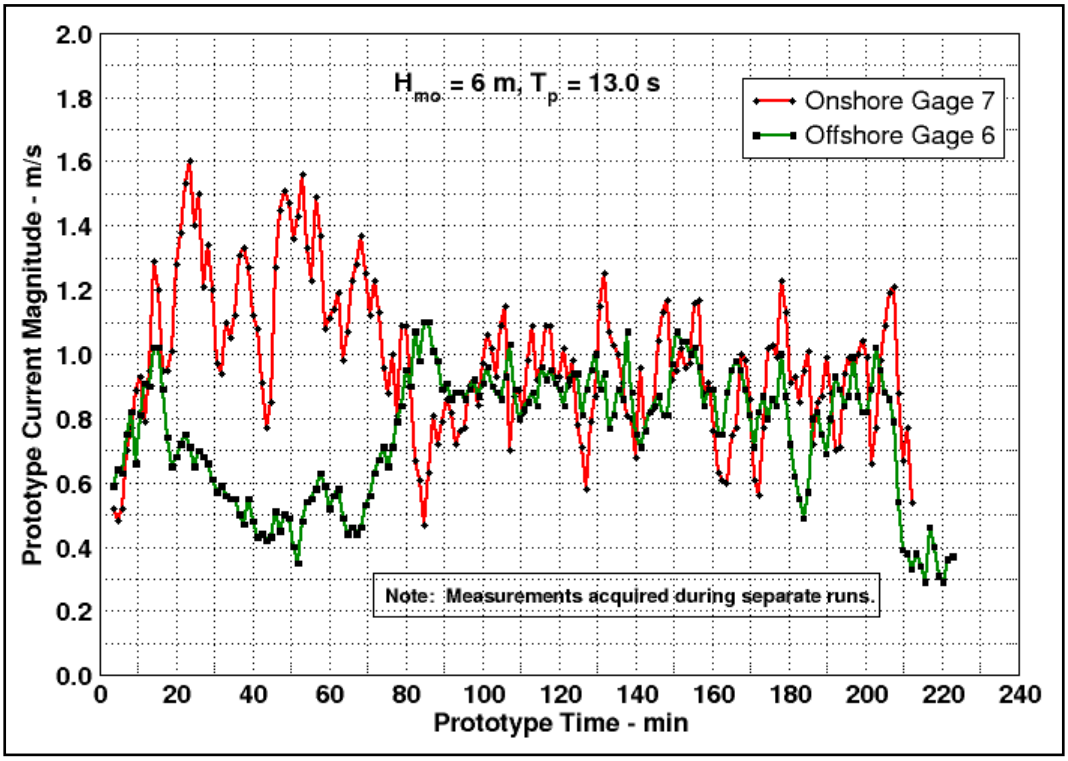

Figure 44. Measured physical model longshore current near Point Chehalis.

Rather than extending the wave-guide landward, an artificial barrier constructed of rubberized horsehair mats was placed as a groin-like structure extending seaward from Point Chehalis and oriented toward the end of the wave machine. Subsequent current and dye measurements indicated this barrier had effectively reduced the unrealistic alongshore current to a minimum with a slight seaward-directed current running parallel to the barrier. Placement of the horsehair barrier was too late to benefit the calibration testing, but it did provide better model response in the eastern portion of Half Moon Bay during evaluation of the existing condition (see Chapter 7).

7 Evaluation of Existing Half Moon Bay Condition

This chapter describes an experiment aimed at evaluating the expected long-term evolution of Half Moon Bay under the assumption that no additional engineering modifications, such as hard structures or beach fills, are made in the future. Expectation at the beginning of the experiment was that the recession position established as the stable beach planform shape in the model would be less than would occur in nature due to sand-transport scale effects and the fact that the model simulated only one water level elevation. In other words, the general planform shape would be reasonably accurate, but the ultimate recession at Half Moon Bay would be greater than estimated by the physical model. The results from this experiment could also serve as the baseline for comparison in the physical model of any engineering alternatives that might be developed if the LTMS deems such comparisons are warranted.

Experiment Setup

At the end of the second calibration experiment, tests were conducted to correct the abnormally strong longshore current near Point Chehalis (see Chapter 6). Installation of a barrier constructed out of rolled rubberized horsehair absorber material extending seaward from Point Chehalis solved the problem and greatly reduced the amount of sand moving past the Point Chehalis revetment. Figure 45 shows the horsehair barrier that was directed seaward on an alignment with the end of the wavemaker. (In the foreground of the photograph note the sand that had overwashed the revetment.)

Figure 45. Barrier structure off Point Chehalis used to reduce strong longshore current.

The success of alternating between 6-m and 3-m regular wave trains during the second calibration runs prompted engineers to develop a viable irregular wave signal with a zeroth-moment wave height of H_{mo} = 3 m and peak period of T_p = 13 sec. Alternating the irregular wave train with the more energetic regular wave train would provide a smoother shoreline response than using only regular wave sequences. The drawback to substituting the irregular wave signal in the run sequence was the longer time required for movable-bed evolution under irregular waves. Wave tests were conducted and measurements acquired to confirm the wavemaker could generate the target wave height in the model. Figure 46 presents a typical measurement of the 3-m, 13-sec irregular wave train measured at model wave Gauge 4 (see Figure 29). Parameter values given for the measured wave spectrum are in model dimensions.

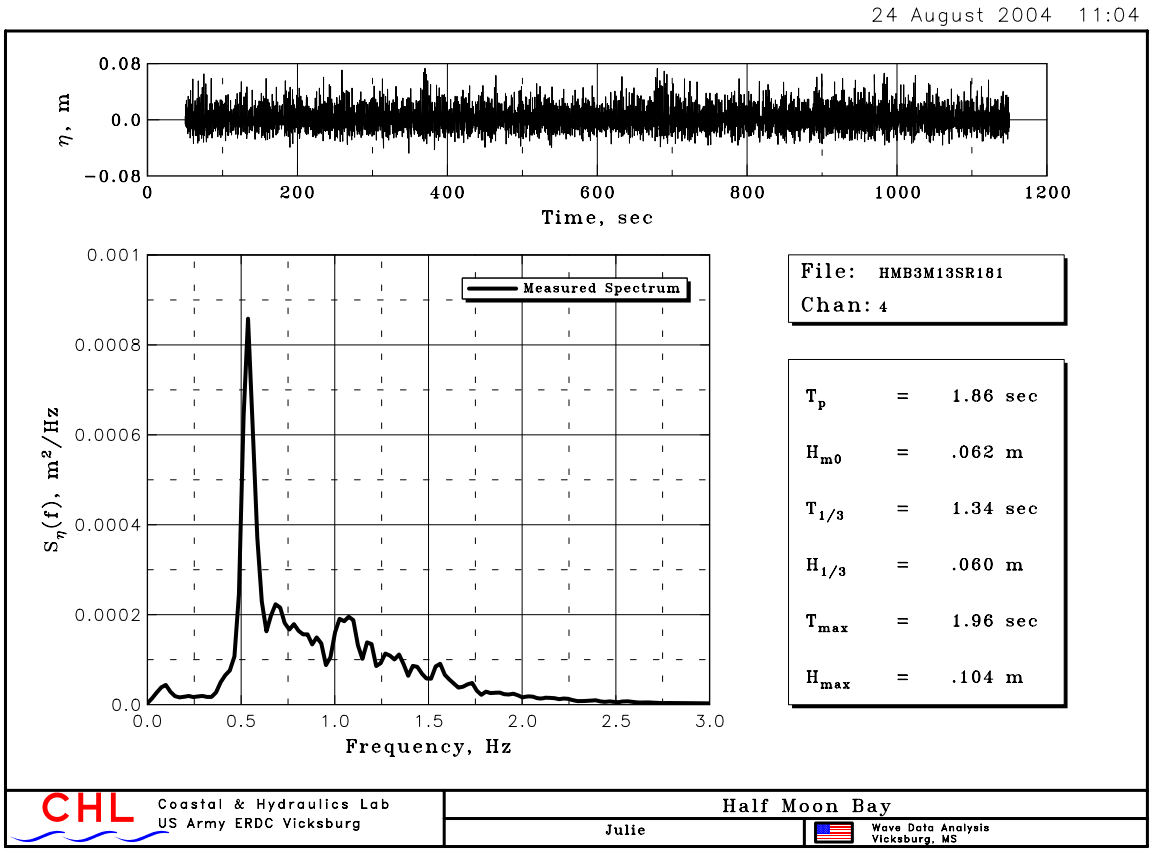

Figure 46. Analysis of irregular waves measured at model wave Gauge 4.

The movable bed portion of the physical model was remolded to the June 2002 configuration, and the gravel transition beach was reconstructed during the third week of July 2004. Profiles P1-P10 were surveyed prior to placement of the nearshore wave gauges in the arrangement shown in Figure 29 in Chapter 5.

Throughout testing of the long-term evolution of the existing Half Moon Bay condition, waves in the physical model were run according to the sequence listed in Table 6. The higher energy, more erosive regular waves were run for only 20 min of every 80-min cycle with the irregular waves acting for 60 min of the cycle. In addition to being more realistic, the irregular waves kept the shoreline, dune scarp, and submerged bathymetry smoother than if only regular waves had been used.

Table 6: Wave sequence used during evaluation of existing condition.

Wave Parameters (Prototype Scale)	Minutes Duration (Model Scale)
Sequence (80 min run time)	
Regular wave H = 6 m, T = 13 sec	20
Basin settling	15
Irregular wave H_{mo} = 3 m, T = 13 sec	20
Basin settling	10
Irregular wave H_{mo} = 3 m, T = 13 sec	20
Basin settling	10
Irregular wave H_{mo} = 3 m, T = 13 sec	20
Basin settling	10

Experiment Results

The model was flooded up to the +12-ft mllw storm surge elevation (prototype equivalent) on 27 July 2004 and subjected to repetitive wave sequences described in Table 6 until 18 August 2004. Over this time span the Half Moon Bay model was exposed to waves for a total of 67 hr. Twenty-five percent of the waves were the more energetic 6-m, 13-sec regular waves, and 75 percent were the less energetic (but more realistic) 3-m, 13-sec irregular waves. This resulted in smoother profiles and more uniform shoreline recession than was seen during the calibration experiments. However, the penalty for using irregular waves was a slower recession rate. Figures 47 through 52 show photographs of the physical model taken on 19 August 2004 after the basin had been drained.

Figure 47 shows the overall recession in the western end of Half Moon Bay. The gravel/cobble protection had been substantially eroded and transported along the beach in an eastward direction. The gravel transition erosion is also evident in the photograph of Figure 48. Once the gravel/cobble protection was removed, the underlying sand was exposed to wave action, and it might be expected that the rate of dune recession would increase. Measurements indicated a slight increase in the rate of recession in the exposed areas, but it was not a substantial increase. This could be a sign that the beach in this area of the model was already near an equilibrium state.

The photographs of Figures 49 and 50 show closer views of the gravel/cobble erosion. The pair of pink survey flags nearest to the camera in Figure 49 mark the original end of the gravel/cobble transition in the model. These are the same flags shown in Figure 50. Because gravel trans-

port meets the model similitude requirements, similar gravel movement should be expected in nature under the same hydrodynamic conditions.

Figure 47. Overhead view of western end of Half Moon Bay.

Figure 48. View from navigation channel looking across diffraction mound.

Figure 49. Erosion of gravel transition region.

Figure 50. Head-on view of gravel transition erosion.

Figure 51. Gravel/cobble transport eastward toward Point Chehalis.

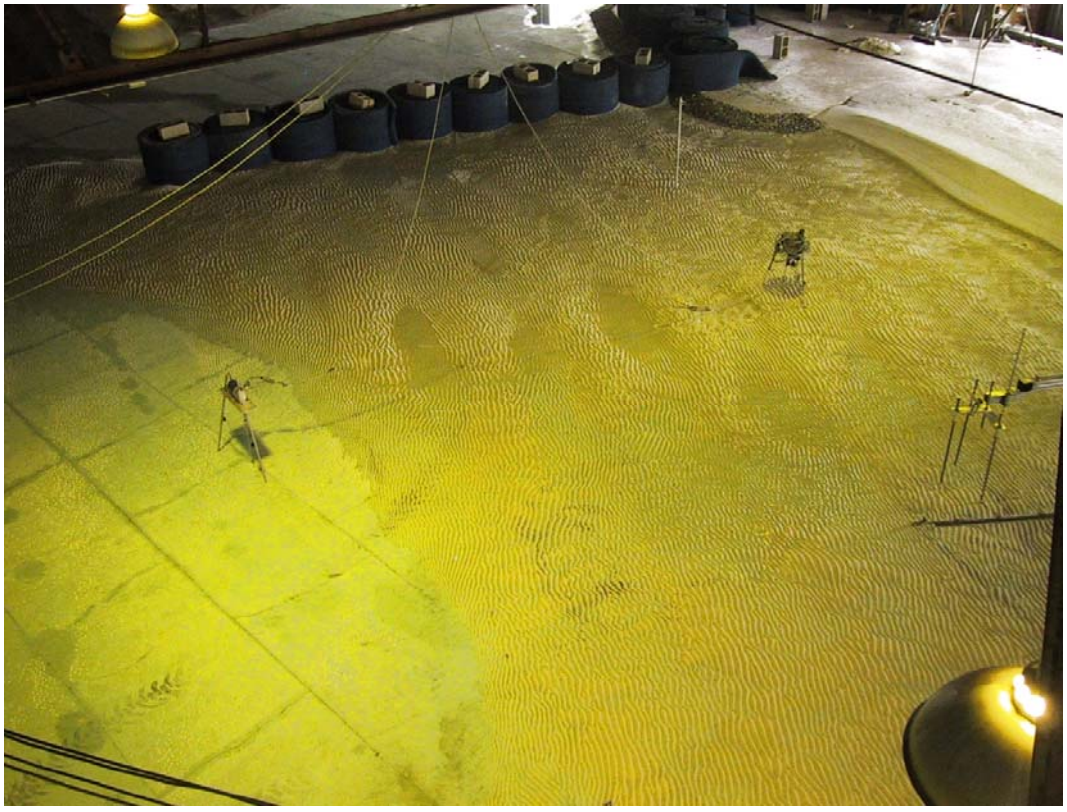

Figure 52. Overhead view of bottom evolution in vicinity of Point Chehalis.

The extent of gravel/cobble transport eastward toward Point Chehalis is evident in Figure 51. The two survey flags mark the original end of the gravel in the model. Most of the gravel and cobble was transported and deposited along a path that roughly corresponded to the elevation of the wave rundown. Some of this deposit would be at elevations above the normal tide range in Half Moon Bay. A lesser quantity of gravel/cobble was deposited at the wave runup limit at the toe of the dune scarp.

The barrier placed at Point Chehalis to reduce the laboratory effect of excessively strong longshore current effectively prevented sand from moving northward past Point Chehalis. Instead, the sand was either deposited at the barrier, or moved seaward along the barrier to be deposited in deeper water. This offshore deposition is shown in the overhead view of the Point Chehalis region in the model in Figure 52. Point Chehalis is in the upper right corner. Despite the placement of the barrier, the profiles near Point Chehalis exhibited the same downward cutting as seen in the second calibration experiment. Prototype survey comparisons do not indicate a similar profile downcutting, and this may be due to periodic placement of dredged material in Half Moon Bay that feeds the beach in the vicinity of Point Chehalis.

Dune Recession

Dune recession relative to the model baseline was recorded at 12 locations around Half Moon Bay. Figure 53 shows the final model recession line (in red) measured on 18 August 2004. Also shown in the figure are the June 2002 (yellow) and March 2003 (purple) shorelines measured in the field. (Note that shoreline refers to the approximate intersection of the beach and normal high-tide level, whereas dune recession is the cutback of the dune.)

The model recession line (scaled to prototype dimensions and referenced to Washington State Planes coordinates) approximates the vegetation line shown in the photograph dated 16 June 2003. Between profile lines P3 and P5, recession in the model was beyond the vegetation line, indicating additional erosion will occur in this region of Half Moon Bay.

During testing of the existing condition, daily measurements were made of the dune recession relative to the model baseline. These measurements were plotted to give an indication of the experiment progression toward a possible equilibrium of the shoreline planform in the model. Figure 54 shows the recession plots for 12 locations identified in Figure 53.

Recession is given in equivalent feet in the prototype whereas time is hours of model run time.

Figure 53. Final model shoreline recession for existing condtion at Half Moon Bay (16 June 2003).

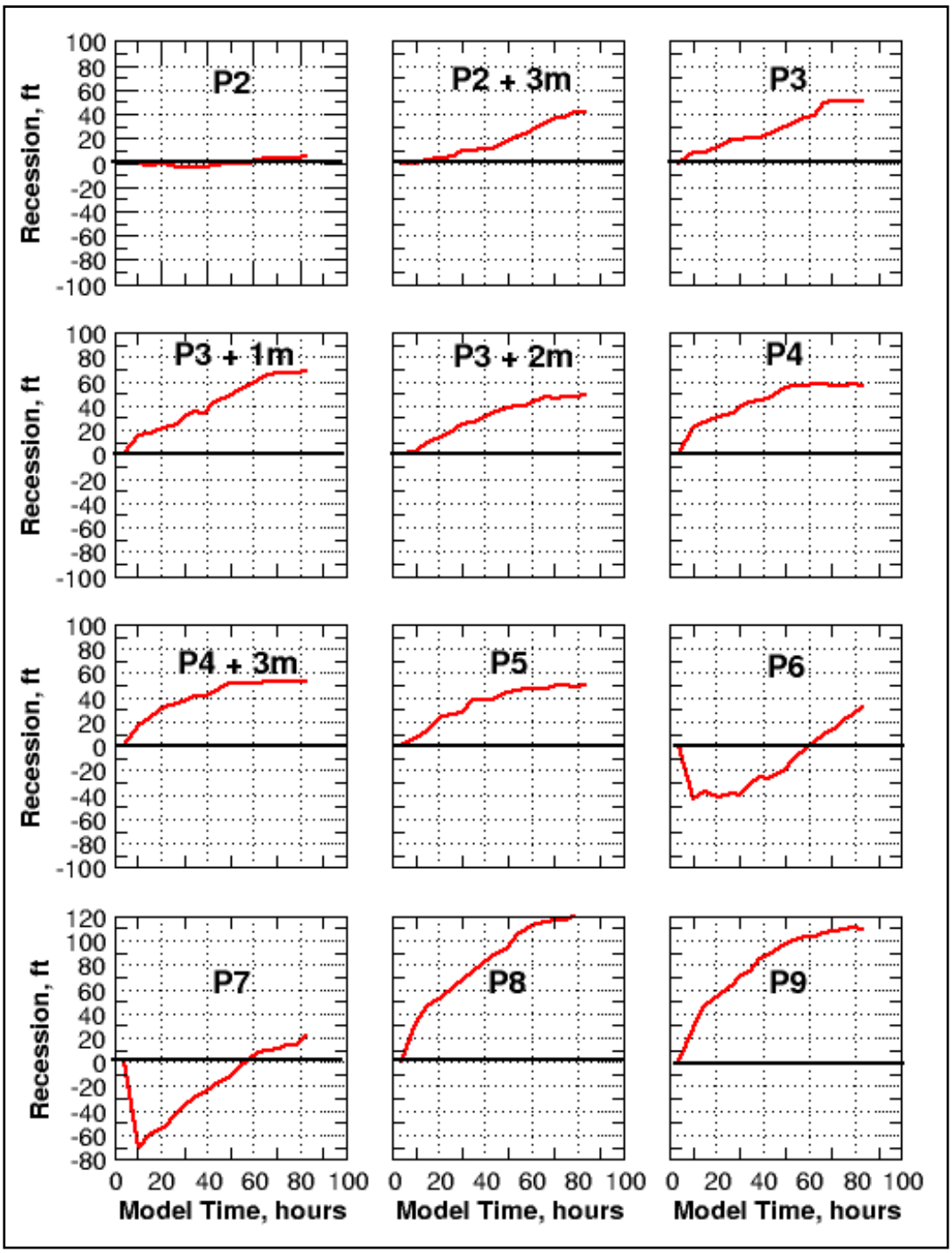

Figure 54. Dune recession during testing of existing condition (scaled to prototype dimensions).

Location P2 was closest to the diffraction mound, and diffracted waves were so small that hardly any gravel/cobble was eroded from this profile. Locations P2+3m and P3 were originally armored with the gravel/cobble protection, but the waves eroded a significant quantity of material and recession occurred at a nearly constant rate. When profiles were measured

on 19 August, 2004, the recession rates at P2+3m and P3 had not leveled out to indicate an equilibrium. The recession rate at location P3+1m was higher than most locations in the western portion of the bay, and equilibrium under fixed water level and wave conditions was not reached by the end of the experiment for this location.

Recession rates at locations P3+2m, P4, P4+3m, and P5 were similar, but at these locations the leveling off of the recession curves indicated an equilibrium position had been reached. Locations P6 and P7 exhibited strange behavior by first accreting and then receding to about the same position. This was probably related to the rapid recession seen at locations P8 and P9 that are closest to Point Chehalis. The eastern portion of the bay has the most exposure to large waves, and dune recession was rapid. This exposure is why the extension of the Point Chehalis revetment was needed. As mentioned in Chapter 6, the severity of beach erosion that occurred during the June 2002 and March 2003 period might have been obscured by subsequent beach recovery before profiles were surveyed in March 2003. This hypothesis remains unproven at this time.

Profile Development

Profiles surveyed in the physical model on 18 August 2004 were scaled to prototype dimensions, referenced to the Washington State Plane coordinate system and plotted. Figures 55, 56, and 57 present the model profiles along with the initial profiles and the field-surveyed profiles of March 2003. Overall, the erosion seen during the existing condition test was similar to that of the second calibration run. Profiles P1 and P2 saw virtually no erosion, as seen in Figure 55; but significant erosion occurred at Profile P3. Once again, the model profile did not erode as deeply as in the prototype. However, model Profiles P4 and P5, shown in Figure 56, closely resembled the prototype profiles with slightly more dune recession seen in the model.

Profiles P6 and P7, shown in Figures 56 and 57, respectively, ended with no dune recession after first accreting during the first early stages of the experiment. However, profile P7 had significant profile erosion, as did profiles P8 and P9 (Figure 57).

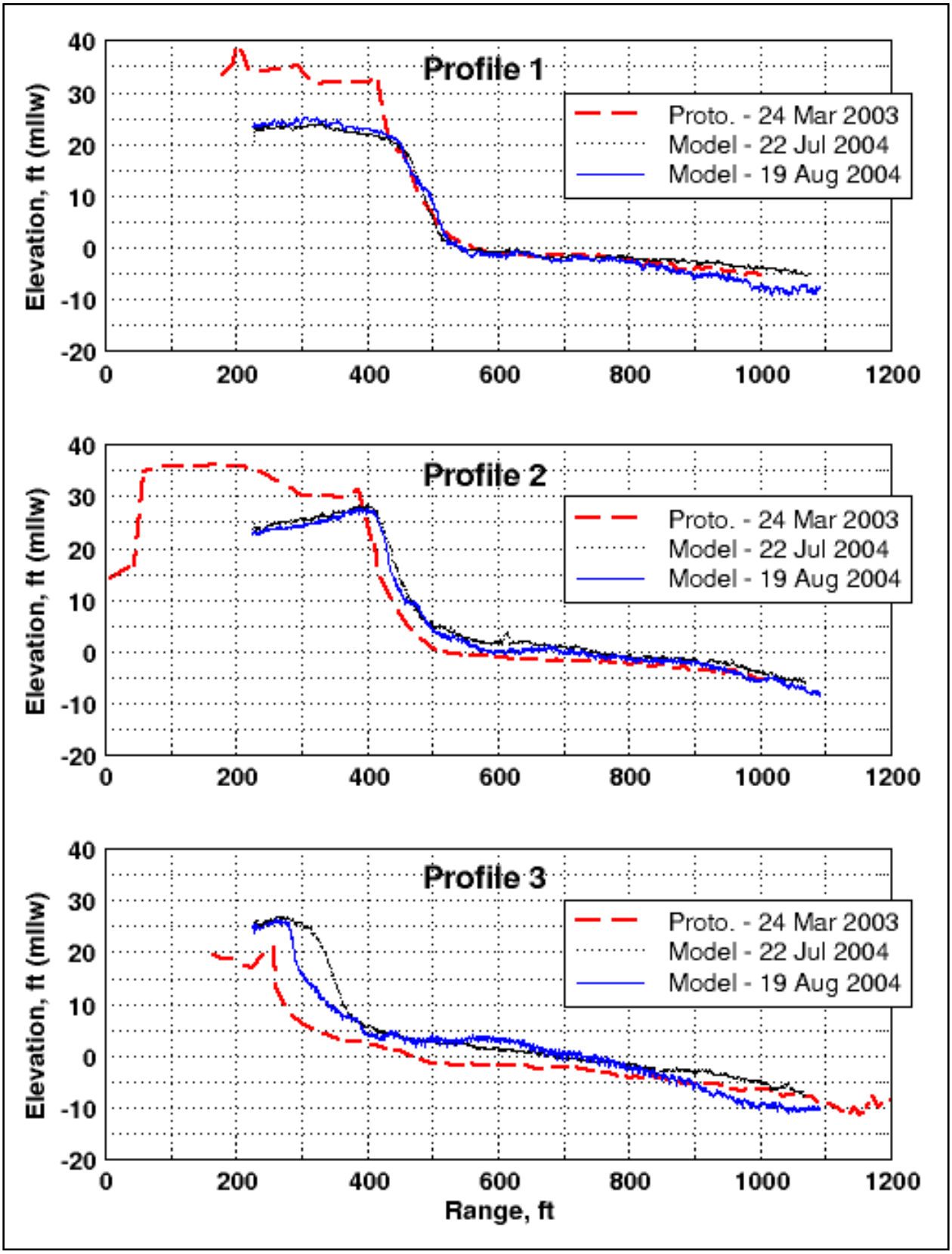

Figure 55. Existing condition test profile comparison, profiles P1, P2, and P3 (vertical scale is exaggerated relative to horizontal scale).

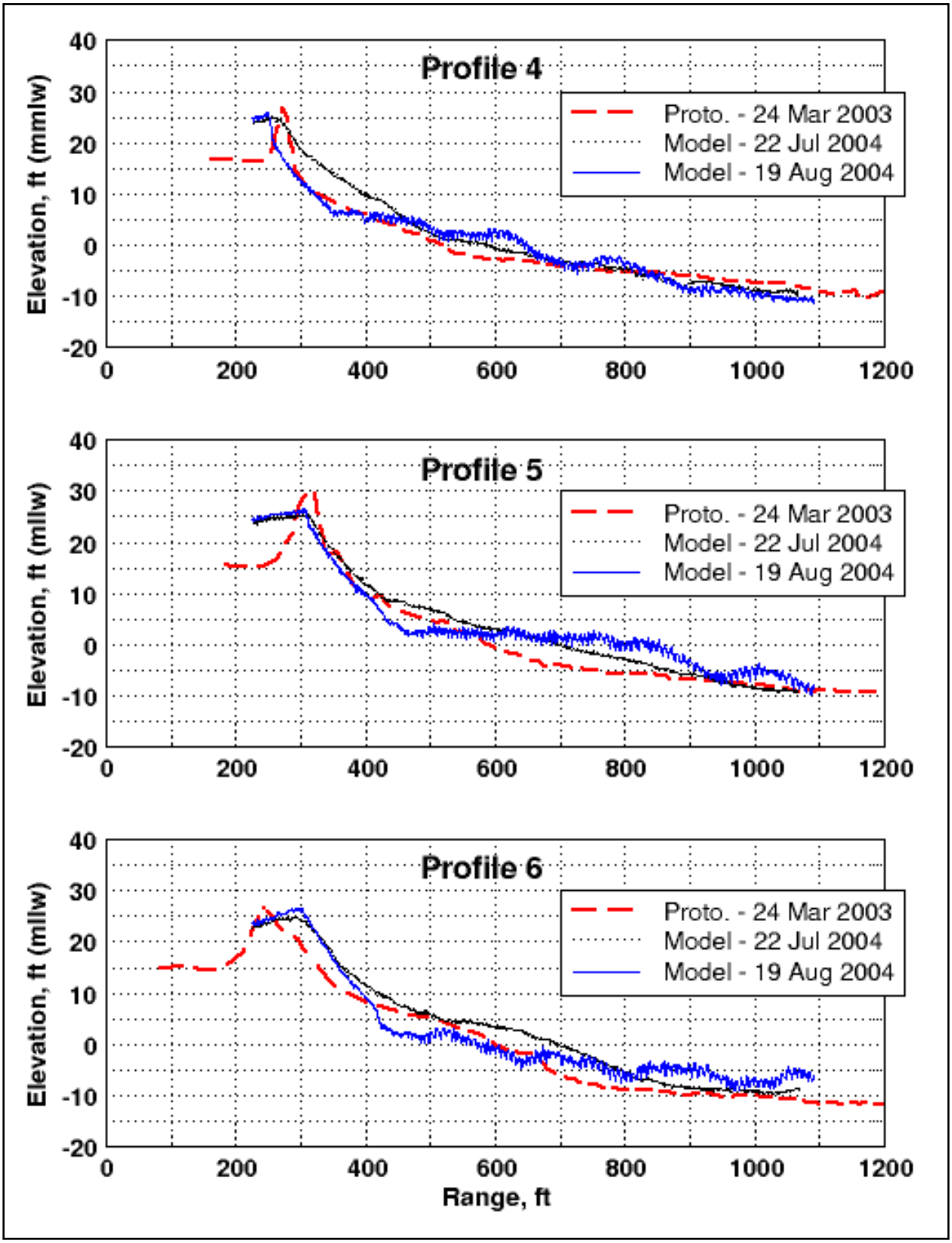

Figure 56. Existing condition test profile comparison, profiles P4, P5, and P6 P3 (vertical scale is exaggerated relative to horizontal scale).

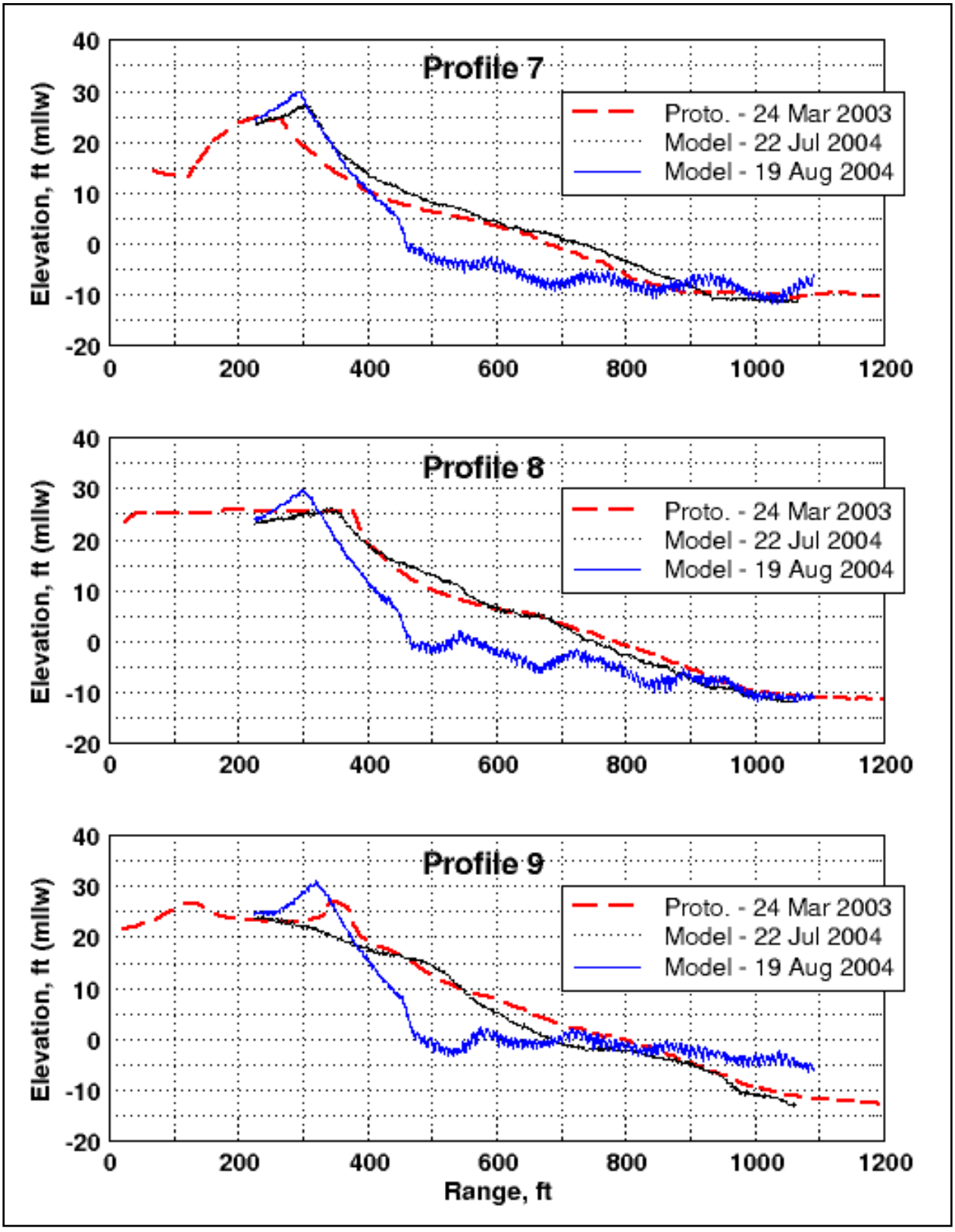

Figure 57. Existing condition test profile comparison, profiles P7, P8, and P9 P3 (vertical scale is exaggerated relative to horizontal scale).

Interpretation of Physical Model Results

Storm waves entering Grays Harbor with an approach direction of 295 deg attacked the Half Moon Bay model shoreline at a storm surge elevation equivalent to +12 ft mllw in the prototype. The model began with the movable bed molded into the field-measured June 2002 shoreline and profile configuration. Erosion occurred on most profile lines at an approximately constant rate until near the end of the experiment when dune recession slowed or stopped at several locations. However, measurement locations in the western end of Half Moon Bay were still eroding at a low rate, and the experiment was continued until dune recession in the model was not occurring at most locations.

Dune recession in the model for Half Moon Bay, as plotted in Figure 53, matched the existing vegetation line at most locations, with some additional erosion appearing past the existing vegetation line in the vicinity of the access road and restroom facility. Recession in the model on the order of 80 ft from the June 2002 dune crest position has already been experienced at Half Moon Bay, that the model reproduced the essential shore behavior of what had already occurred. Because of the relatively good replication in the model of the known erosion, the model is considered to be correctly simulating the erosion process to a reasonable extent given the simplified hydrodynamic forcing. The final shoreline position in the model is most likely still seaward of where it would be in the prototype if subjected to the same storm conditions and surge levels.

This physical model simulation is a simplification of complicated erosion processes that have historically modified the morphology of Half Moon Bay. After formation in 1946, Half Moon Bay continued to enlarge between 1946 and 1993, requiring the construction of the Pt. Chehalis revetment and revetment extension. Sand transported into the bay after the 1993 breach partially filled the bay, and 1994 to 2004 was a period of readjustment to the breaching. The apparent stability of the vegetation line of Half Moon Bay may have been due to the protection provided by the material that was deposited in the bay during the breach. The Seattle District gave the following summary of District analyses and activities that have influenced the Half Moon Bay morphology.[1]

[1] Mr. Dennis A. Fischer, Chief, Civil/Soils Section, U.S. Army Engineer District, Seattle, 20 December 2004.

> "Long-term volume change analysis indicated that since 1995, approximately 60,000 yd^3/year eroded from the shoreline area above -10 ft mllw and 100,00 to 200,000 yd^3/year eroded from the area below -10 ft mllw. Placement of maintenance-dredged material (in the -10 to -20 ft mllw depths) at an average annual rate of about 225,000 yd^3/year probably has prevented the nearshore recession rate from being higher. It is not known whether the shoreline and dune locations of 2004 have approached equilibrium."

However, the Half Moon Bay shoreline has exhibited the classic open-coast crenulate-bay planform (Silvester 1991) for many years. Significant change in the planform shape of the shoreline occurs when the hard points that define the crenulate shape are changed, and thus, cause an increase in longshore sand transport. Storms and high-water levels can cause a landward migration of the planform shape by eroding the beach and dune, transporting the material seaward. The breach of 1993 was one instance where the bay planform shape adapted in response to boundary hard point change, and the other recent change was when the diffraction mound was constructed and the jetty terminus was lowered in 1999. Between 1999 and 2004, the western end of Half Moon Bay experienced erosion as the bay adapted to the changed anchor point at the eastern end of the south jetty. This adjustment necessitated placement of the gravel/cobble transition beach to stem further erosion of the breach fill between the bay and South Beach.

The erosion that occurred in the western end of the bay between 2002 and 2004 has remolded Half Moon Bay toward a new planform shape, and the physical model reproduced similar dune recession as observed in the prototype. However, known scale effects dictate that additional shoreline recession should be expected at Half Moon Bay beyond that given by the model for the same water level and wave conditions run in the model simulation. Erosion in the physical model would have been greater if the storm waves acted at a storm surge level greater than +12 ft mllw, and dune recession would have been more pronounced. Waves occasionally overtopped the Point Chehalis revetment in the model, and higher water levels would have had greater overtopping volumes. No additional sand was added to the physical model during the simulation, whereas dredged material is added periodically to Half Moon Bay. The placed sand may

nourish the beach near Point Chehalis, resulting in less erosion of the profile than observed in the physical model.

In summary, if the Seattle District continues placement of dredged material in the subaqueous regions of Half Moon Bay, and breaching of the breach fill between the bay and South Beach is prevented, the planform shoreline shape should reach a stable configuration similar to its existing shape. However, if the bay is subjected to an extended storm acting at the +12 ft mllw elevation, the entire planform shape is expected to translate landward of the position predicted by the physical model because the model had scale effects associated with sand transport. Additional landward recession due to cross-shore sand transport is expected for storms with water levels greater that +12 ft mllw. The bay shoreline adjacent to the breach fill and protected by gravel/cobble remained stable in the physical model, so any new breaching will be largely a result of erosion and dune recession from the Pacific Ocean side.

Cumulative shoreline change over longer time periods will be a result of individual storms followed by longer periods of milder waves that reshape the nearshore bathymetry, but cannot replace eroded dunes. The movable-bed physical model was only capable of examining the response of a single storm event of a given magnitude acting at a static water level of +12 ft mllw. Consequently, this single test cannot be referenced to predict the long-term location of the Half Moon Bay shoreline caused by numerous storms of varied strength acting at different water levels.

The model validation, to the extent validation was achieved, only applies to perturbations in the modeled region shoreline being driven by similar hydrodynamic forcing that was used to calibrate the model. Large system perturbations such as large changes to the initial Half Moon Bay shoreline configuration, substantial changes to the bay bathymetry (e.g., significant infilling of the bay using dredge material placement), or vastly different characteristic hydrodynamic conditions could not be simulated using this physical model without additional validation.

The physical model demonstrated the gravel/cobble transition material is mobile with substantial erosion and transport of the gravel from the area of original placement toward the eastern portion of the bay. Because gravel/cobble transport was considered to be in similitude in the model, more confidence can be given to this result. Over time, additional erosion of the gravel material and subsequent redistribution of the gravel along the

Half Moon Bay beach should be anticipated. With the loss of gravel material presently protecting the western shoreline of the bay, additional erosion of the breach fill from the bay side would increase breaching potential.

Finally, simulation of the existing condition in the movable-bed physical model has provided a baseline case for physical model comparison with any engineering alternatives that might be developed in the LTMS for strengthening the breach fill between South Beach and Half Moon Bay or reducing or preventing erosion along the bay shoreline.

8 Summary and Conclusions

A small-scale physical model of Half Moon Bay, Grays Harbor, WA, was constructed at the ERDC, CHL, in Vicksburg, MS. The purpose of the physical model was to support the LTMS studies being conducted by the Seattle District. Specifically, the model results will be used to assess the potential long-term response of the Half Moon Bay shoreline to expected storm waves and surge levels, provided the breach fill between South Beach and the bay remains intact. The long-term response will also serve as a comparison baseline if further physical model studies are undertaken in the LTMS to evaluate performance of engineering alternatives aimed at stabilizing the shoreline and/or strengthening the sand breach fill separating the bay from the Pacific Ocean.

Summary of Study Tasks

The physical model was designed and constructed at a prototype-to-model length scale of 50-to-1, and the hydrodynamics were scaled according to the Froude similitude relationships. The model reproduced the Half Moon Bay bathymetry with a concrete fixed-bed extending from the -10-ft mllw elevation to -40 ft mllw (prototype equivalents). The bathymetry then became a constant 1:10 slope to the horizontal bottom of the wave basin at the -50-ft contour. All bathymetry and beach topography between -10 ft mllw and +25 ft mllw was molded with fine grained (dm = 0.12 mm) non-cohesive quartz sand. The distribution of gravel/cobble protective material placed on the Half Moon Bay foreshore and dune face was scaled to model size and placed between the +4-ft to +25-ft mllw contours.

Potential scale and laboratory effects were analyzed with the following conclusions:

a. Hydrodynamics were in similitude, so that all wave-generated physical processes such as wave refraction, diffraction, shoaling, and wave-induced current would represent those of the prototype.
b. Gravel/cobble transport would be in similitude, and thus the model was expected to reproduce accurately the movement of gravel and cobble material.
c. Bedload sediment transport of sand in the physical model was not in similitude because the model sediment could not be reduced to the correct size without introducing cohesive forces. Consequently, erosion in the

model will not be as severe as in nature, sediment incipient motion under bed-load conditions will require a relatively larger flow speed than in nature, and sediment in motion will settle at relatively greater flow speeds than the prototype. Despite this scale effect, the model was expected to indicate the correct locations of erosion and deposition of sand, but the absolute magnitudes will be less than expected in nature.

d. Sand thrown into suspension by turbulent fluid motion with the surf zone and transported in suspended mode was nearly in similitude, so that erosion produced by energetic wave action with strong breaking and turbulence generation was nearly correct. Eventually, suspended sand grains will settle out of the water column in less turbulent regions.

e. The primary laboratory effect was simulating an entire winter storm season of varying wave conditions and fluctuating water levels by long-crested regular and irregular waves at a single, constant storm surge elevation and at a single approach angle associated with the worst storms. This compromise was necessary due to time and cost limitations involved with simulating the actual storm sequence.

f. An unrealistically strong longshore current in the Point Chehalis vicinity was caused by diffraction of the wave crests into the northern part of the model as the waves passed the end of the wave guide. This problem was recognized and alleviated after the calibration tests were completed.

Despite the inherent limitations of the physical model due to scale and laboratory effects, the model still responded well to the wave forcing with all the nonlinear wave processes accurately reproduced. Because of the recognized sand transport scaling effect, care must be taken when interpreting model results in terms of absolute dune recession expected to occur at Half Moon Bay.

Calibration of the movable-bed response to wave forcing centered around reproducing cumulative shoreline recession and profile change observed at Half Moon Bay during the time period June 2002 to March 2003. Interest was focused on profile P3 that experienced 75 ft of dune recession over the course of the storm season. The first model calibration experiment provided experience on how the movable bed reacted to different wave conditions, wave directions, and wave types (regular versus irregular). With knowledge gained from this experience, the sand bed was remolded and gravel replaced for a second, iterative calibration experiment.

The second calibration experiment was run at a constant surge water level of +12 ft mllw. Regular wave trains having H = 6 m, T = 13 sec were alter-

nated with regular wave trains with H = 3 m, T = 13 sec. Wave direction was from 295 deg. The higher waves promoted dune recession, and the smaller waves proved to be more effective at distributing the eroded sand in the alongshore direction. Overall the dune recession observed in the model was similar to that measured in the prototype, particularly in the western end of Half Moon Bay. However, the model profiles did not erode downward nearly as much as the prototype. This discrepancy is believed to be related to conducting the experiment at a constant water level. In the field, waves at lower water levels cut the profiles lower during less stormy periods, but this hypothesis remains untested. On the eastern end of Half Moon Bay, significantly more profile erosion occurred than was measured in the prototype. The primary cause was an unrealistically strong longshore current moving northward past Point Chehalis. Measurements proved this current to be a laboratory effect created by wave diffraction, and corrections were made at the end of the calibration tests. A secondary reason for the observed discrepancy between laboratory and field might be post-storm waves contributing to profile rebuilding, thus obscuring the true extent of the erosion as compared to the model.

After the model calibration tests, the movable-bed was remolded to the June 2002 bathymetry, and water level was set to +12 ft mllw (prototype equivalent). Energetic regular wave trains with H = 6 m and T = 13 sec were alternated with irregular wave trains with H_{mo} = 3 m and T_p = 13 sec. The regular waves (25 percent of the time) promoted dune recession, and the irregular waves (75 percent of the time) distributed sand within the active transport regions and assured smoother beach profiles and shoreline. Waves were run for a total of 68 hr in the model, at which point most of the shoreline recession approached equilibrium. The final dune recession line closely matched the existing vegetation line at Half Moon Bay with erosion beyond the vegetation line seen in the western end of the bay. Profile comparisons between the model and the prototype March 2003 measurements were favorable.

Study Conclusions

The movable-bed physical model was originally constructed to evaluate potential alternatives for long-term stabilization of the Half Moon Bay shoreline. After construction of the model, the study scope was narrowed by the Seattle District to evaluating future erosion of Half Moon Bay due to storms and elevated surge water levels. This simulation represented the existing condition, and it assumed no additional engineering modifications

to the bay, and erosion would be caused by wave and water level conditions similar to (or less than) those recorded in the past.

The physical model eroded the June 2003 shoreline until a near equilibrium was achieved in the model with the dune recession line closely matching the existing vegetation line. This result indicated Half Moon Bay is approaching an equilibrium shoreline planform shape as postulated by the crenulate bay theory of Silvester (1991) as it adjusts from an influx of sediment resulting from the 1993 breach. However, scale effects in the physical model related to sand transport mean that the dune recession reached in the model for a constant water level and wave energy is less than what would occur in Half Moon Bay under the same constant conditions. Therefore, some additional erosion of the dune should be expected in the coming years. Recent shoreline planform change has largely been adjustment caused by modification to the crenulate bay anchor point at the landward terminus of the South Jetty. The physical model did not include simulation of beach rebuilding during milder wave climate. Some of the sediment eroded from the beach and dune moved past Point Chehalis and was lost to the bay. A similar loss of sediment occurs in the prototype, but periodic placement in Half Moon Bay of material dredged from the navigation channel has decreased the impacts of this sediment loss. Over time, continued loss of sediment may induce additional erosion if placement of dredged material in Half Moon Bay is not continued. The physical model simulation could not be run sufficiently long to estimate the magnitude of any potential problem due to sediment loss in the bay over long time periods.

In summary, if the Seattle District continues placement of dredged material in the subaqueous regions of Half Moon Bay, and breaching of the breach fill between the bay and South Beach is prevented, the planform shoreline shape should reach a stable configuration similar to its existing shape. However, if the bay is subjected to an extended storm acting at the +12-ft mllw elevation, the entire planform shape is expected to translate landward of the position predicted by the physical model because the model had scale effects associated with sand transport. Additional landward recession due to cross-shore sand transport is expected for storms with water levels greater than +12 ft mllw. The bay shoreline adjacent to the breach fill and protected by gravel/cobble remained stable in the physical model, so any new breaching will be largely a result of erosion and dune recession from the Pacific Ocean side.

Cumulative shoreline change over longer time periods will be a result of individual storms followed by longer periods of milder waves that reshape the nearshore bathymetry, but cannot replace eroded dunes. The movable-bed physical model was only capable of examining the response of a single storm event of a given magnitude acting at a static water level of +12 ft mllw. Consequently, this single test cannot be referenced to predict the long-term location of the Half Moon Bay shoreline caused by numerous storms of varied strength acting at different water levels.

The physical model did not include the benefits of placing dredged material in Half Moon Bay, and this probably explains why the physical model lost sediment on the profiles close to Point Chehalis when compared to the prototype. If this periodic nourishment with dredged material decreases in the future, the first effect would likely be sediment loss from the profiles closest to Point Chehalis. Over time this loss might cause sediment to be removed from the profiles farther westward in the bay, but any potential loss of dunes is unknown.

The model demonstrated the gravel/cobble transition material is mobile with substantial erosion and transport of the gravel from the area of original placement toward the eastern portion of the bay. Over time, additional erosion of the gravel material and subsequent redistribution of the gravel along the Half Moon Bay beach should be anticipated. With the loss of gravel material presently protecting the western shoreline of the bay, additional erosion of the breach fill from the bay side might increase breaching potential, although major erosion of the breach fill is also expected to be from the ocean side.

Finally, simulation of the existing condition in the movable-bed physical model provided a baseline case for physical model comparison with engineering alternatives that might be developed in the LTMS for strengthening the breach fill between South Beach and Half Moon Bay or for mitigating or preventing recession of the bay shoreline.

References

Batten, B. K., and N. C. Kraus. 2004. Regional Morphology Analysis Package (RMAP): Part 1. Overview, Technical Note ERDC/RSM-TN-16. Vicksburg, MS: U.S. Army Engineer Research and Development Center.

Dalrymple, R. A., and W. W. Thompson. 1976. Study of equilibrium beach profiles, *Proceedings 15th Coastal Engineering Conference*, Vol 2, American Society of Civil Engineers (ASCE), 1,277-1,296.

Dean, R. G. 1973. Heuristic models of sand transport in the surf zone, *Proceedings Conference on Engineering Dynamics in the Surf Zone*, Sydney, Australia, 208-214.

Hallermeier, R. J. 1981. Terminal settling velocity of commonly occurring sand grains, *Sedimentology* 28(6), 859-865.

Hudson, R. Y., F. A. Herrmann, R. A. Sager, R. W. Whalin, G. H. Keulegan, C. E. Chatham, and L. Z. Hales. 1979. Coastal hydraulic models, Special Report No. 5. Vicksburg, MS: U.S. Army Engineer Waterways Experiment Station.

Hughes, S. A. 1993. Physical models and laboratory techniques in coastal engineering. In *Advanced series on ocean engineering* 7. Singapore: World Scientific.

Hughes, S. A. 2003. Physical modeling considerations for coastal structures. In *Advances in coastal structure design*, R. Mohan, ed., ASCE, 97-115.

Hughes, S. A., and J. E. Fowler. 1990. Validation of movable-bed modeling guidance. *Proceedings 22nd Coastal Engineering Conference* 3:2,457-2,470, ASCE.

Kamphuis, J. W. 1975. Coastal mobile bed model -- Does it work? *Proceedings 2nd Symposium on Modeling Techniques* 2:993-1,009, ASCE.

Kamphuis, J. W. 1991. Physical modeling. In *Handbook of coastal and ocean engineering* 2, J. B. Herbich, ed. Houston, TX: Gulf Publishing Company.

Le Méhauté, B. 1976. Similitude in coastal engineering. *Journal of the Waterways, Harbors and Coastal Engineering Division* 102(WW3):317-335, ASCE.

Osborne, P. D., T. V. Wamsley, and H. T. Arden. 2003. South jetty sediment processes study, Grays Harbor Washington: Evaluation of engineering structures and maintenance measures. Coastal and Hydraulics Laboratory Technical Report, ERDC/CHL TR-03-4. Vicksburg, MS: U.S. Army Engineer Research and Development Center.

Silvester, R. 1991. Natural shaping of bays. In *Handbook of coastal and ocean engineering* 2, J. B. Herbich, ed. Houston, TX: Gulf Publishing Company.

U.S. Army Engineer District, Seattle. 1997. Long-term maintenance of the South Jetty at Grays Harbor, Washington, Evaluation Report. Seattle, WA: U.S. Army Engineer District, Seattle.

Wamsley, T.V., M. A. Cialone, and N. C. Kraus. 2006. Breach history and susceptibility study, south jetty and navigation project, Grays Harbor, Washington. Coastal and Hydraulics Laboratory Technical Report ERDC/CHL TR-06-XX. Vicksburg, MS: U.S. Army Engineer Research and Development Center.

Warnock, J. E. 1950. Hydraulic similitude. In *Engineering hydraulics*, H. Rouse, ed, 136-176. New York: John Wiley & Sons.

REPORT DOCUMENTATION PAGE

Form Approved
OMB No. 0704-0188

1. REPORT DATE *(DD-MM-YYYY)*	2. REPORT TYPE	3. DATES COVERED *(From - To)*
September 2006	Final report	

4. TITLE AND SUBTITLE

Half Moon Bay, Grays Harbor, Washington: Movable-Bed Physical Model Study

5a. CONTRACT NUMBER

5b. GRANT NUMBER

5c. PROGRAM ELEMENT NUMBER

6. AUTHOR(S)

Steven A. Hughes and Julie Cohen

5d. PROJECT NUMBER

5e. TASK NUMBER

5f. WORK UNIT NUMBER

7. PERFORMING ORGANIZATION NAME(S) AND ADDRESS(ES)

U.S. Army Engineer Research and Development Center
Coastal and Hydraulics Laboratory
3909 Halls Ferry Road
Vicksburg, MS 39180-6199

8. PERFORMING ORGANIZATION REPORT NUMBER

ERDC/CHL TR-06-15

9. SPONSORING / MONITORING AGENCY NAME(S) AND ADDRESS(ES)

U.S. Army Engineer District, Seattle
P.O. Box 3755
Seattle, WA 98124-3755

10. SPONSOR/MONITOR'S ACRONYM(S)

11. SPONSOR/MONITOR'S REPORT NUMBER(S)

12. DISTRIBUTION / AVAILABILITY STATEMENT

Available for public release; distribution is unlimited.

13. SUPPLEMENTARY NOTES

14. ABSTRACT

A 1-to-50 scale physical model of Half Moon Bay, Grays Harbor, WA, was constructed at the U.S. Army Engineer Research and Development Center's Coastal and Hydraulics Laboratory in Vicksburg, MS. The purpose of the physical model was to support studies being conducted by the U.S. Army Engineer District, Seattle. Specifically, the model results will be used to assess the potential long-term response of the Half Moon Bay shoreline to expected storm waves and surge levels, provided the breach fill between South Beach and the bay remains intact. The physical model eroded the June 2003 shoreline until a near equilibrium was achieved in the model with the dune recession line closely matching the existing vegetation line. This result indicated Half Moon Bay is approaching an equilibrium shoreline planform shape as it adjusts from an influx of sediment resulting from the 1993 breach. However, scale effects in the physical model related to sand transport mean that the dune recession reached in the model for a constant water level and wave energy is less than what would occur in Half Moon Bay under the same constant conditions. Therefore, some additional erosion of the dune should be expected in the coming years. The physical model did not include the benefits of placing dredged material in Half Moon Bay. The model demonstrated the gravel/cobble transition material is mobile with substantial erosion and transport of the gravel from the area of original placement toward the eastern portion of the bay.

15. SUBJECT TERMS

Half Moon Bay	Physical model	Shoreline evolution
Movable-bed model	Equilibrium shoreline	Grays Harbor
	Gravel transition	Point Chehalis

16. SECURITY CLASSIFICATION OF:			17. LIMITATION OF ABSTRACT	18. NUMBER OF PAGES	19a. NAME OF RESPONSIBLE PERSON
a. REPORT	b. ABSTRACT	c. THIS PAGE			19b. TELEPHONE NUMBER *(include area code)*
UNCLASSIFIED	UNCLASSIFIED	UNCLASSIFIED		118	